DNA Origami

Invented by Paul Ruthemund in 2005

DNA Origami Papers

1. 2005, Rothemund – Design of DNA Origami
2. Mar 2006, Rothemund –
   Folding DNA to create nanoscale shapes and patterns
3. May 2009, Shih et al –
   Self-assembly of DNA into nanoscale three-dimensional shapes
4. Aug 2009, Shih et al –
   Folding DNA into Twisted and Curved Nanoscale Shapes
5. Apr 2009, Andersen et al -
   Self-assembly of a nanoscale DNA box with a controllable lid
6. April 2011, Han et al –
   DNA Origami with Complex Curvatures in Three-Dimensional Space
7. Nov 2011, Arbona et al – Modeling the folding of DNA Origami
8. Nov 2009, Shih et al –
   Multilayer DNA Origami Packed on a Square Lattice
9. Jan 2012, Shih et al –
   Multilayer DNA Origami Packed on Hexagonal and Hybrid Lattices

Comparison of Nanofabrication Methods

Lithography (Top down)

- Eg. Electron beam lithography, photolithography
- Expensive
- Serial
- Precise
- Ultra-high vacuum, ultra-clean conditions or cryogenic temperatures

Self-assembly (Bottom up)

- Eg. DNA origami, self-assembled monolayers, lipid bilayers and micelles
- Cheaper
- Massively parallel synthesis
- Less exact
- Simple aqueous environments

2005 – Design of DNA Origami
2006 – Folding DNA to create nanoscale shapes and patterns
Paul Rothemund

2005 – Design of DNA Origami
2006 – Folding DNA to create nanoscale shapes and patterns
Paul Rothemund

- Origami → folding
- One long strand → “scaffold”
- Many short strands → ”helpers”, later “staples”
- Used Matlab to design origami (clunky → never released → made obsolete anyway…)
- Major leaps here are:
  - One-pot reaction
  - High yield

How DNA Origami Self-Assembles

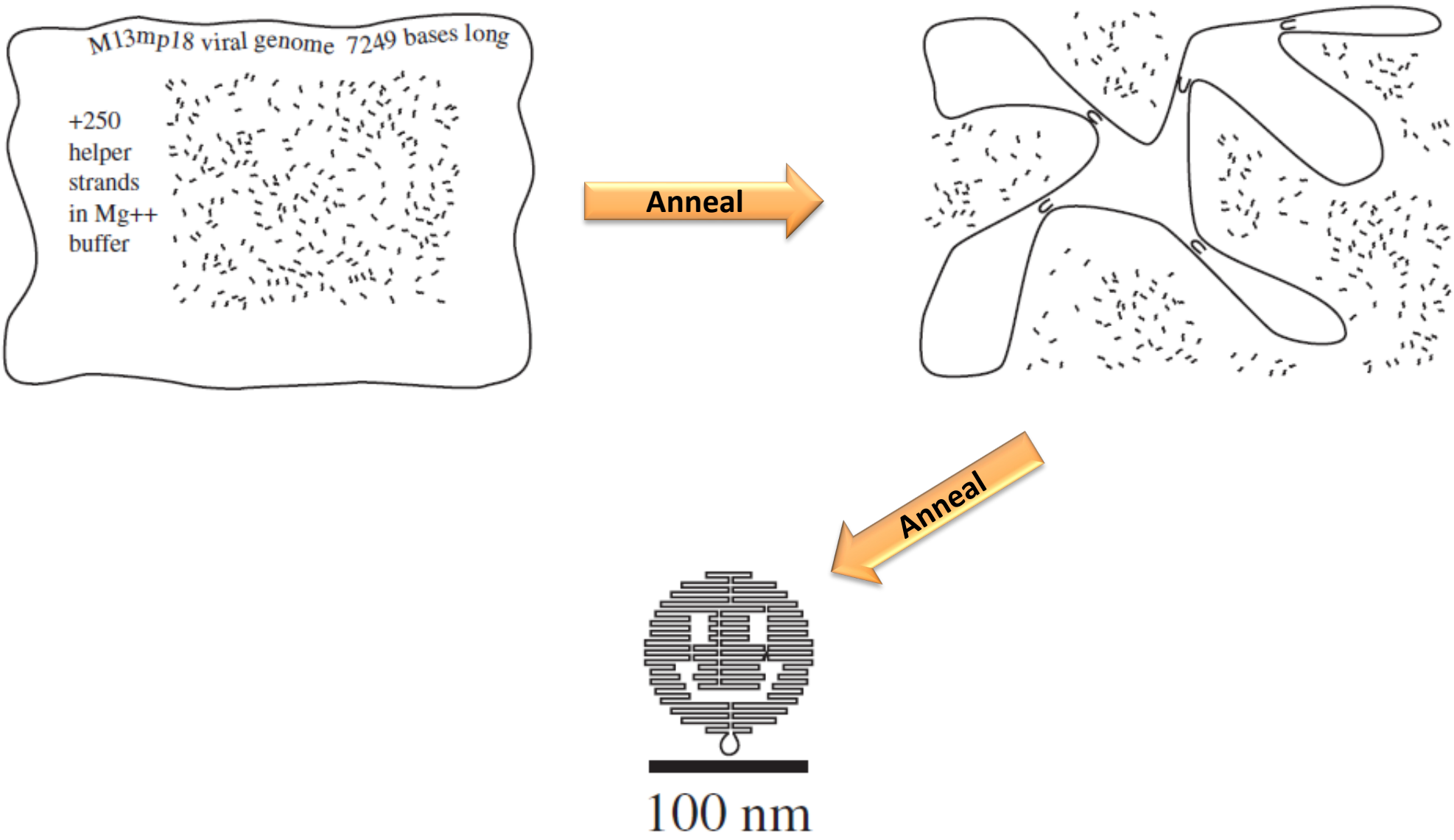

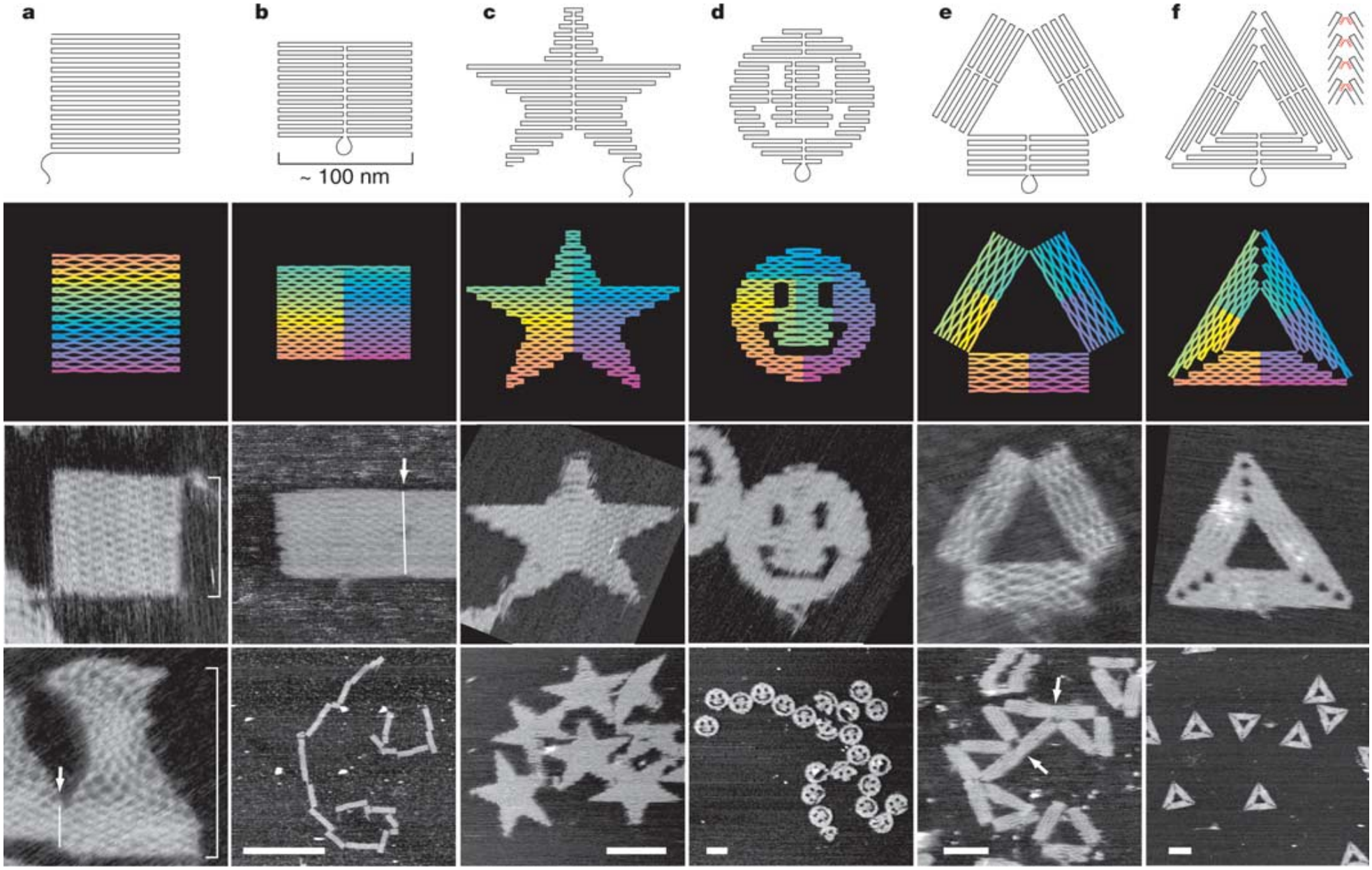

Figure 2 | **DNA origami shapes.** Top row, folding paths. **a**, square; **b**, rectangle; **c**, star; **d**, disk with three holes; **e**, triangle with rectangular domains; **f**, sharp triangle with trapezoidal domains and bridges between them (red lines in inset). Dangling curves and loops represent unfolded sequence. Second row from top, diagrams showing the bend of helices at crossovers (where helices touch) and away from crossovers (where helices bend apart). Colour indicates the base-pair index along the folding path; red is the 1st base, purple the 7,000th. Bottom two rows, AFM images. White lines and arrows indicate blunt-end stacking. White brackets in **a** mark the height of an unstretched square and that of a square stretched vertically (by a factor >1.5) into an hourglass. White features in **f** are hairpins; the triangle is labelled as in Fig. 3k but lies face down. All images and panels without scale bars are the same size, 165 nm × 165 nm. Scale bars for lower AFM images: **b**, 1 μm; **c**–**f**, 100 nm.

DUKE
COMPUTER SCIENCE

Design of 2D Origami

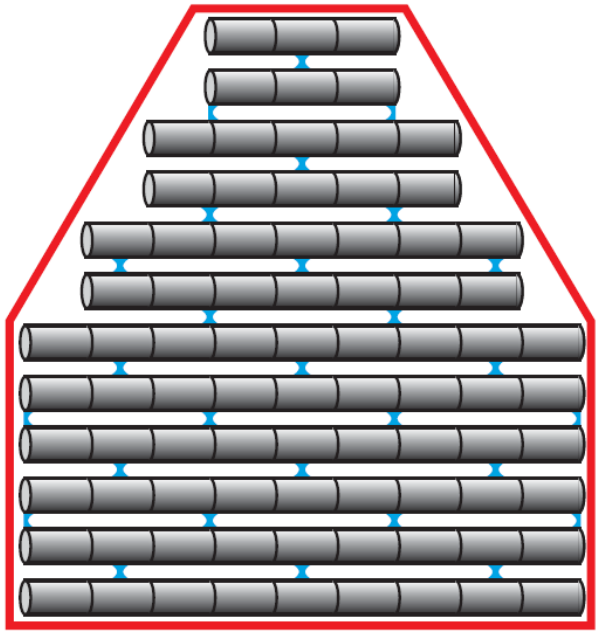

- Scaffold crossover
- Staple crossover

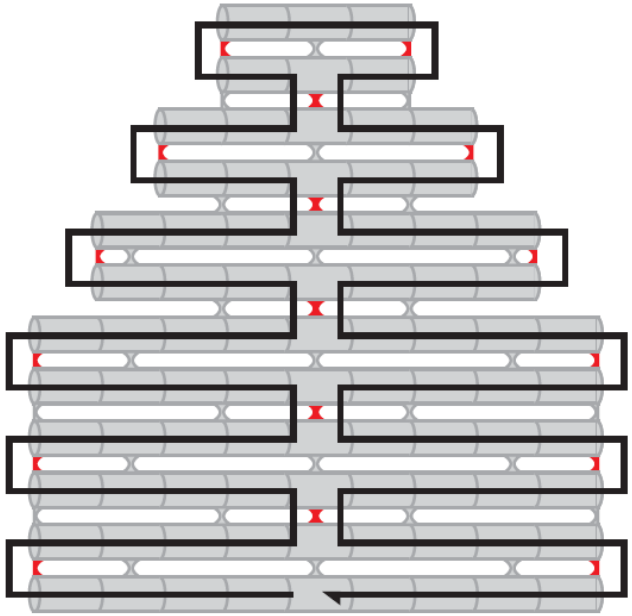

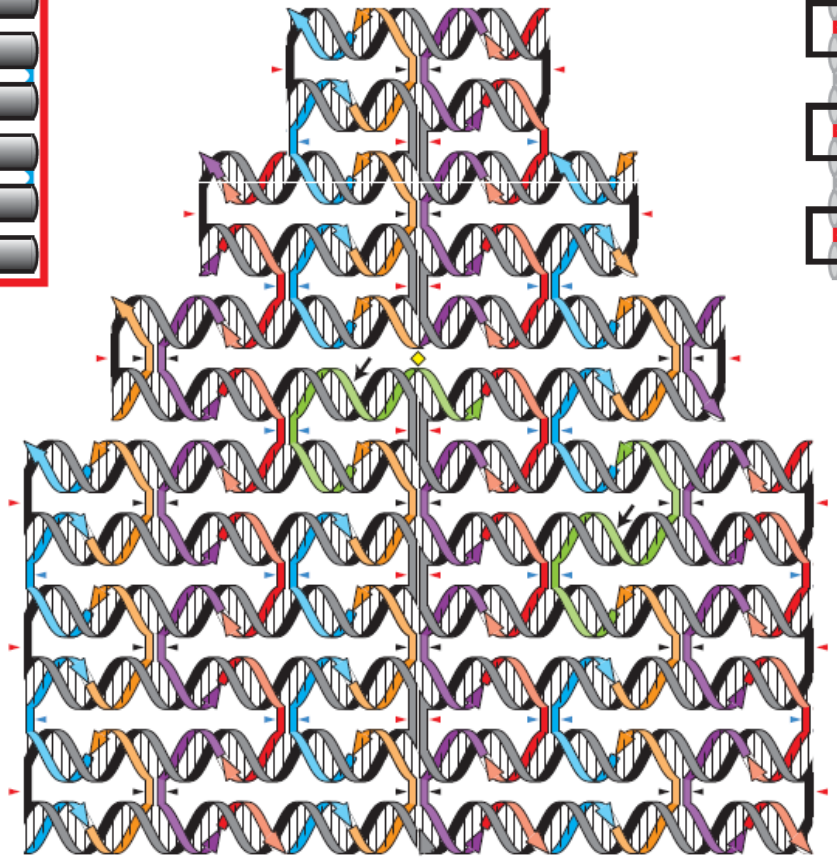

Step 1 – Approximate Shape & Add Blue Crossovers

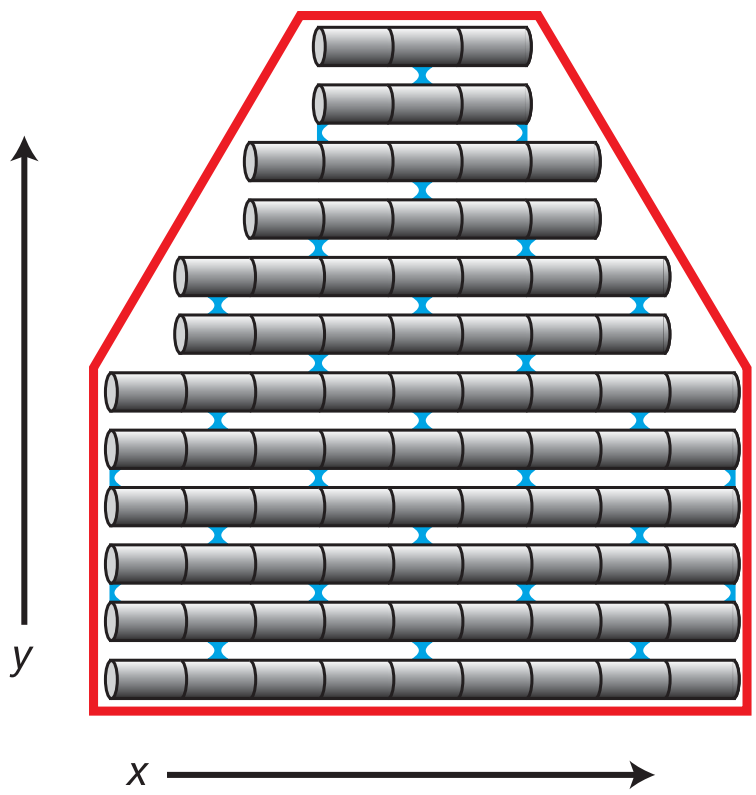

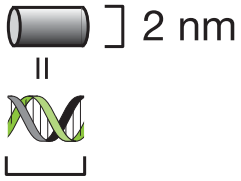

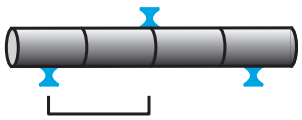

- y depends on the gap between helices, typically ~2.6 nm if crossovers are tight (no excess bases)
- Odd number of half-turns = ??
- Even number of half-turns = ??

Q: Why 16 base pairs?

2006 - **Folding DNA to create nanoscale shapes and patterns**

Step 2:
Raster Fill & Add Scaffold Crossovers

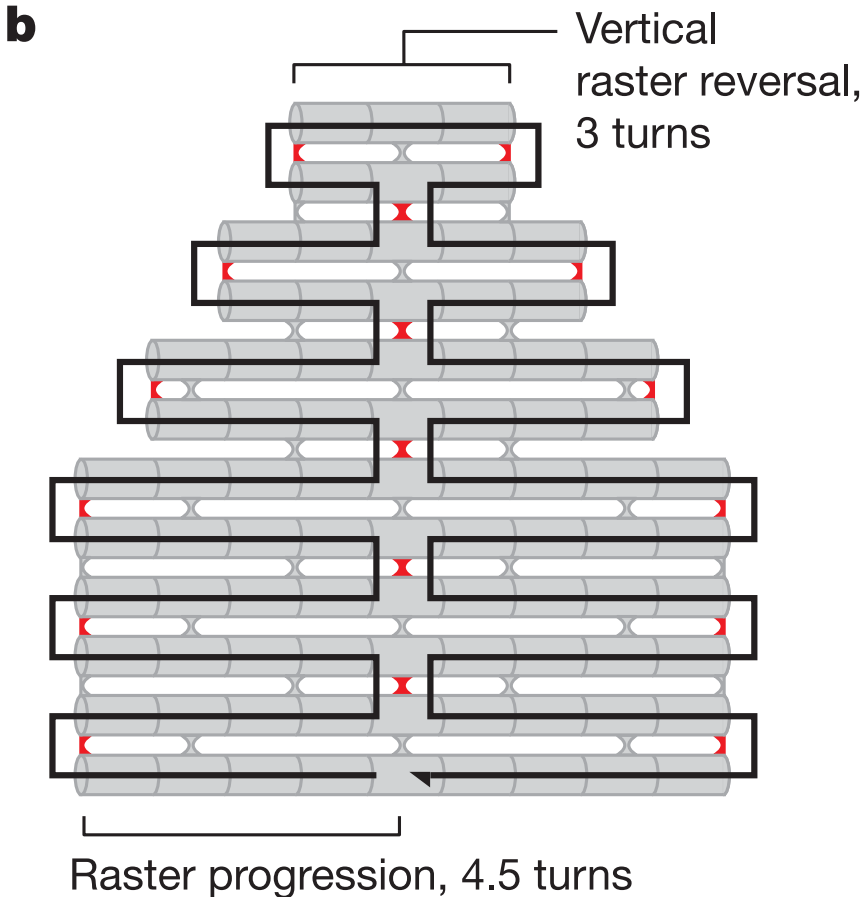

- Red - ‘scaffold crossovers’
- Distance must be an odd number of half-turns
- Seam → contour that the path does not cross

2006 - **Folding DNA to create nanoscale shapes and patterns**

Step 3 – Fill in Staple Strands & Sequences

- 250 staples, each 32 bases long
- Provide complements for scaffold

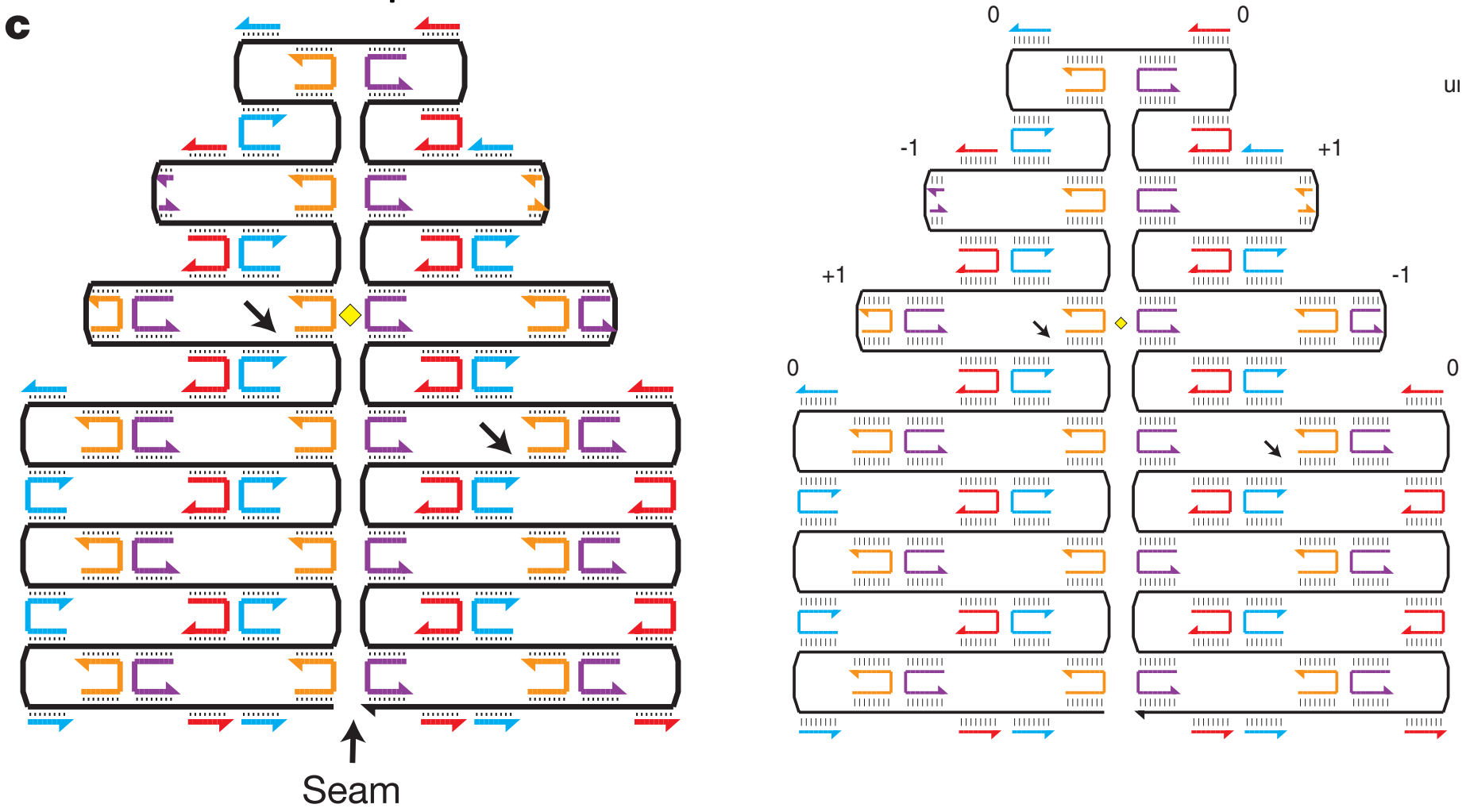

2006 - **Folding DNA to create nanoscale shapes and patterns**

Step 4: Minimize Strain & Recompute Staple Sequences

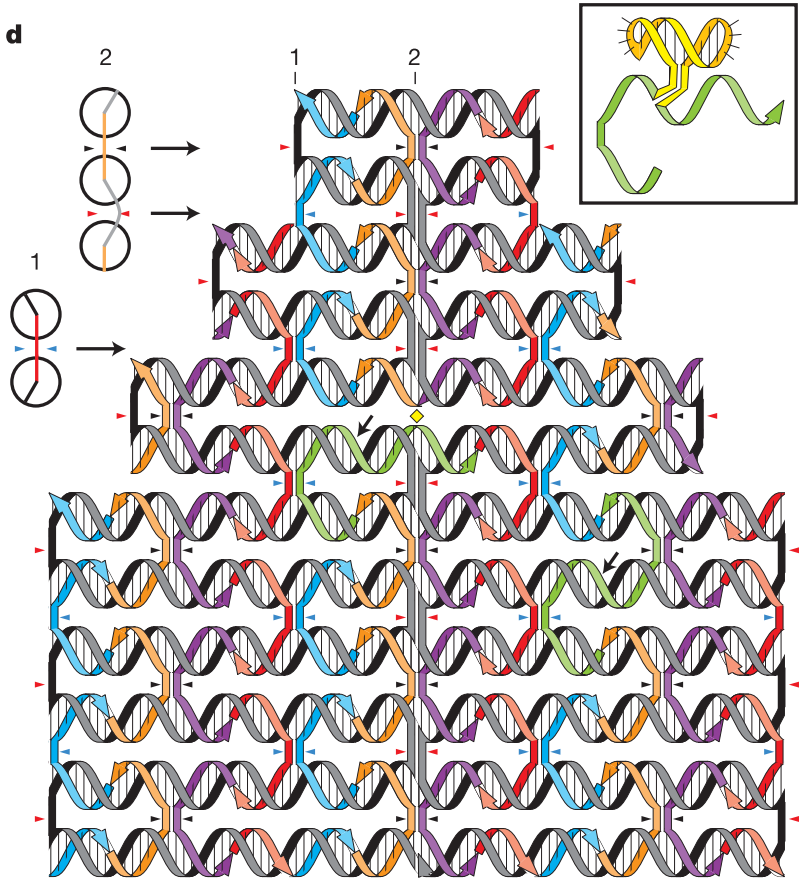

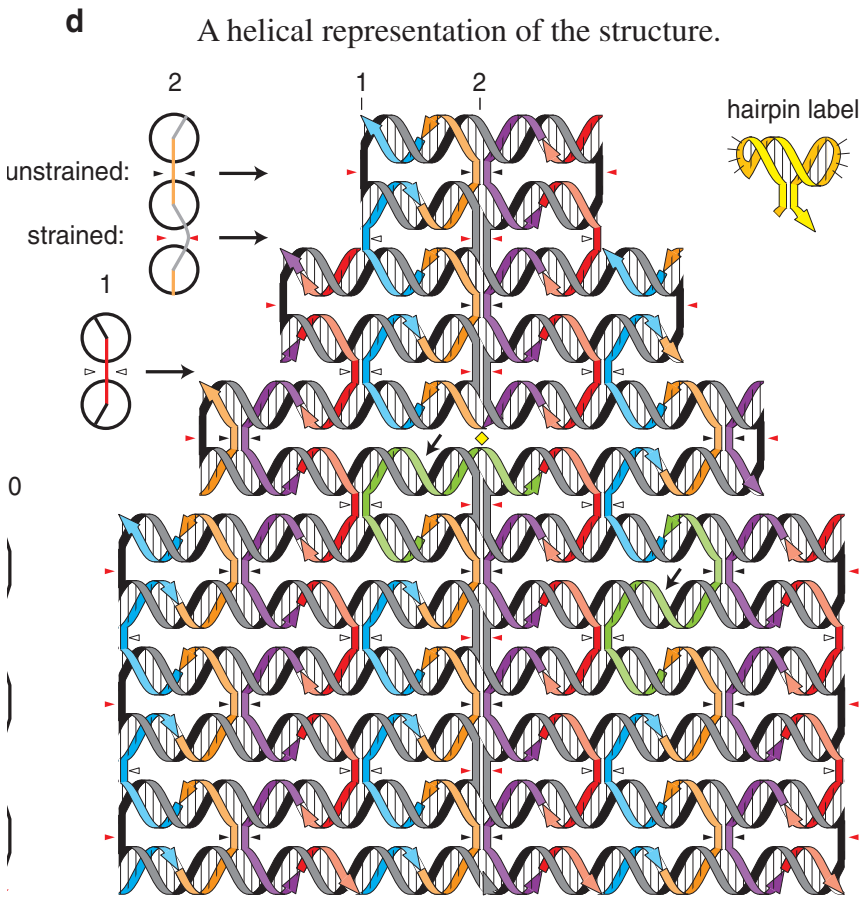

2006 - **Folding DNA to create nanoscale shapes and patterns**

Step 5 - Merge Staples

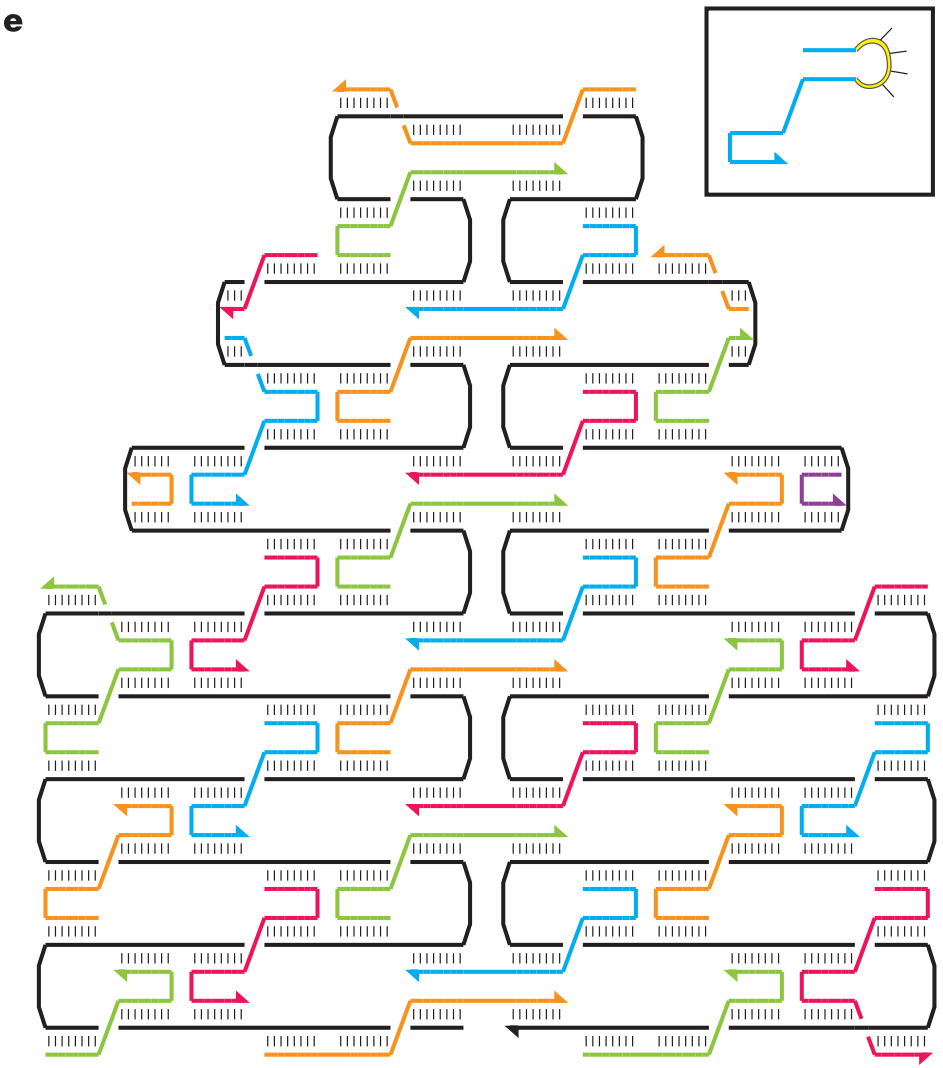

If using a full m13mp18 scaffold, shapes typically ~ 150 staples, 20-60 bases long

2006 - **Folding DNA to create nanoscale shapes and patterns**

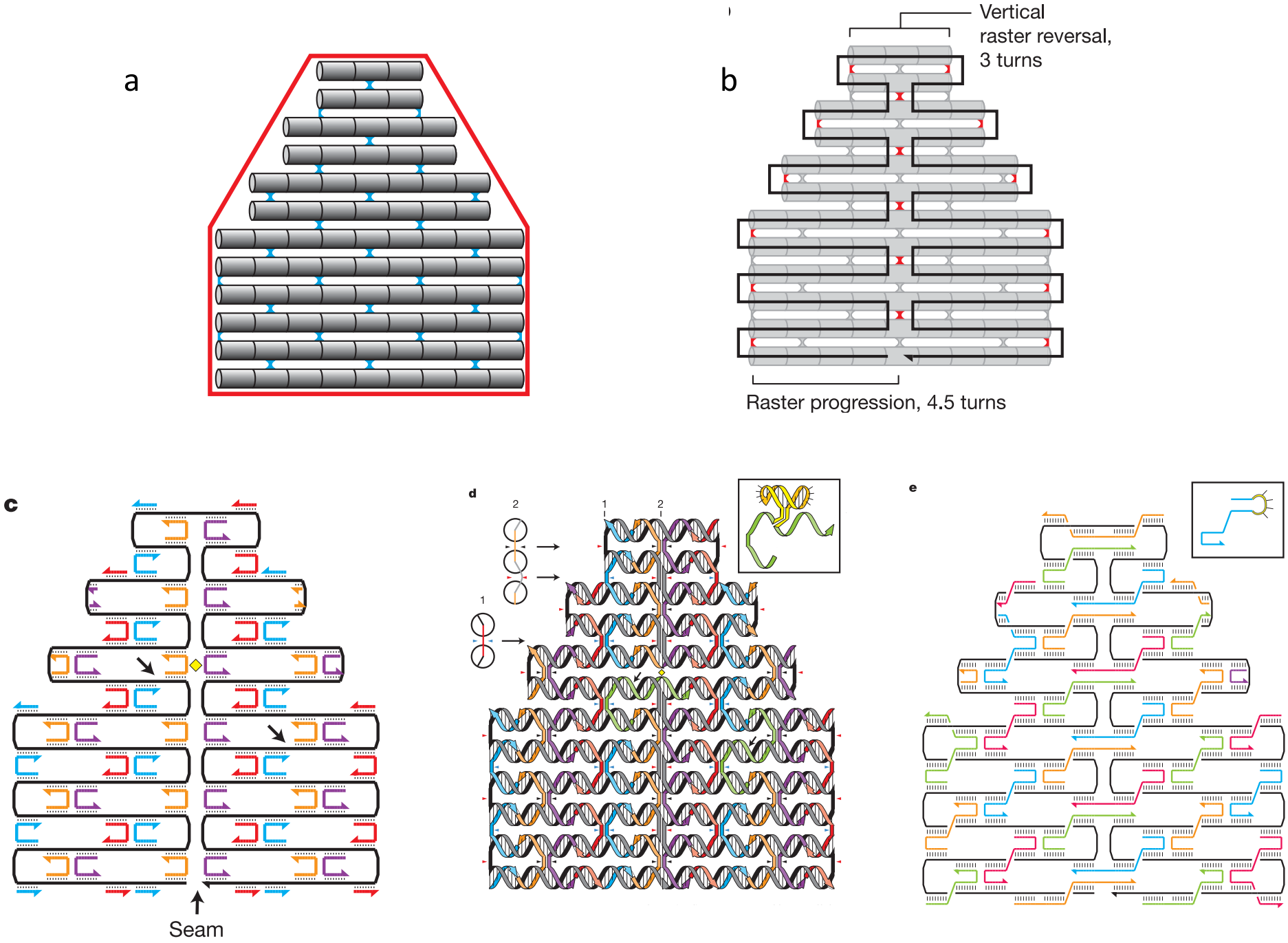

2006 - **Folding DNA to create nanoscale shapes and patterns**

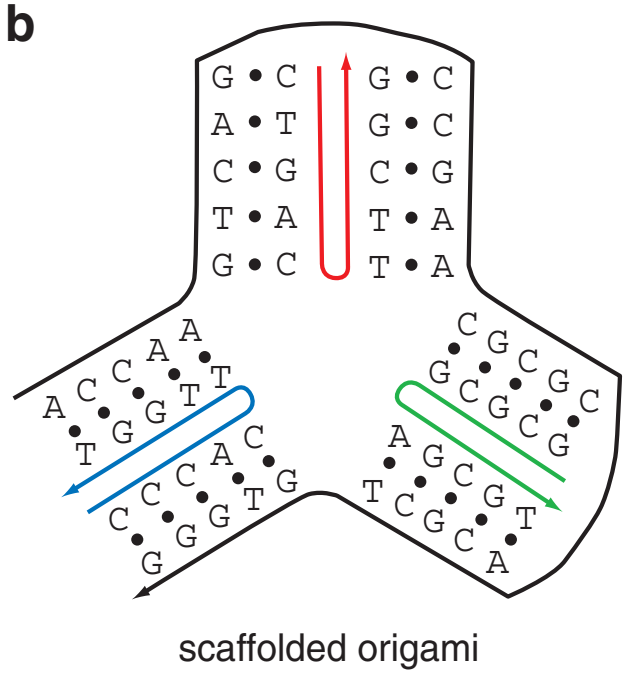

- Origami
  - Allows excess of staples to be used (no need for exact stoichiometry)
  - Uniquely addressable

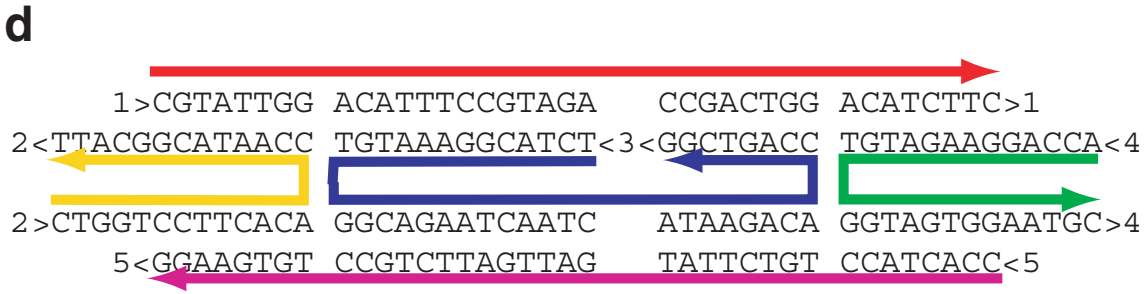

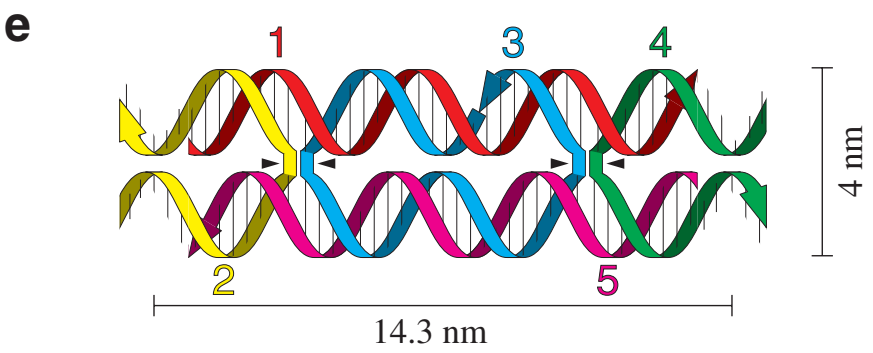

Fig. 1. Examples of non-canonical, branched DNA structures. 3-prime ends (usually written 3', here '3') of DNA strands are marked by arrowheads.

2006 - **Folding DNA to create nanoscale shapes and patterns**

Experimental Method for Forming DNA Origami

- >100 staple strands, each 20-60 bases long
  - 5 uL of each strand solution → "master mix"
- Scaffold, 3000-50,000 nts long
- Buffer (pH control)
- Magnesium salt (Magnesium Mg++ ions neutralize negative charges on the DNA and allow the single-stranded DNA to come together and form the double helix)
- Heating to 90 C then cooling to 20 C in under 2 hrs (in 2006 papers, says 95 C in over 2 hours).
- Characterize with AFM, TEM, or gel electrophoresis

2006 - **Folding DNA to create nanoscale shapes and patterns**

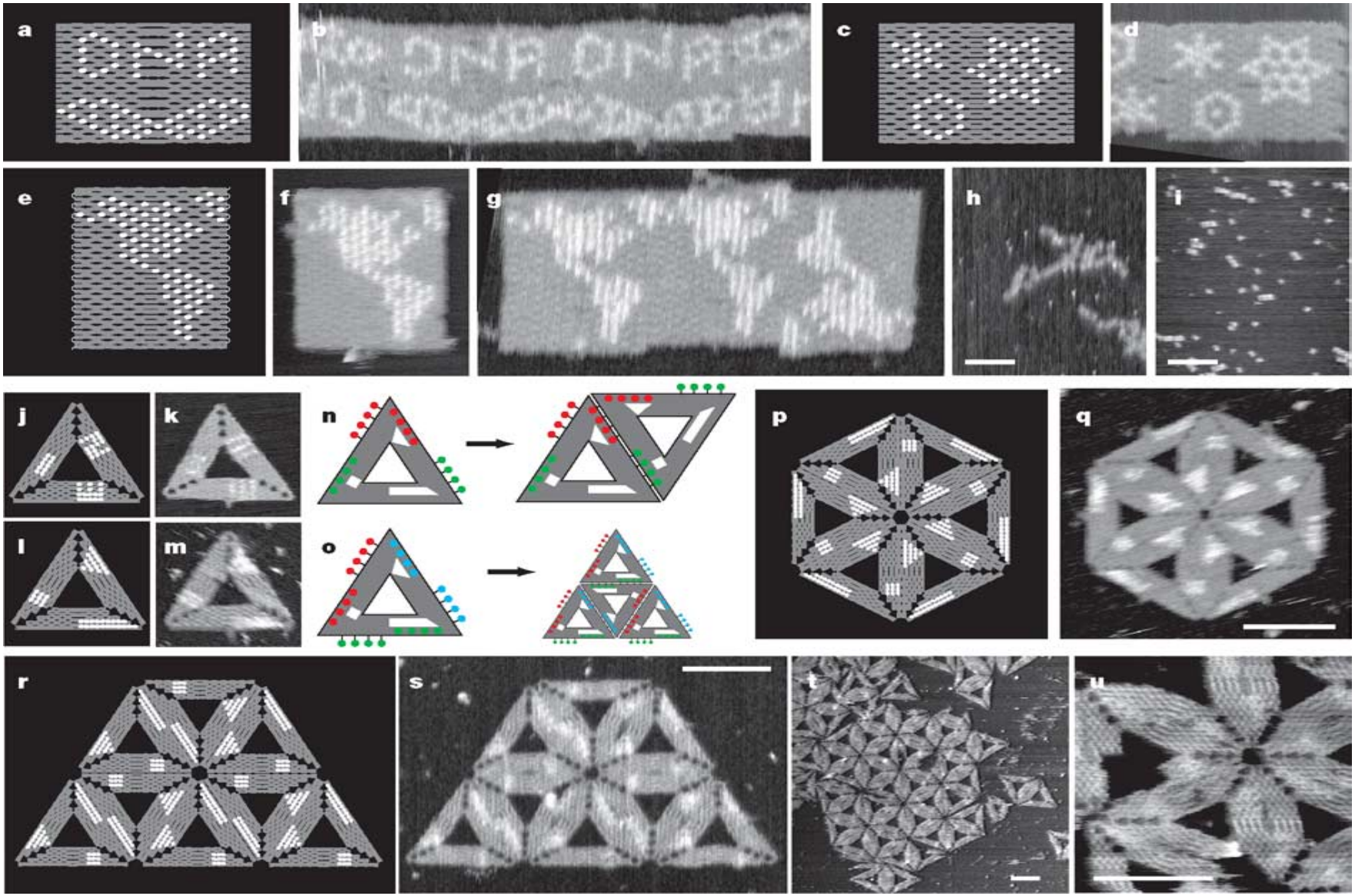

Patterning and combining DNA origami. **a**, Model for a pattern representing DNA, rendered using hairpins on a rectangle (Fig. 2b). **b**, AFM image. One pixelated DNA turn (~100 nm) is 30× the size of an actual DNA turn (~3.6 nm) and the helix appears continuous when rectangles stack appropriately. Letters are 30 nm high, only 6× larger than those written using STM in ref. 3; 50 billion copies rather than 1 were formed. **c**, **d**, Model and AFM image, respectively, for a hexagonal pattern that highlights the nearly hexagonal pixel lattice used in **a**–**i**. **e**–**i**, Map of the western hemisphere, scale 1:2 × 10^{14}, on a rectangle of different aspect ratio. Normally such rectangles aggregate (**h**) but 4-T loops or tails on edges (white lines in **e**) greatly decrease stacking (**i**). **j**–**m**, Two labellings of the sharp triangle show that each edge may be distinguished. In **j**–**u**, pixels fall on a rectilinear lattice. **n**–**u**, Combination of sharp triangles into hexagons (**n**, **p**, **q**) or lattices (**o**, **r**–**u**). Diagrams (**n**, **o**) show positions at which staples are extended (coloured protrusions) to match complementary single-stranded regions of the scaffold (coloured holes). Models (**p**, **r**) permit comparison with data (**q**, **s**). The largest lattice observed comprises only 30 triangles (**t**). **u** shows close association of triangles (and some breakage). **d** and **f** were stretched and sheared to correct for AFM drift. Scale bars: **h**, **i**, 1 μm; **q**, **s**–**u**, 100 nm.

Summary of DNA Origami

Templated self-assembly of DNA into custom two-dimensional shapes on with a multiple-kilobase ‘scaffold strand’ that is folded into a *flat* array of antiparallel helices by interactions with hundreds of oligonucleotide ‘staple strands’

2006 - **Folding DNA to create nanoscale shapes and patterns**

Notes on DNA Origami

- Prior to Rothemund, attempts were made, but inhibited.
- Yield is 70%
- He ignored 3 criteria in his method:
  - Sequences must be optimized to avoid secondary structure or undesired binding interactions
  - Strands must be purified
  - Strands must be equimolar

  (legacy of Seeman)

2006 - **Folding DNA to create nanoscale shapes and patterns**

Why DNA Origami Works so Well?

- Suggested factors that helped this succeed:
  1. strand invasion
  2. an excess of staples (why? proposed 5:1)
  3. cooperative effects
  4. design that intentionally does not rely on binding between staples.

  DNA origami may be used as a 'nanobreadboard' to which diverse components can be added.

Modeling the folding of DNA origami Arbona et al

Arbona, J. M., Elezgaray, J., & Aimé, J. P. (2011). Modelling the folding of DNA origami. arXiv preprint arXiv:1111.7130. Retrieved from http://arxiv.org/abs/1111.7130

Modeling the folding of DNA origami
Arbona et al

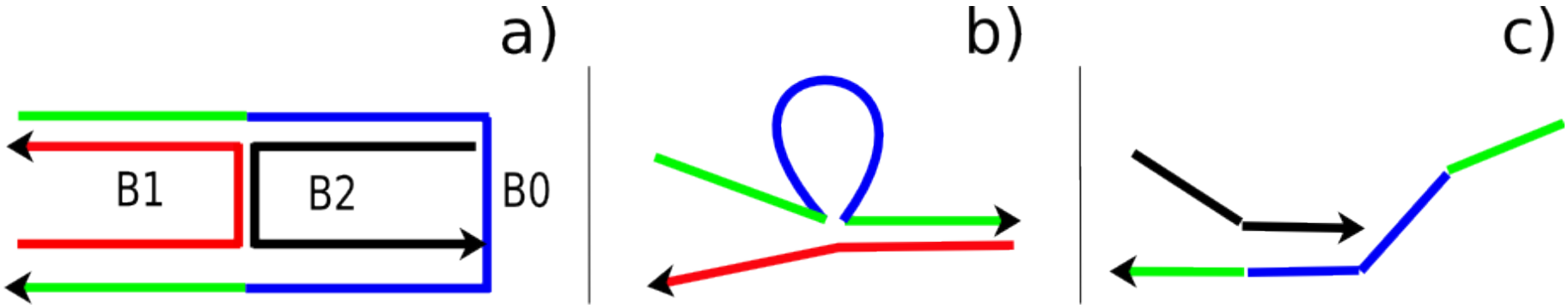

(a) Schematic representation of the connectivity of the small origami.(b) B1 staple is in the 'outer' position,(c) B2 staple in the 'inner' position. (b) and (c) show that the binding of staples in the outer (b) or inner (c) positions are very different.

Modeling the folding of DNA origami
Arbona et al

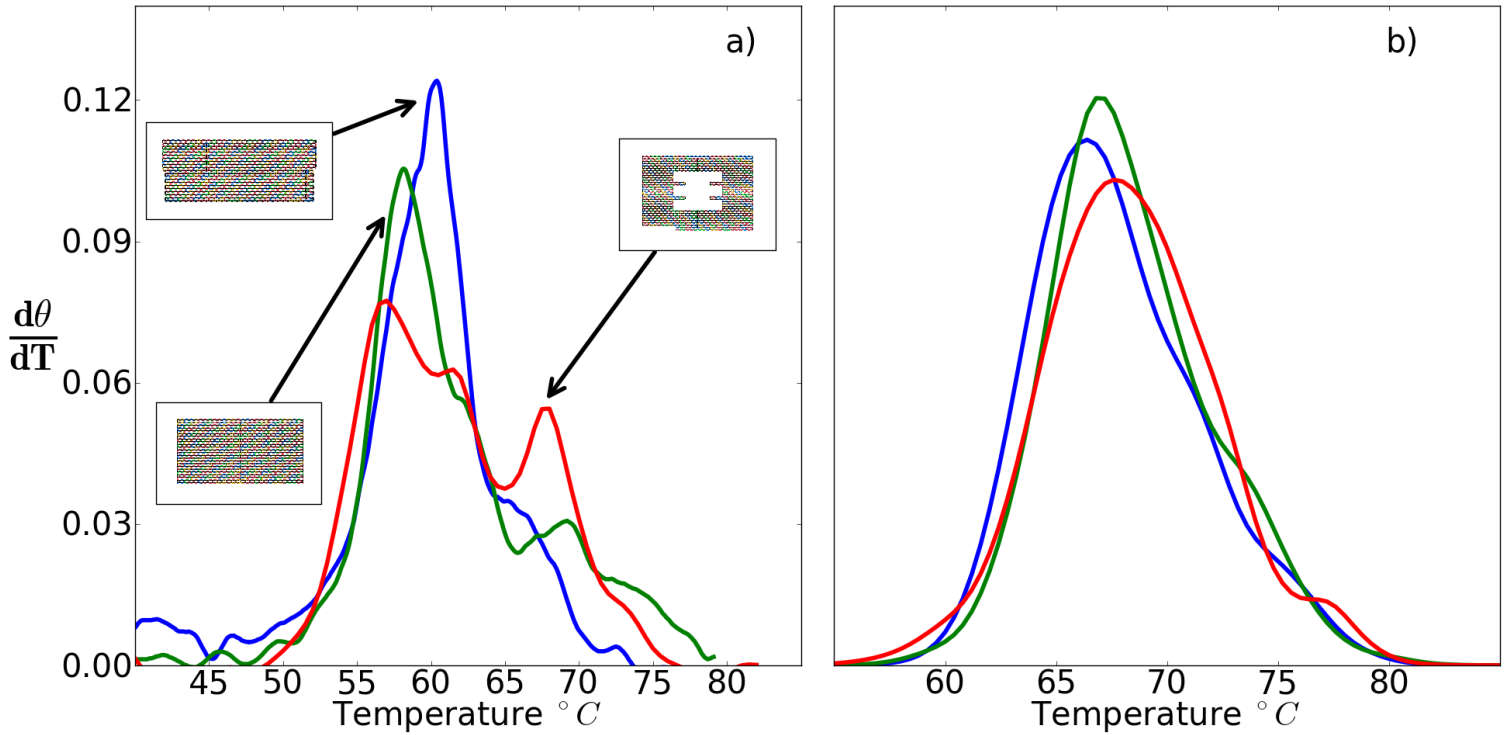

(a)Derivative $d\theta/dT$ of the degree of pairing with respect to temperature for the three DNA origamis represented in the insets. (b) $d\theta/dT$ for a model where

Modeling the folding of DNA origami
Arbona et al

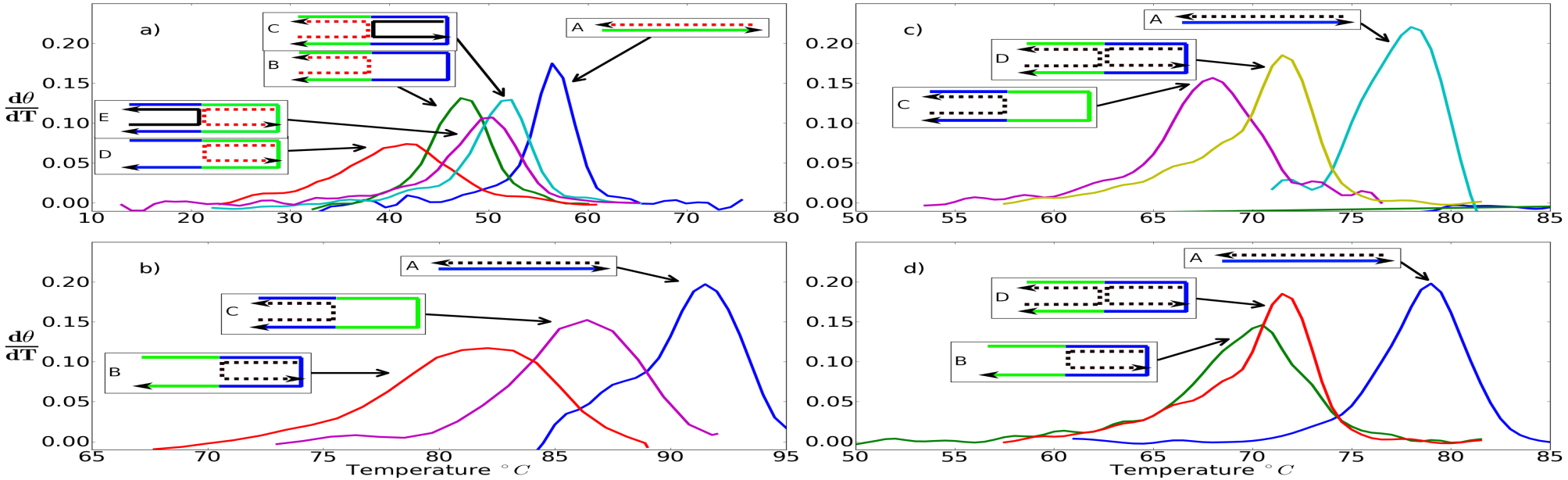

The derivative $d\theta/dT$ reported in the four figures corresponds to the folding of the dotted staple. a) experimental data on the folding of B1(AT) cases (A,B,D) in the absence of B2(GC), cases (C,E) with B2 already folded; b) experimental data on B2 without B1; c) experimental data on B1m; d) experimental data on B2m

Modeling the folding of DNA origami
Arbona et al

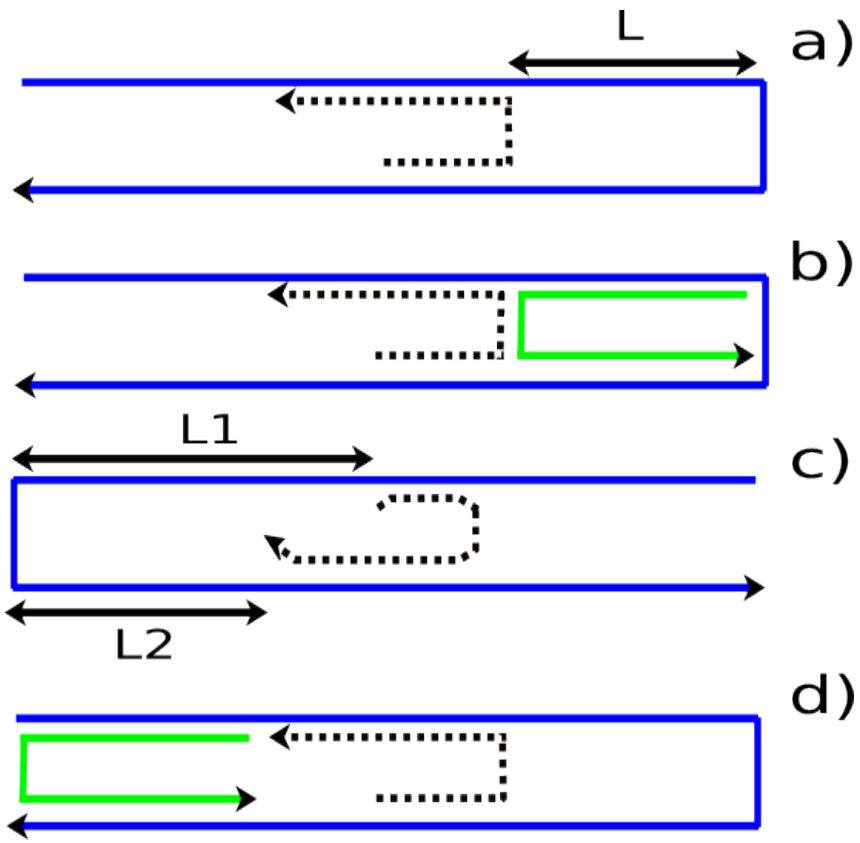

Computing the entropic penalty for the three different local intermediate states (LIS). The staple to be inserted is represented by the dotted line, the scaffold by the continuous line. (a) LIS1 (b) LIS2 (c) LIS3. Here, we assume that, because of the curvature constraints imposed by this configuration, the staple remains partly unfolded. (d) A typical situation where two types of LIS (LIS1 at the right side of the staple, LIS3 at the left side) can be attributed to a given crossover.

Modeling the folding of DNA origami
Arbona et al

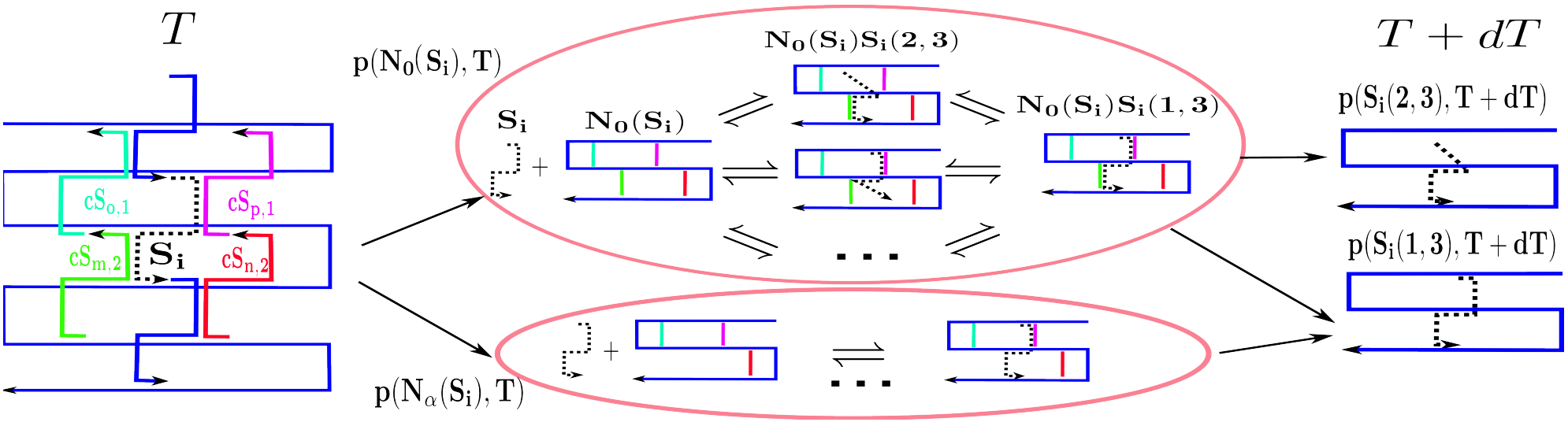

. To evaluate the fraction of the staple S_i folded at the temperature $T + dT$, one considers the nearby staples of the staple i at T and calculates the probability of the different neighbouring crossovers configurations ($cS_{m,2}, cS_{p,1}$,etc) around S_i. The origami is then subdivided in different partially folded state(eg $N_\alpha(S_i)$) with a given probability (eg $p(N_\alpha(S_i))$..). For each of these partial states the equilibrium constant for a partial folded configuration ($N_\alpha(S_i)S_i(m,n)$) of the staple within this restricted local state is calculated as explained in the energy model. The law of mass action for each partial configuration folded gives a set of coupled equations. Once solved they allow to determine the fraction of partial configuration folded in this environment $p(N_\alpha(S_i), T + dT)$. Then we can calculate the total fraction of each configuration folded $p(S_i(m,n), (T + dT)$, as the sum of the fraction of those configurations in the different local states, weighted by the probability of each state.

Modeling the folding of DNA origami
Arbona et al

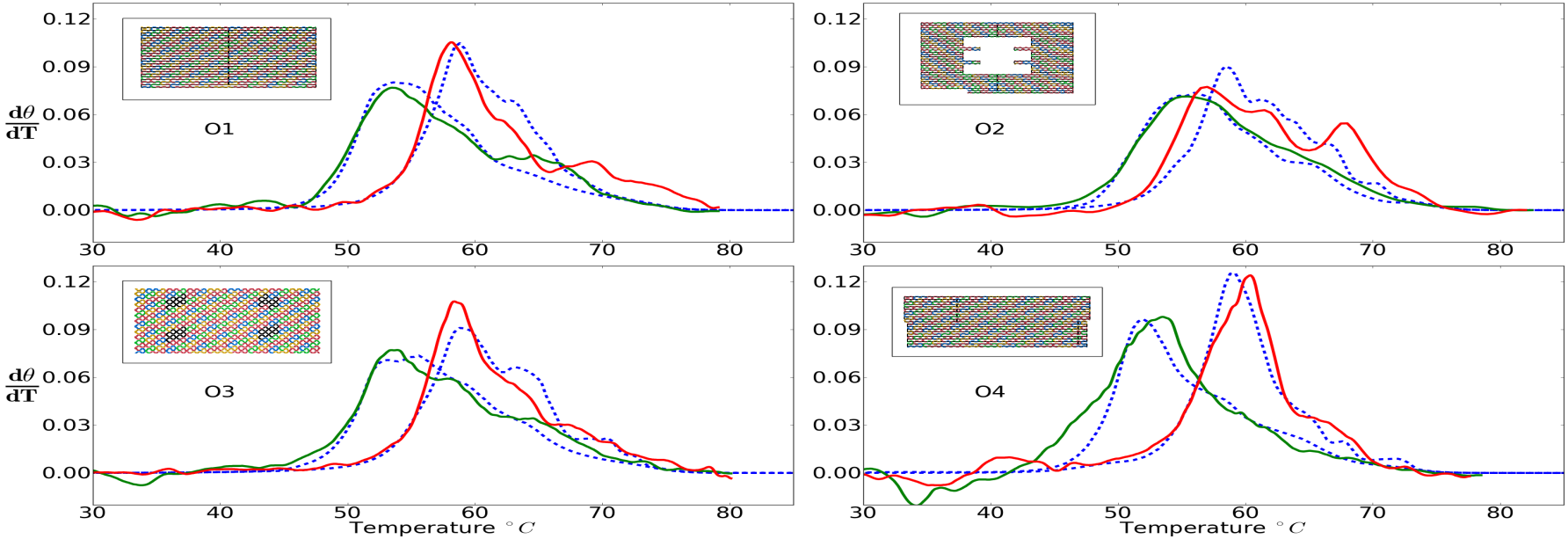

. Derivative of the pairing degree versus temperature. The data corresponding to annealing are in red, melting in green, the model is in blue for both processes.

Modeling the folding of DNA origami
Arbona et al

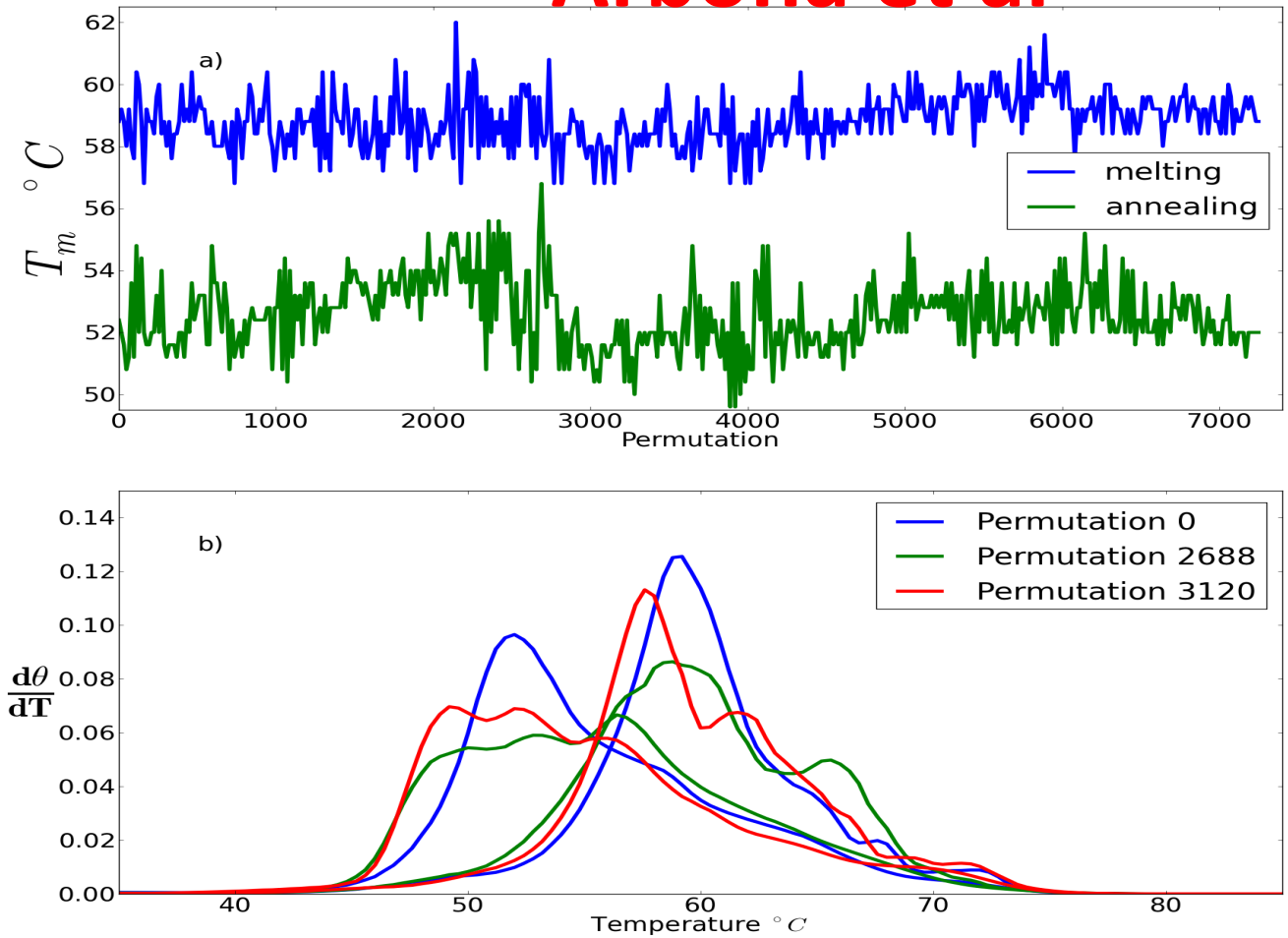

(a) Distribution of melting temperatures (annealing and melting) as a function of the order of the circular permutation of the scaffold strand. (b) two different melting curves corresponding to two permutations with the lowest and highest annealing temperatures.

Modeling the folding of DNA origami
Arbona et al

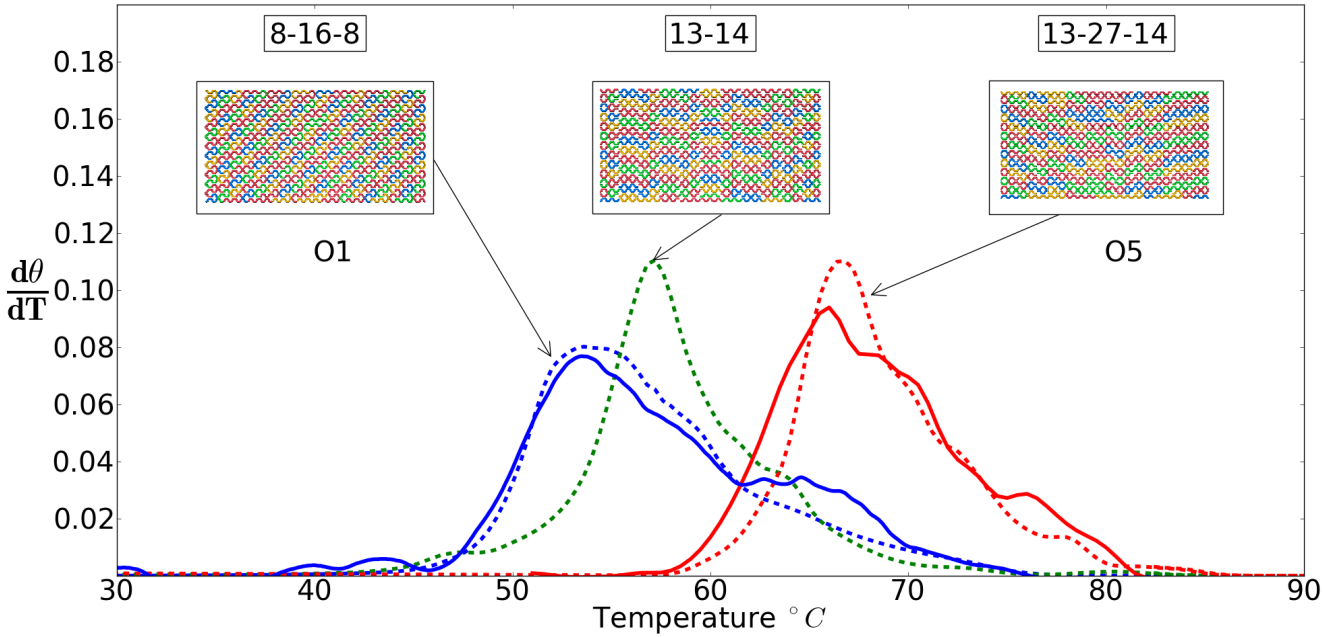

Annealing curves of the O1 and O5 origamis. The two origamis correspond to the same scaffold pattern, but different staple pattern (solid line = experimental data, dashed line = theoretical curves)

DNA Origami Software

DNA Origami Software

- **caDNAno**
  - http://cadnano.org
  - Shawn Douglas (now @ UCSF) while @ William Shih's lab
- **Cando**
  - https://cando-dna-origami.org
  - Mark Bathe (MIT)

caDNAno Software for Design of DNA Origami

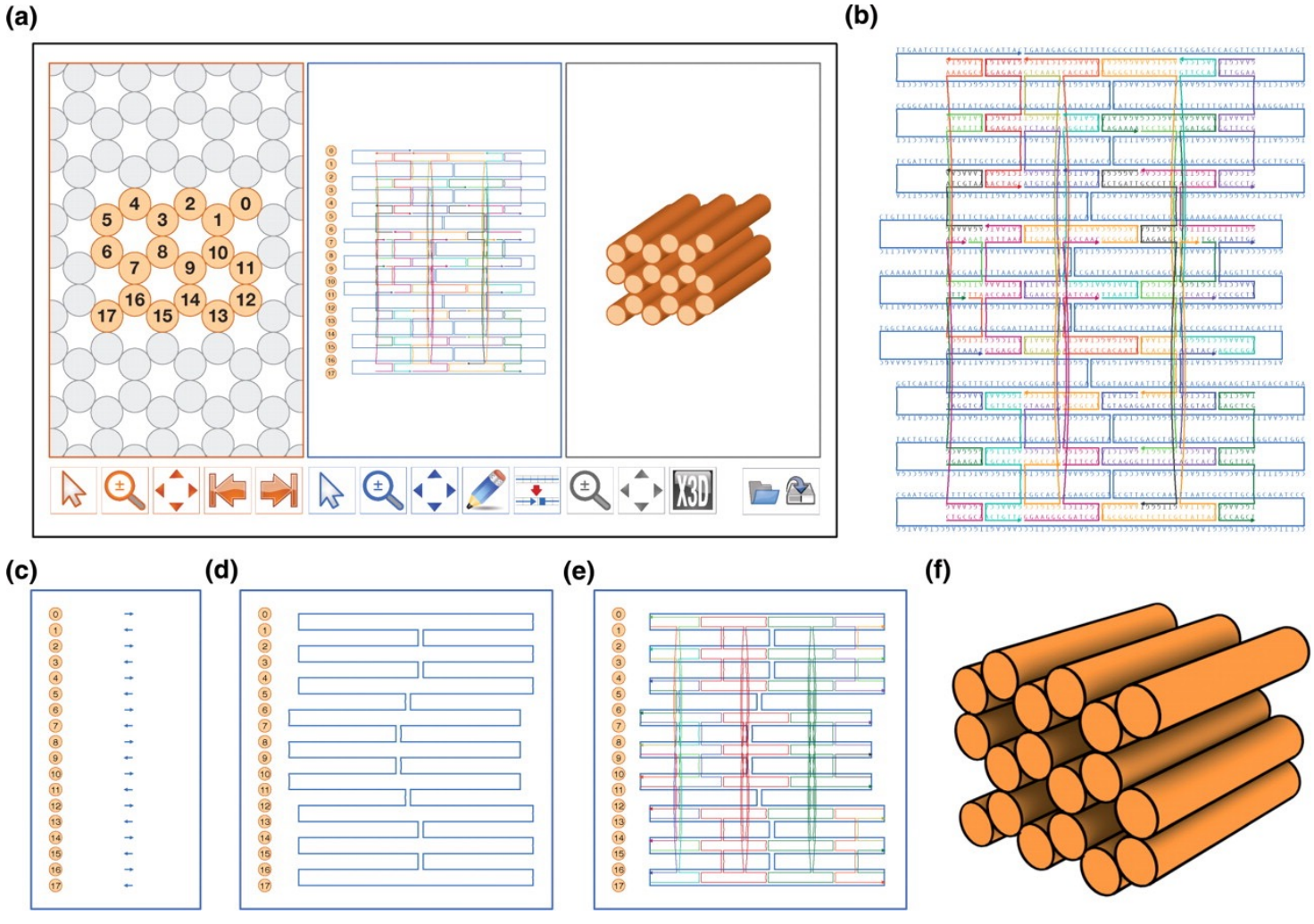

Legacy version (from Douglas et al. 2009)

caDNAno Software for Design of DNA Origami

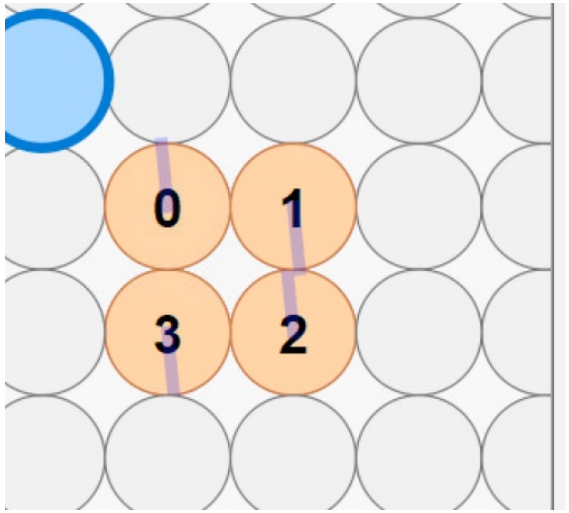

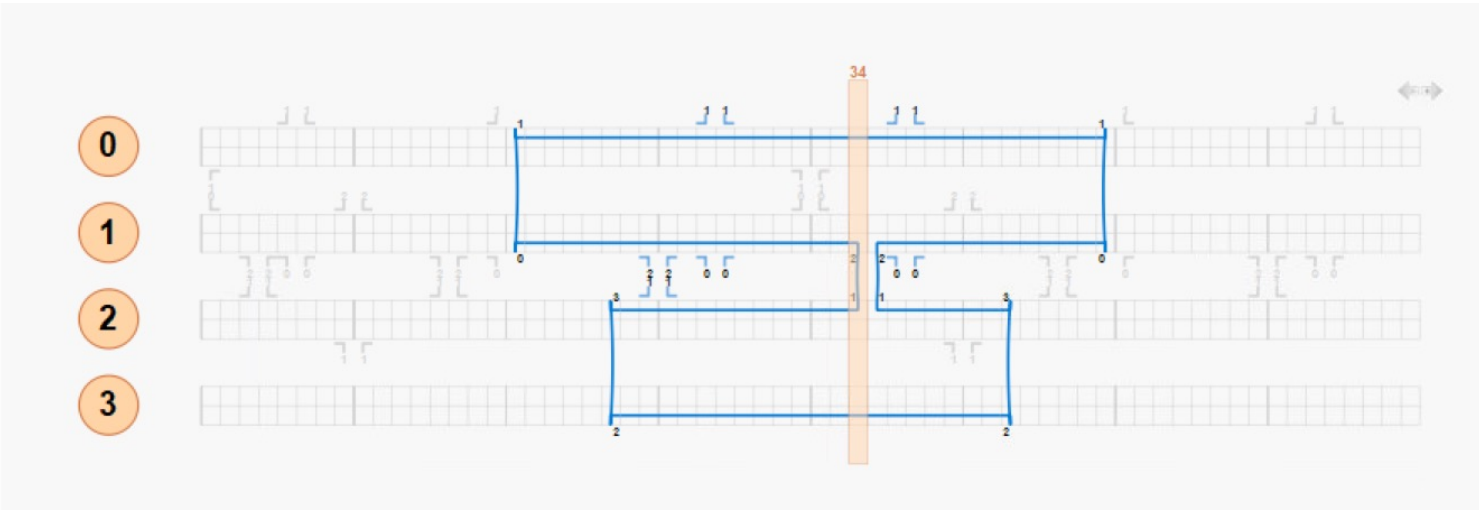

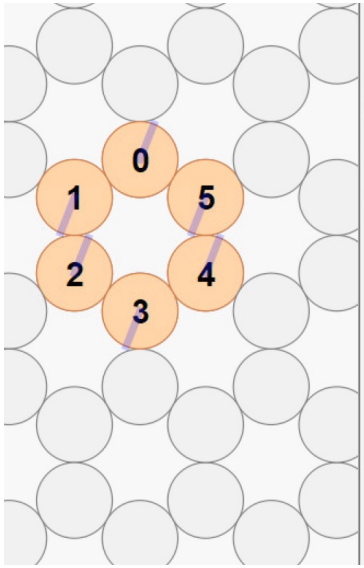

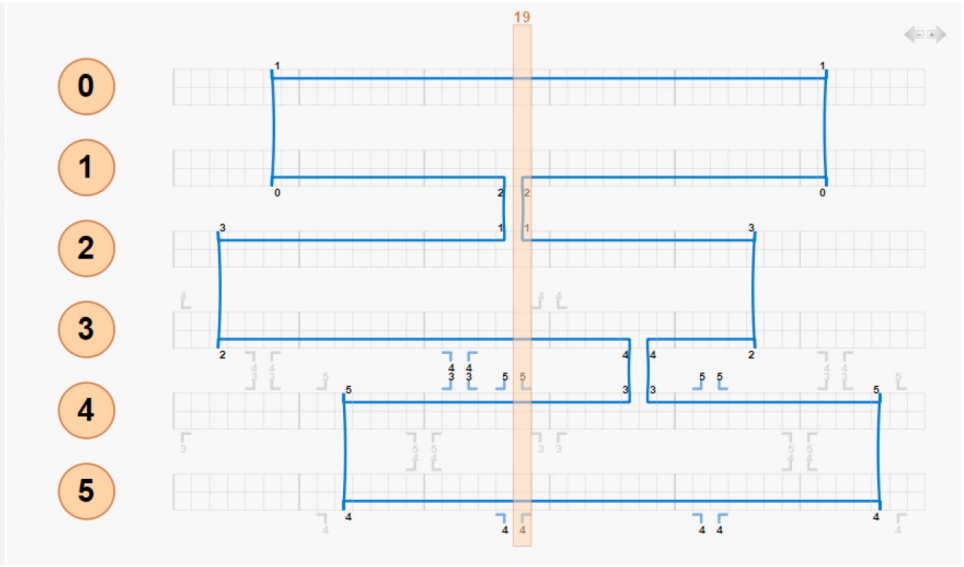

Version 2

Cando Software for Design of DNA Origami

- Input
  - JSON (caDNAno)
  - DAT (Tiamat)
  - or CNDO (Cando) formats
- Output
  - Fluctuations movies
  - Relaxed shape
  - Atomic model

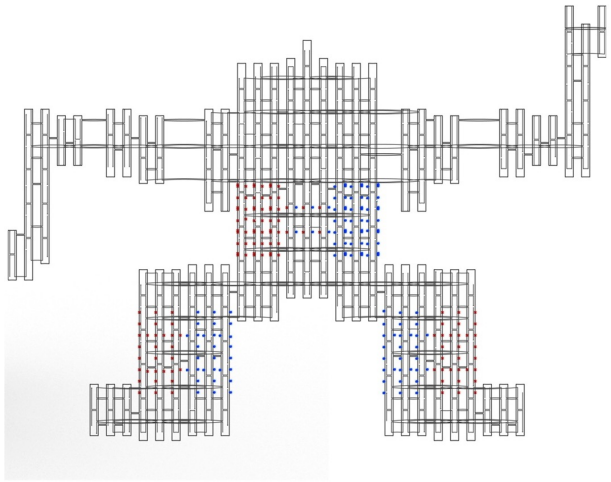

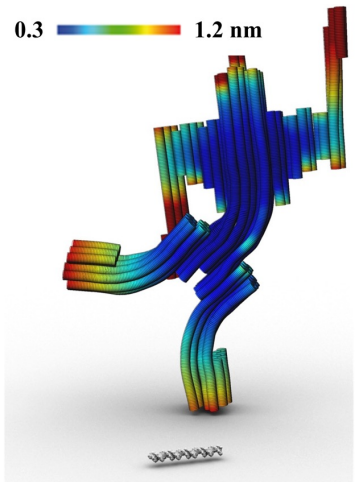

From Castro et al, “A primer to scaffolded DNA origami”, 2011
Also founds in Examples from Cando!

Andersen et al - Self-assembly of a nanoscale DNA box with a controllable lid

Andersen et al - Self-assembly of a nanoscale DNA box with a controllable lid

- Extended the DNA origami method into three dimensions by creating an addressable DNA box 42 X 36 X 36 nm^3 in size that can be opened in the presence of externally supplied DNA ‘keys’.
- Used package at http://cdna.au.dk/software/

Andersen et al - Self-assembly of a nanoscale DNA box with a controllable lid

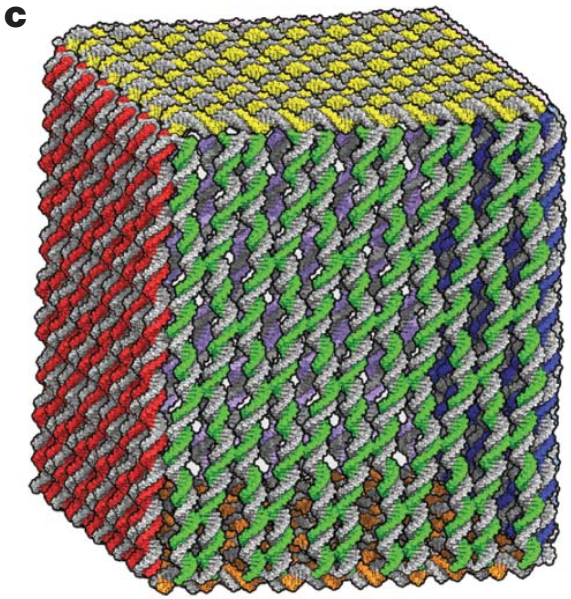

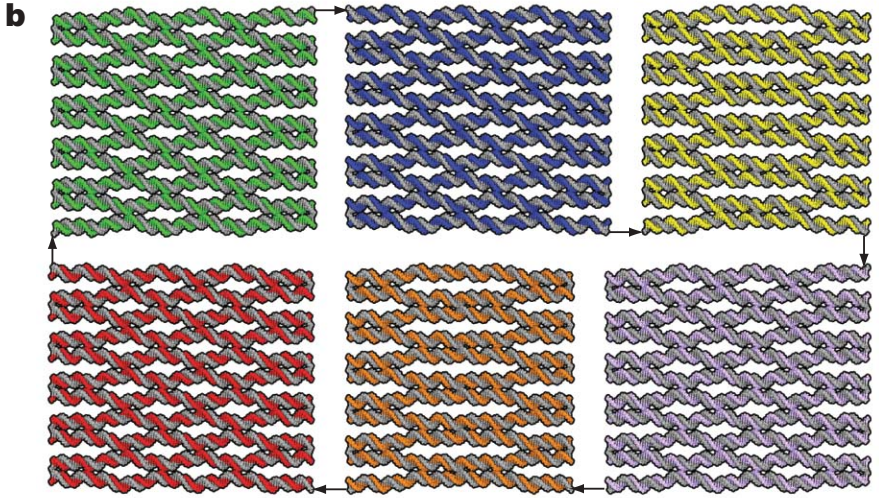

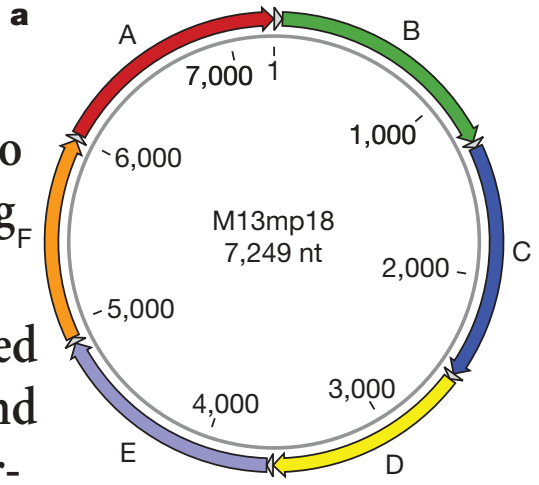

Design of a DNA origami box. **a**, Sequence map of the circular, single-stranded DNA genome of the M13 bacteriophage with regions used to fold the six DNA sheets shown as coloured arrows (A–F). Base numbering starts from a 44-nucleotide spacer region between sheets A and B that contains a stable hairpin structure[9]. Spacers of 33 nucleotides are positioned between each face. **b**, **c**, Molecular models of the six DNA sheets in a flat and cubic higher-order structure, respectively. The six DNA sheets are colour-coded as in **a**.

Andersen et al - Self-assembly of a nanoscale DNA box with a controllable lid

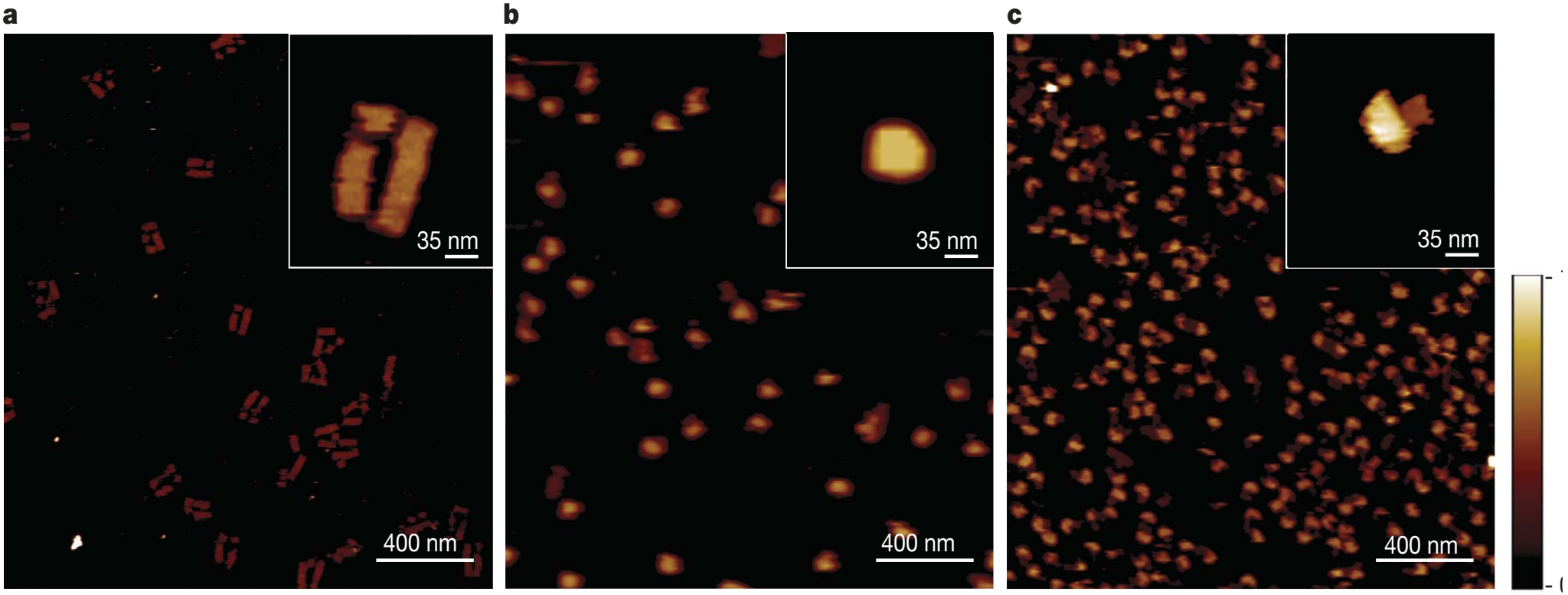

AFM imaging of two- and three-dimensional DNA origami structures. **a**, AFM image of a sample in which the six DNA sheets were folded along the M13 backbone. Inset, magnified view of a preferred arrangement of the six sheets. **b**, AFM image of a sample in which the edges of the DNA sheets were linked to form a box. Inset, magnified view of a box-like particle. **c**, AFM image of a sample in which one lid of the DNA box was left open. Inset, magnified view of a structure in which the lid is protruding from the body of the box. The colour scale shows the height above the surface in the range 0–15 nm.

Andersen et al - Self-assembly of a nanoscale DNA box with a controllable lid

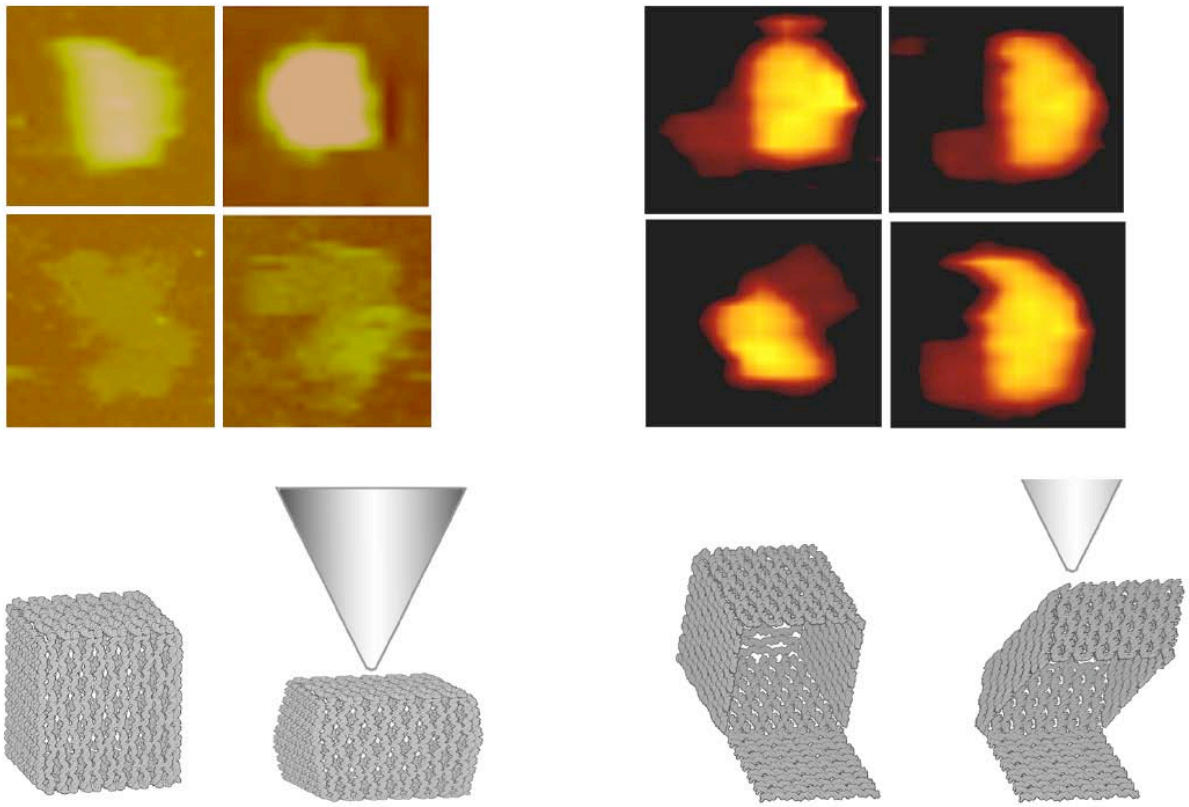

Collapse of box structure during AFM imaging. a, AFM images of the DNA box. Two images on top show box-like dimensions. The two images below show particle-structures that upon AFM imaging changed shape into double- or single-layer DNA sheets. Cartoon below illustrate how the AFM tip might distort the soft and hollow DNA box. **b**, Four representative images of DNA box particles with an open lid. The cartoon below illustrates how the elongated main part of the particle is likely the result of a sideway collapse of main box, while the lid is laying flat on the surface.

Explanation for disparity in height of box between 4-12 nm:
→ Over time structures were observed to collapse from 3D into flat structures

Andersen et al - Self-assembly of a nanoscale DNA box with a controllable lid

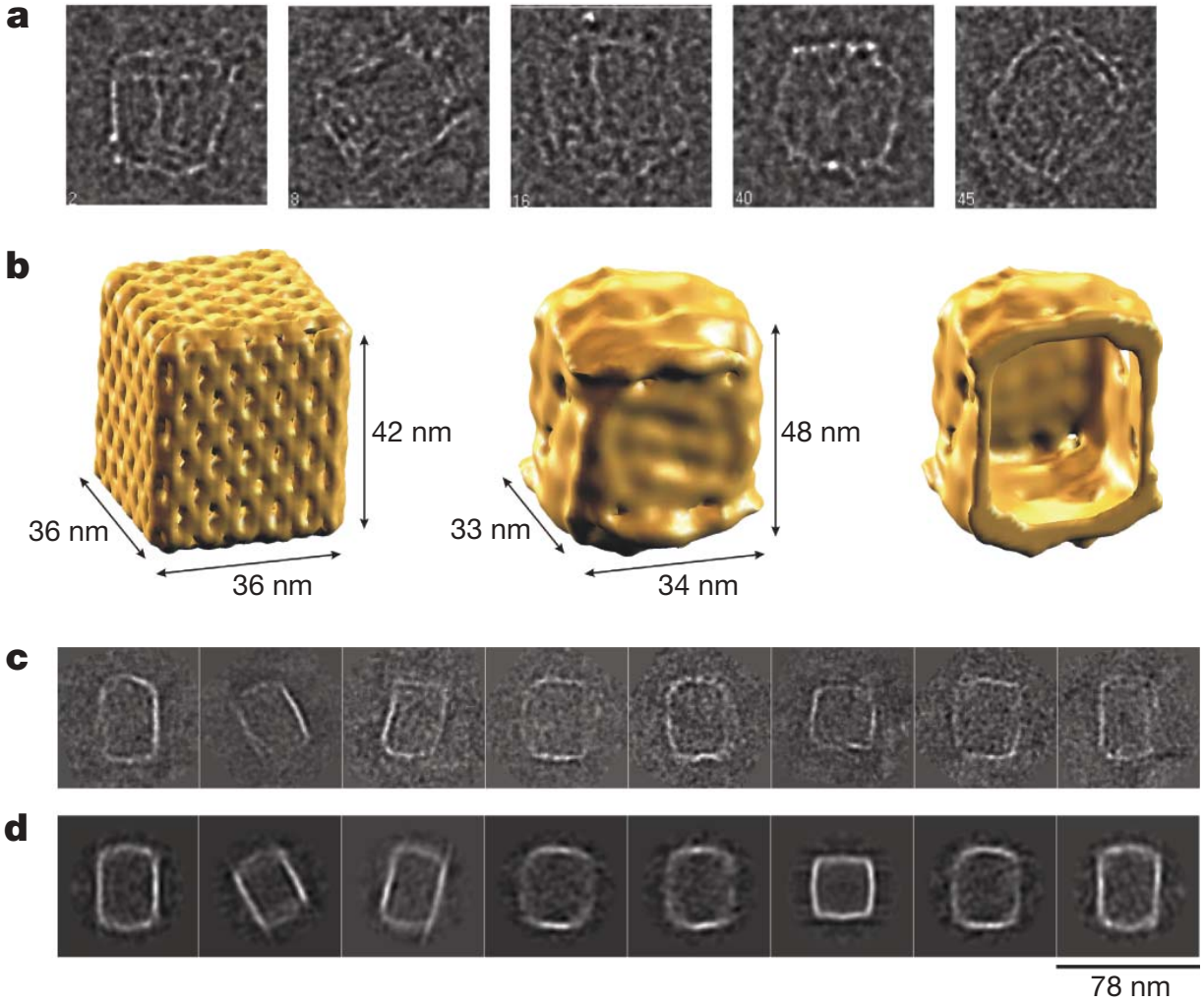

Used cryo-electron microscopy and SAXS for imaging.

Cryo-EM:

- http://www.youtube.com/watch?v=BJKkC0W-6Qk
- http://www.eicn.ucla.edu/cryoem

SAXS:

- http://www.youtube.com/watch?v=2QOsh2vgY2Q
- http://www.stack.nl/~brian/LookingAtNothing_WordPress/wp-content/uploads/2007/08/2dsaxs_annotated_web.mov
- http://www.stack.nl/~brian/LookingAtNothing_WordPress/wp-content/uploads/2007/08/1dsaxs.mov

Characterization of DNA origami box by cryo-EM and small-angle *x*-ray scattering (SAXS). **a**, Single-particle cryo-EM images of box-shaped assemblies. **b**, Single-particle reconstruction of the DNA box applying D2 symmetry. Left, theoretical model. Middle, surface representation of the cryo-EM map. Right, cut-open view showing the interior cavity of the cryo-EM map. **c**, **d**, Comparison of the class averages of the DNA boxes (**c**) with the corresponding two-dimensional re-projections corresponding fits from different approaches: red dashed curve, fit using the theoretical atomic coordinates for the box; blue dotted curve, typical Debye background[25] for modelling the excess oligonucleotides; dash–dot curve, fit using the theoretical atomic coordinates for the box with the Debye background added; solid curve, fit using a semi-analytical model for a box with three different side lengths with the Debye background added. $I(q)$, SAXS intensity; q, momentum transfer modulus (Methods). Inset, semi-

Andersen et al - Self-assembly of a nanoscale DNA box with a controllable lid

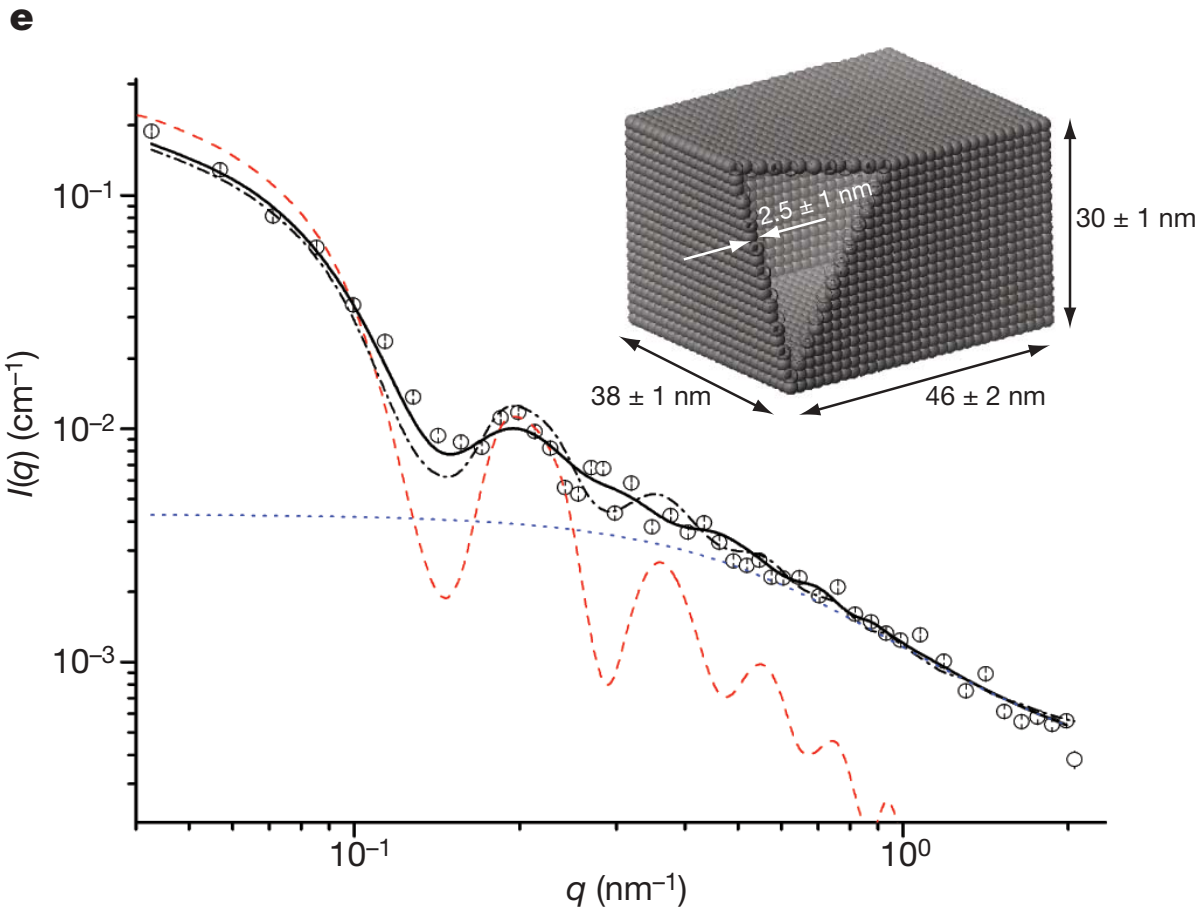

Used cryo-electron microscopy and SAXS for imaging.

Characterization of DNA origami box by cryo-EM and small-angle x-ray scattering (SAXS). **a**, Single-particle cryo-EM images of box-shaped assemblies. **b**, Single-particle reconstruction of the DNA box applying D2 symmetry. Left, theoretical model. Middle, surface representation of the cryo-EM map. Right, cut-open view showing the interior cavity of the cryo-EM map. **c**, **d**, Comparison of the class averages of the DNA boxes (**c**) with the corresponding two-dimensional re-projections of the 3D cryo-EM map (**d**). **e**, Experimental SAXS data (circles) with corresponding fits from different approaches: red dashed curve, fit using the theoretical atomic coordinates for the box; blue dotted curve, typical Debye background[25] for modelling the excess oligonucleotides; dash–dot curve, fit using the theoretical atomic coordinates for the box with the Debye background added; solid curve, fit using a semi-analytical model for a box with three different side lengths with the Debye background added. $I(q)$, SAXS intensity; q, momentum transfer modulus (Methods). Inset, semi-analytical box model with the estimated side lengths and wall thickness.

Andersen et al - Self-assembly of a nanoscale DNA box with a controllable lid

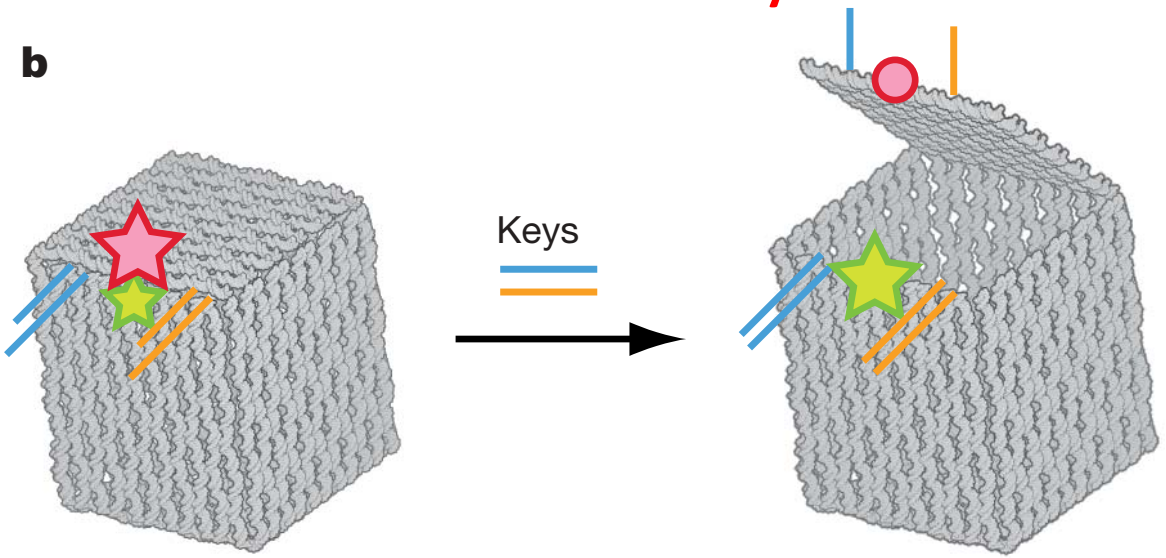

Programmed opening of the box lid. **a**, **b**, Illustrations of the unlinked faces of the box (**a**) and the controlled opening of the box lid (**b**). The emission from the Cy5 and Cy3 fluorophores are marked with red and green stars, respectively. Loss of emission from Cy5 is denoted by a red circle and the independent lock–key systems are indicated in blue and orange.

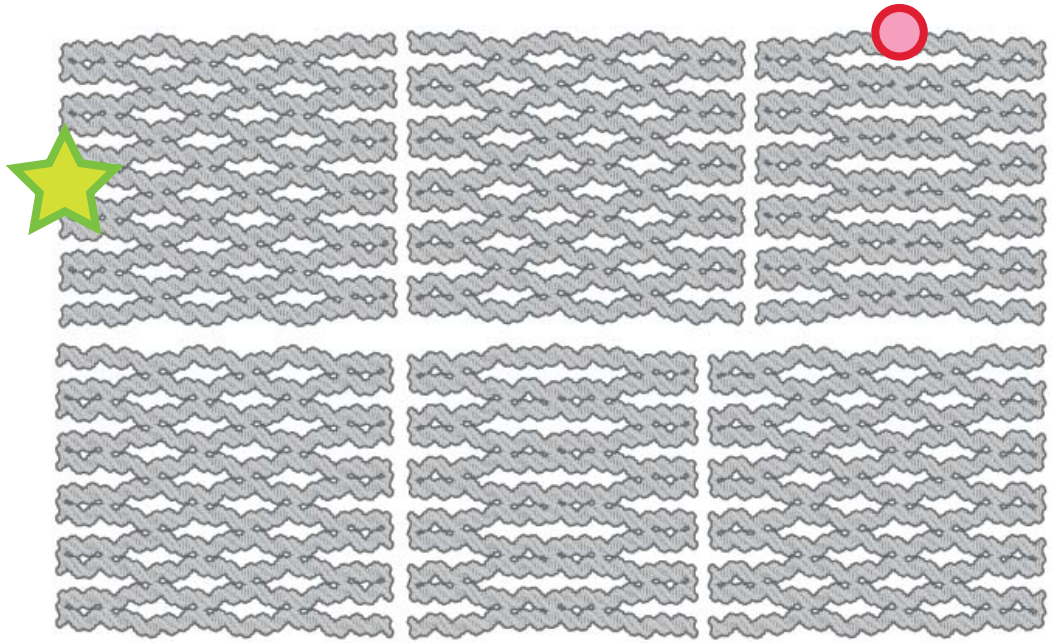

Lock: DNA duplexes attached to both faces B,D (lid and front lateral) with a toehold on the helix attached to B.

Key: signaling DNA sequence that displaces the lid's part of the lock.

Andersen et al - Self-assembly of a nanoscale DNA box with a controllable lid

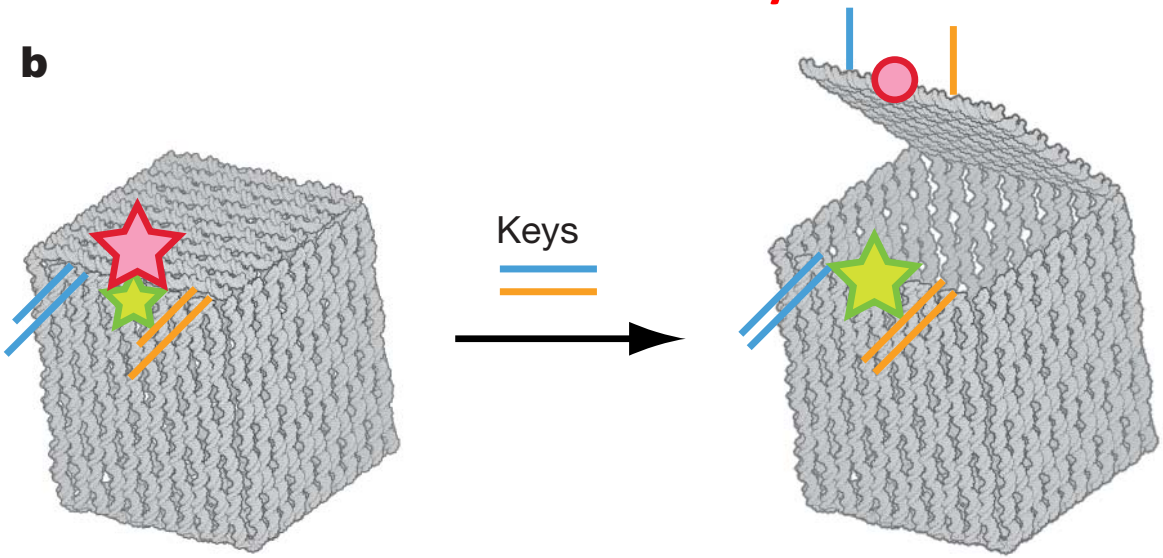

Programmed opening of the box lid. **a**, **b**, Illustrations of the unlinked faces of the box (**a**) and the controlled opening of the box lid (**b**). The emission from the Cy5 and Cy3 fluorophores are marked with red and green stars, respectively. Loss of emission from Cy5 is denoted by a red circle and the independent lock–key systems are indicated in blue and orange.

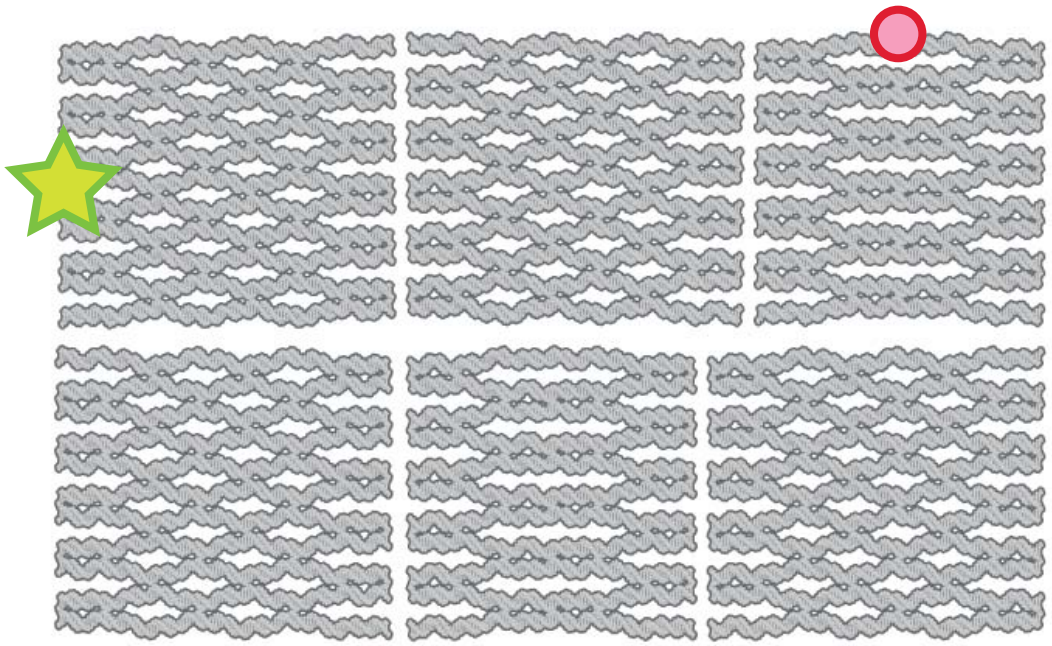

FRET using Cy3 and Cy5:

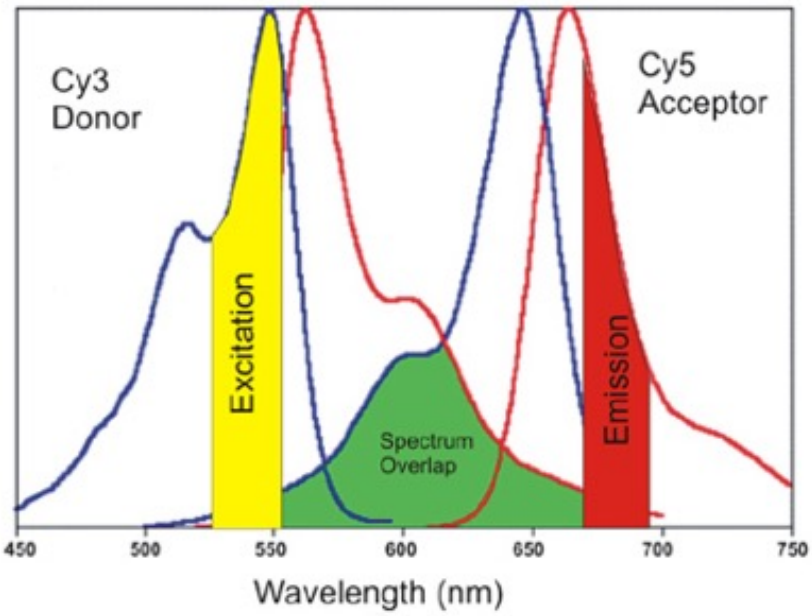

Source: Held, P. (2006).
An Introduction to Fluorescence Resonance Energy Transfer (FRET) Technology and its Application in Bioscience.
Retrieved from
http://www.biotek.com/resources/articles/fluorescence-resonance-energy-transfer.html

Dye	Absorbance Max	Emission Max
Cy3	550 nm	570 nm
Cy5	649 nm	670 nm

Source: Wikipedia.org/wiki/Cyanine

Andersen et al - Self-assembly of a nanoscale DNA box with a controllable lid

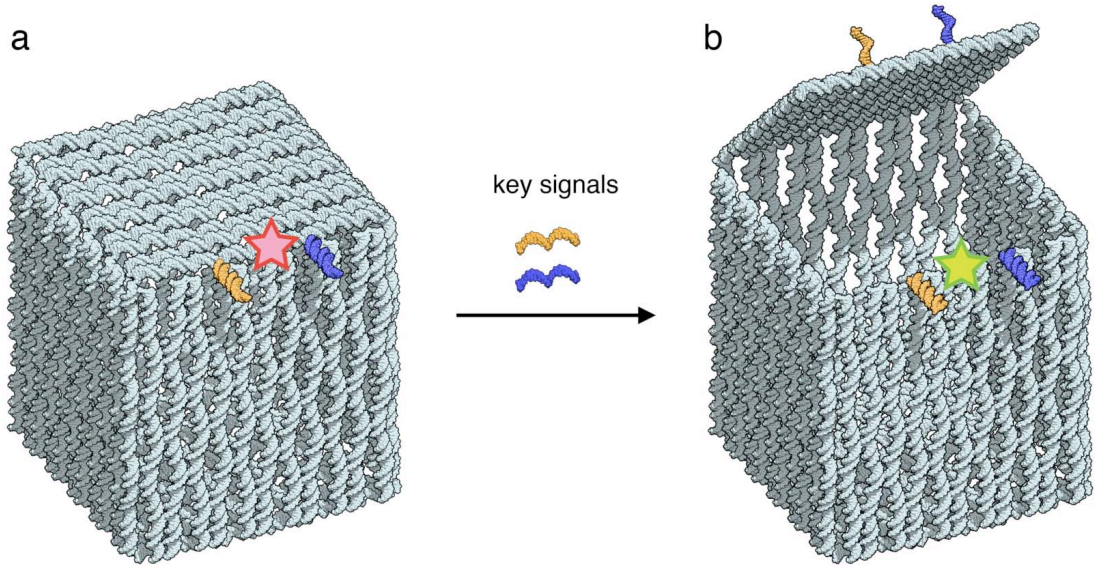

Mechanism for signal-induced opening of the DNA box. a, An atomic model of the DNA box held closed by "locks" (orange and blue) that are double helices formed by two short strands protruding from the lid and the main box, respectively. Each "lock" has a small sticky-end where a "key" sequence signal can bind and open the "lock" by strand displacement. If both "locks" are opened the lid of the box is effectively opened (b). The reporter system for detecting the lid opening is a Cy3-Cy5 FRET system. In the closed state the two fluorophores are in close proximity resulting in FRET emission from Cy5 (red star) when Cy3 is excited. In the open state the two flurophores are far apart and excitation of Cy3 only results in emission from Cy3 (green star).

Methods

- SARSE program for creating realistic 3D models, which facilitated the design of the 3D edge-to-edge staple strand crossovers
- Deposited the samples on a mica surface and performed the AFM imaging in a buffer solution.
- Cryo-EM. The sample was adsorbed on carbon film and plunge-frozen in liquid ethane.
- SAXS. Collected data using a high-resolution set-up of a laboratory-based small-angle x-ray scattering.
- FRET. To detect the opening process, we functionalized the box with Cy3 and Cy5 fluorophores and a lock–key system.

Andersen, E. S., Dong, M., Nielsen, M. M., Jahn, K., Subramani, R., Mamdouh, W., Golas, M. M., et al. (2009). Self-assembly of a nanoscale DNA box with a controllable lid. *Nature*, *459*(7243), 73–76. doi:10.1038/nature07971

Douglas et al - Self-assembly of DNA into nanoscale three-dimensional shapes

Douglas et al - Self-assembly of DNA into nanoscale three-dimensional shapes

- Extended Rothmund's method to 3D pleated (folded) layers of helices constrained into a honeycomb lattice
- Approximated 6 shapes

Douglas et al - Self-assembly of DNA into nanoscale three-dimensional shapes

d

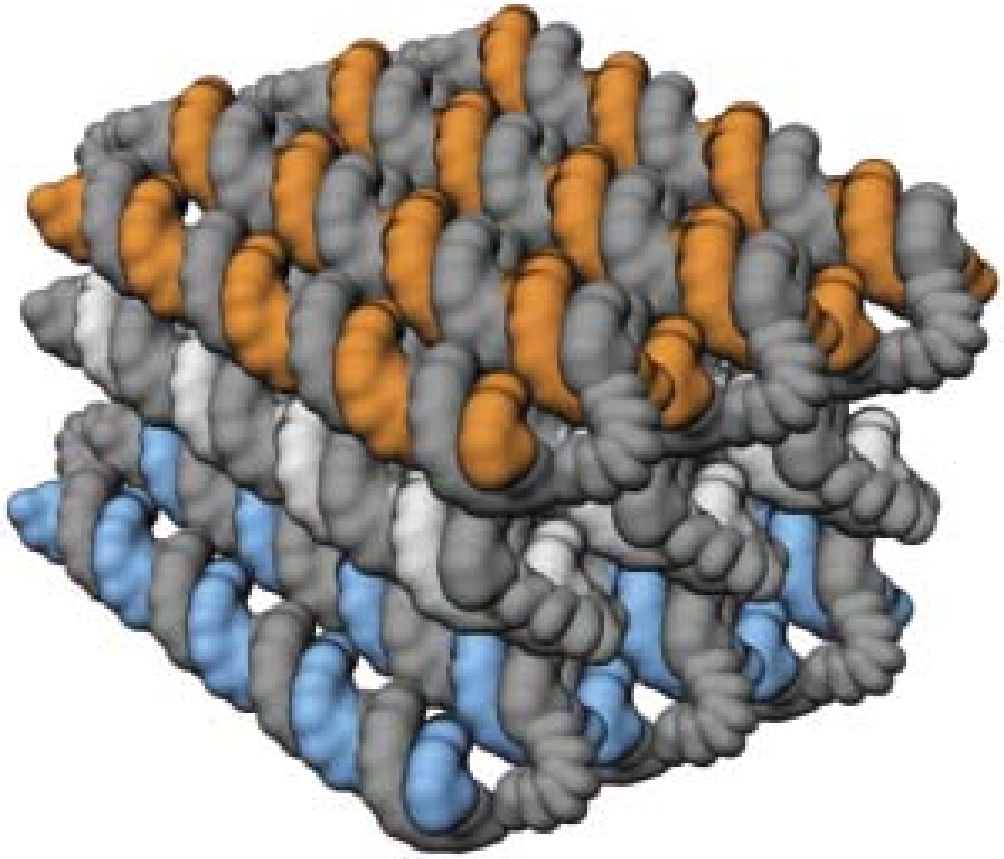

Honeycomb lattice block

Complementary staple strands wind in an antiparallel direction around the scaffold strands to assemble B-form double helices

Douglas et al - Self-assembly of DNA into nanoscale three-dimensional shapes

Douglas et al - Self-assembly of DNA into nanoscale three-dimensional shapes

b, Cylinder model of a half-rolled conceptual intermediate. Cylinders represent double helices, with loops of unpaired scaffold strand linking the ends of adjacent helices. **c**, Cylinder model of folded target shape. The honeycomb arrangement of parallel helices is shown in cross-sectional slices (i–iii) parallel to the *x*–*y* plane, spaced apart at seven base-pair intervals that repeat every 21 base pairs. All potential staple crossovers are shown for each cross-section. **d**, Atomistic DNA model of shape from **c**.

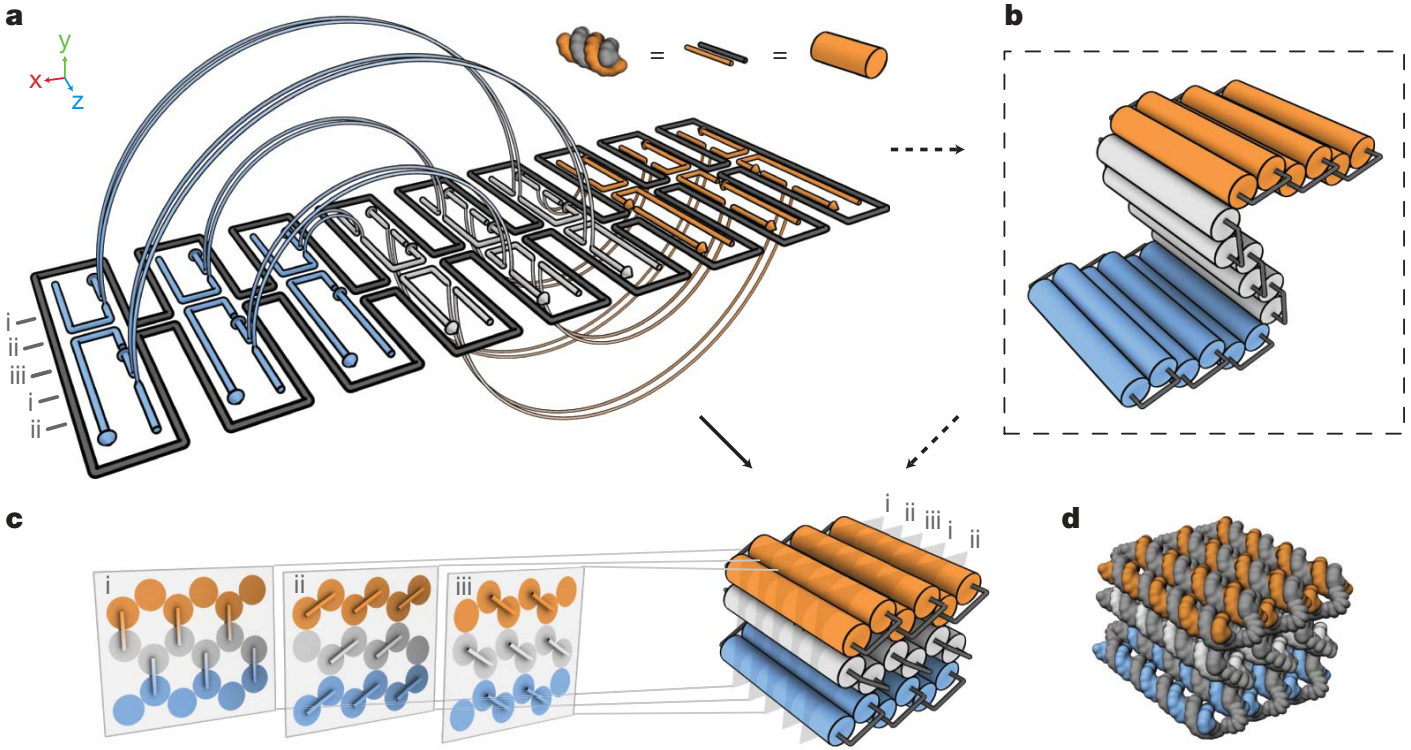

Assembly of a target three-dimensional shape using the honeycomb-pleat-based strategy described here can be conceptualized as laying down the scaffold strand into an array of antiparallel helices (Fig. 1a) where helix *m+1* has a preferred attachment angle to helix *m* of ±120 degrees with respect to the attachment of helix *m−1* to helix *m* (Fig. 1b, c); this angle is determined by the relative register along the helical axes of the Holliday-junction crossovers that connect helix *m+1* to helix *m* versus those that connect helix *m−1 to* helix *m*.

Douglas et al - Self-assembly of DNA into nanoscale three-dimensional shapes

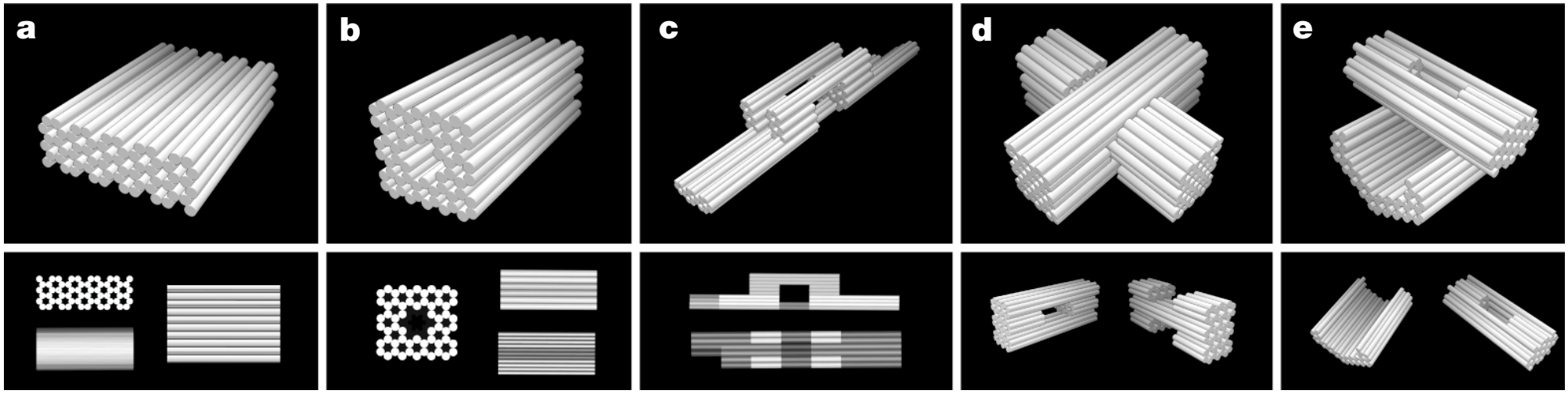

monolith | square-nut | railed bridge | stacked cross | slotted cross

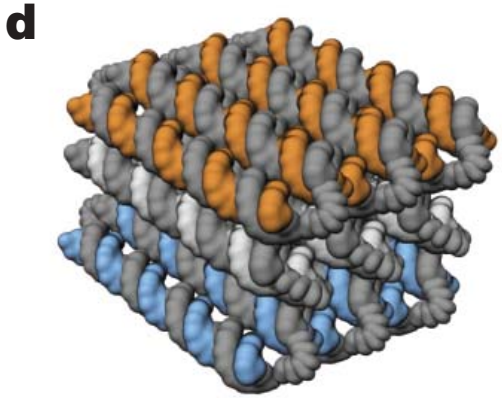

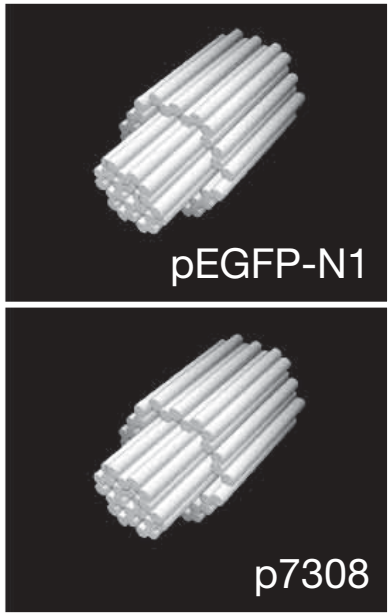

genie bottle

Douglas et al - Self-assembly of DNA into nanoscale three-dimensional shapes

Douglas et al - Self-assembly of DNA into nanoscale three-dimensional shapes

Ex: square-nut

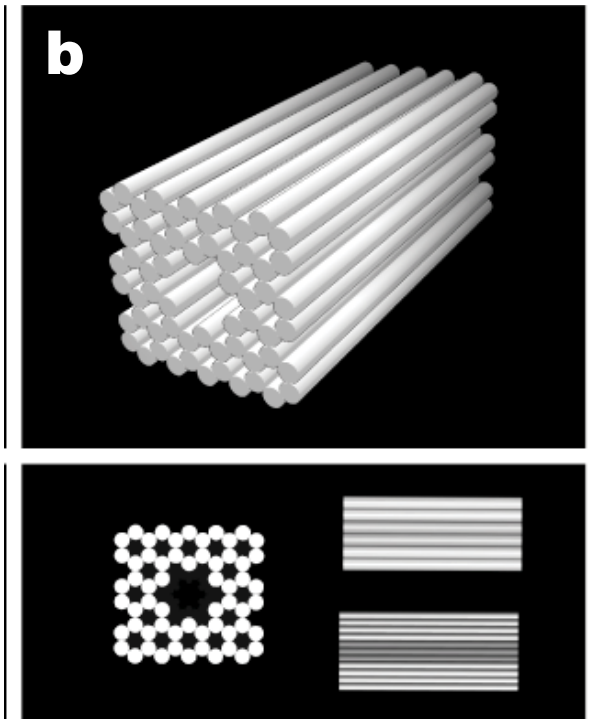

Honeycomb Lattice:

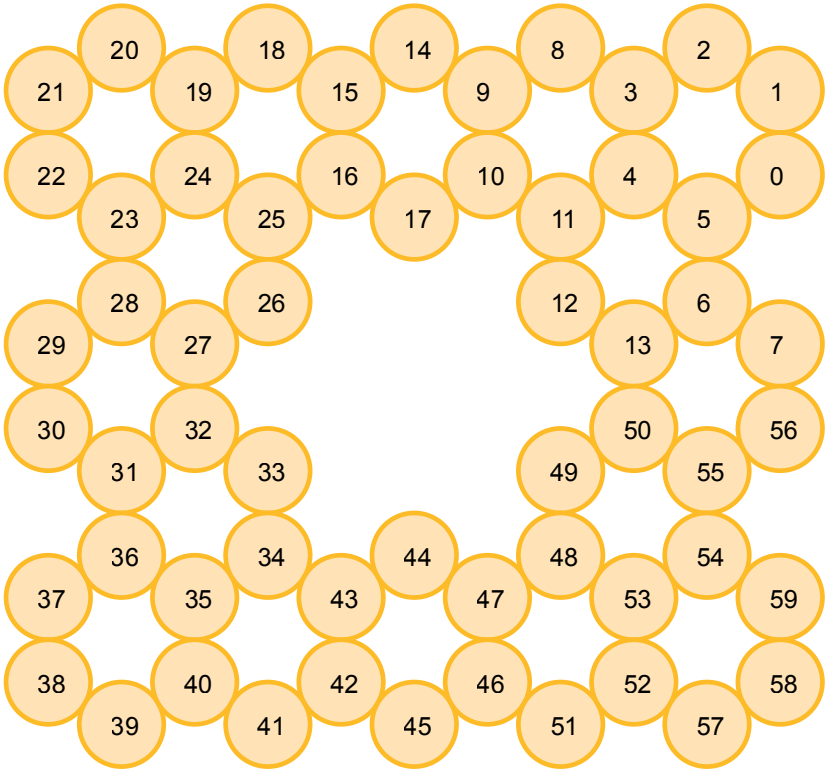

Douglas et al - Self-assembly of DNA into nanoscale three-dimensional shapes

Douglas et al - Self-assembly of DNA into nanoscale three-dimensional shapes

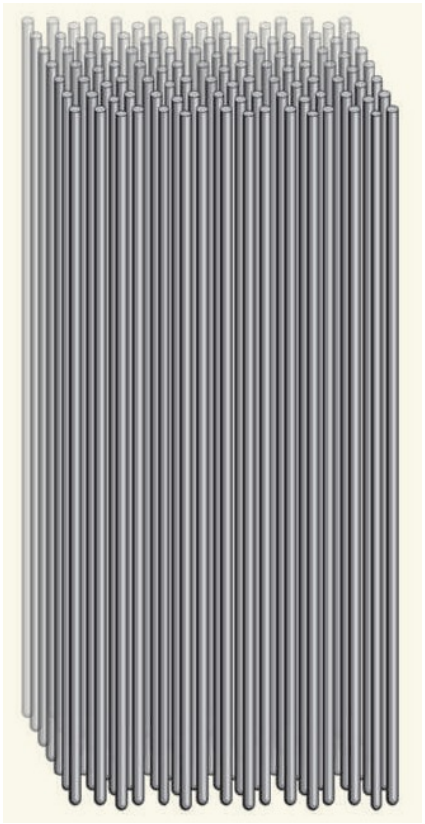

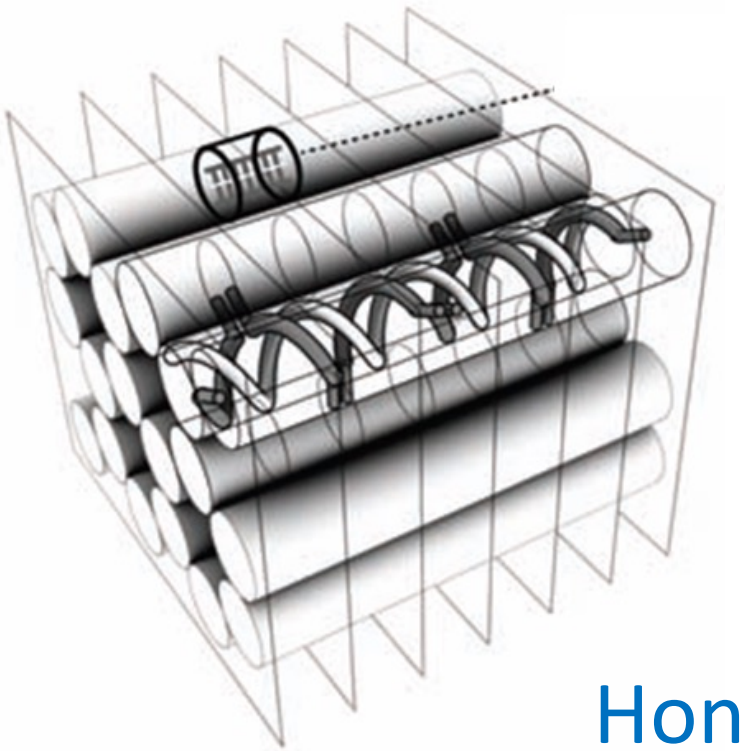

Honeycomb Lattice:

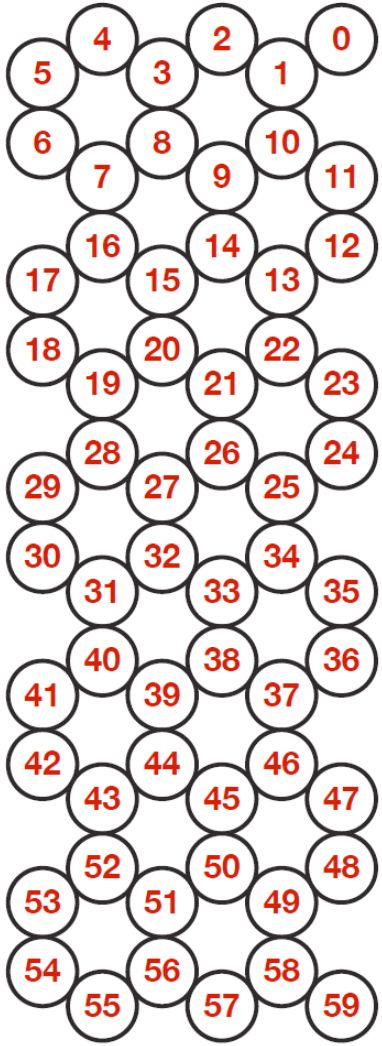

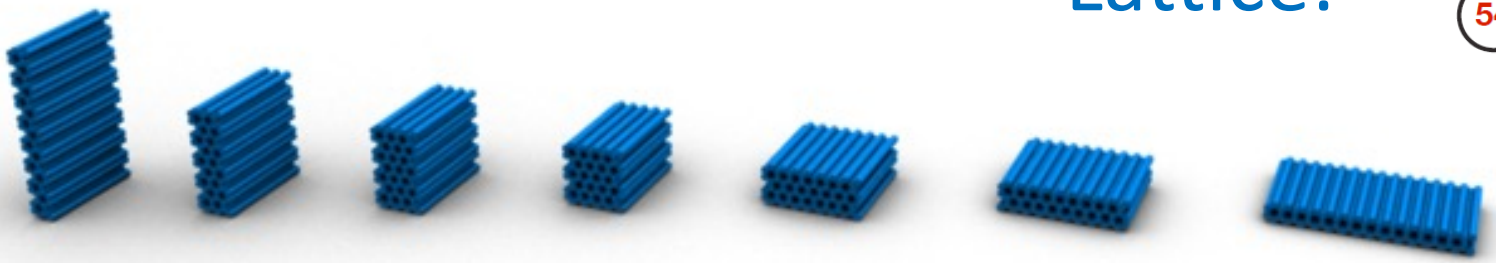

Douglas et al - Self-assembly of DNA into nanoscale three-dimensional shapes

Douglas et al - Self-assembly of DNA into nanoscale three-dimensional shapes

Design Rules for the Honeycomb Lattice

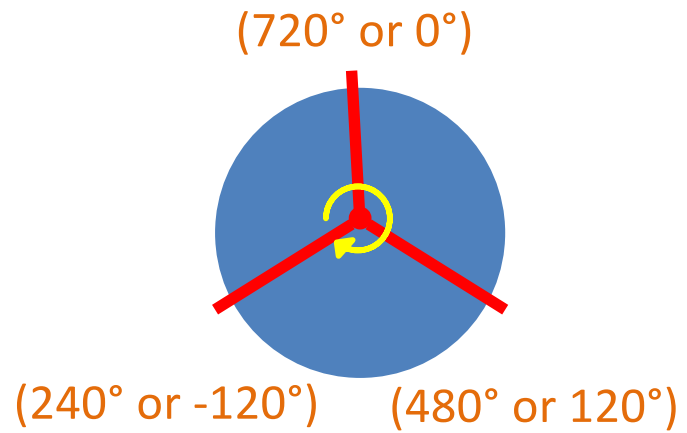

- Potential crossovers every 7 bases
  - 7 bases = ⅔rd turns (240° or -120°)
  - 14 bases = 1 ⅓rd turns (480° or 120°)
  - 21 bases = 2 turns (720° or 0°)
- Entire origami made up of 7 base cylinder
- Scaffold crosses over at position 2 or 5
- We make staple crossover at every potential crossover point
  - Except when the scaffold crossover is 5 bases away
  - Maintains uniform cross over density
- Cut staples such that length = (18,49)
  - Mean = (30, 42)

Douglas et al - Self-assembly of DNA into nanoscale three-dimensional shapes

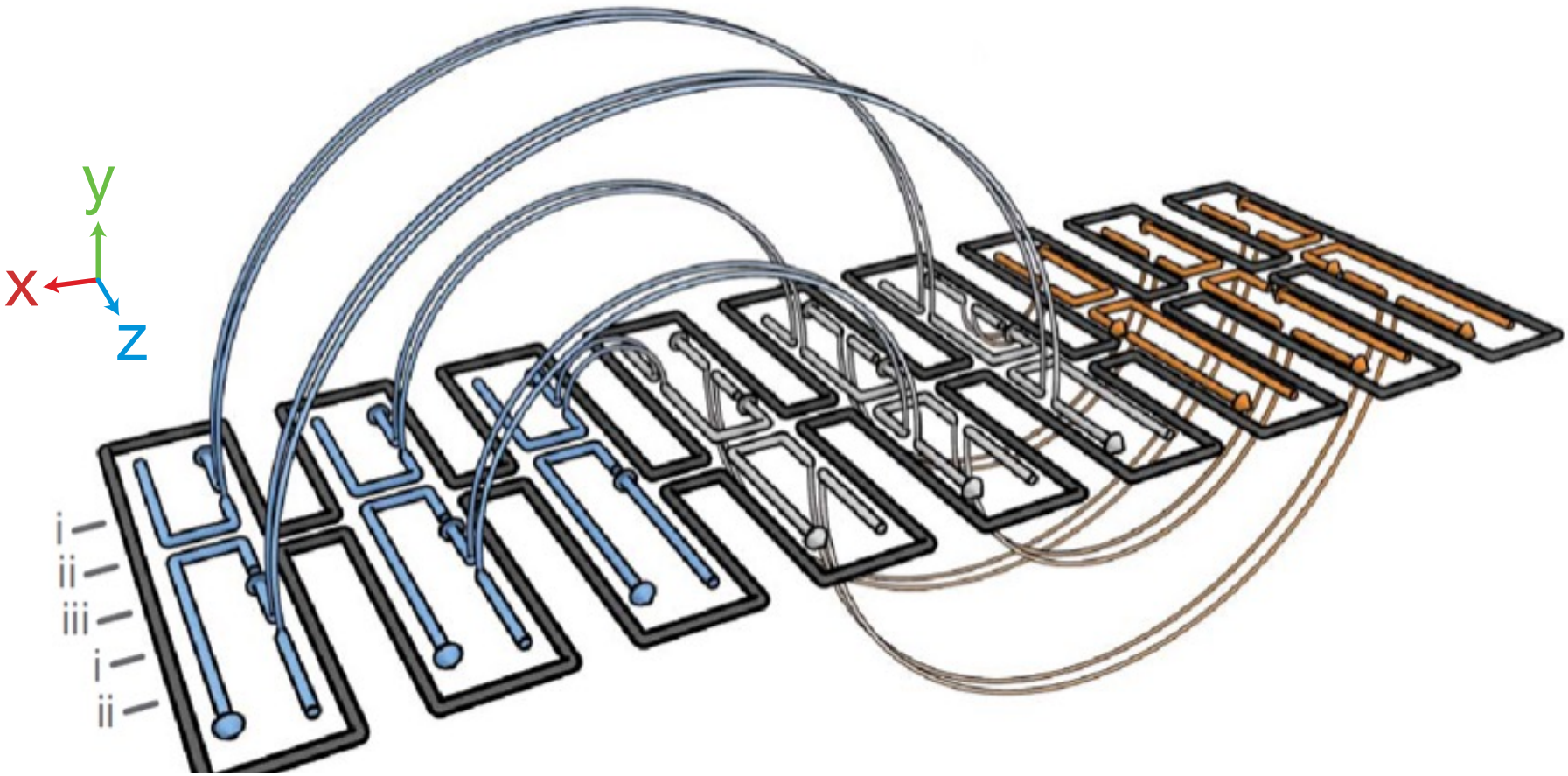

Design of three-dimensional DNA origami. **a**, Double helices comprised of scaffold (grey) and staple strands (orange, white, blue) run parallel to the z-axis to form an unrolled two-dimensional schematic of the target shape. Phosphate linkages form crossovers between adjacent helices, with staple crossovers bridging different layers shown as semicircular arcs.

Douglas et al - Self-assembly of DNA into nanoscale three-dimensional shapes

Crossover Rules:

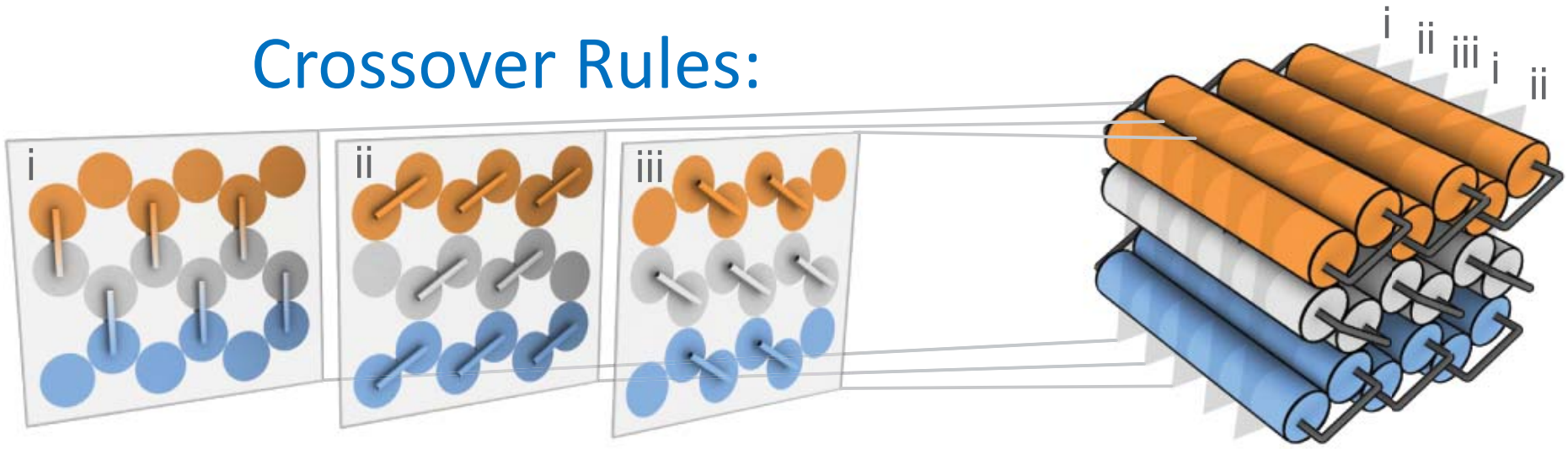

Locations of Crossovers between adjacent staple helices:

- **Are restricted to intersections between the block and every third layer of a stack of planes orthogonal to the helical axes.**
- **Spaced apart at intervals of seven base pairs or two-thirds of a turn.**

Douglas et al - Self-assembly of DNA into nanoscale three-dimensional shapes

Design Examples: Monolith

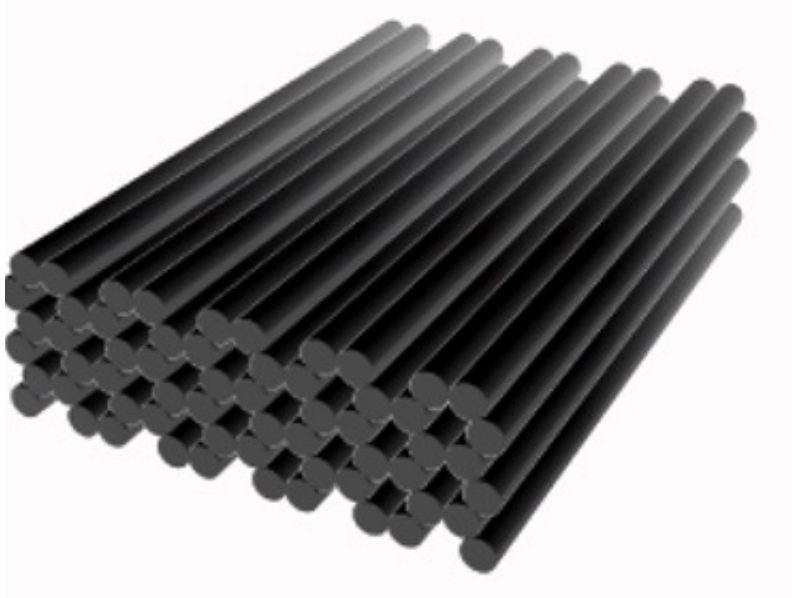

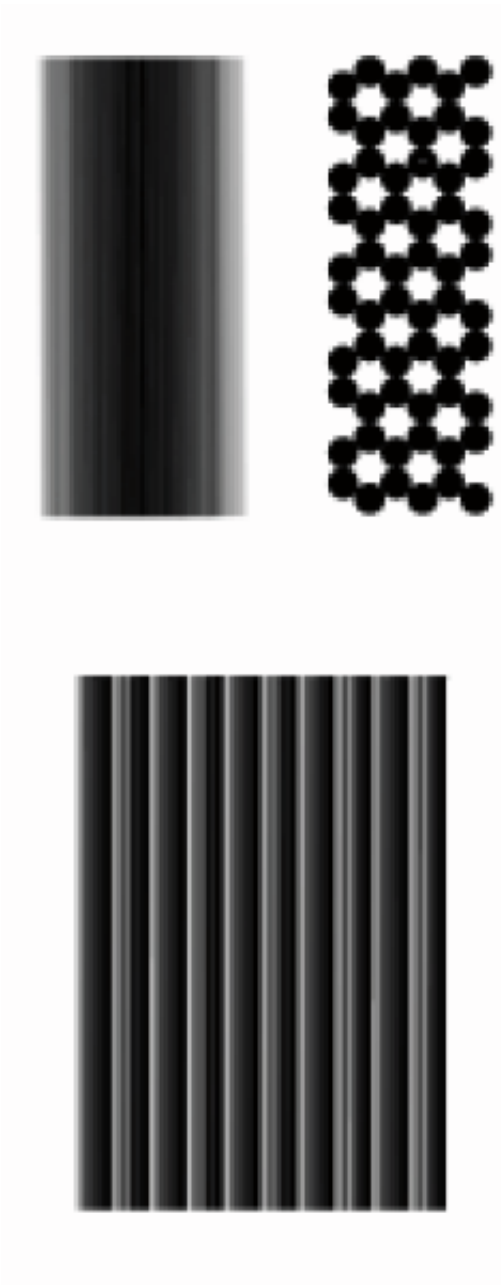

Douglas et al - Self-assembly of DNA into nanoscale three-dimensional shapes

Design Example: Square Nut

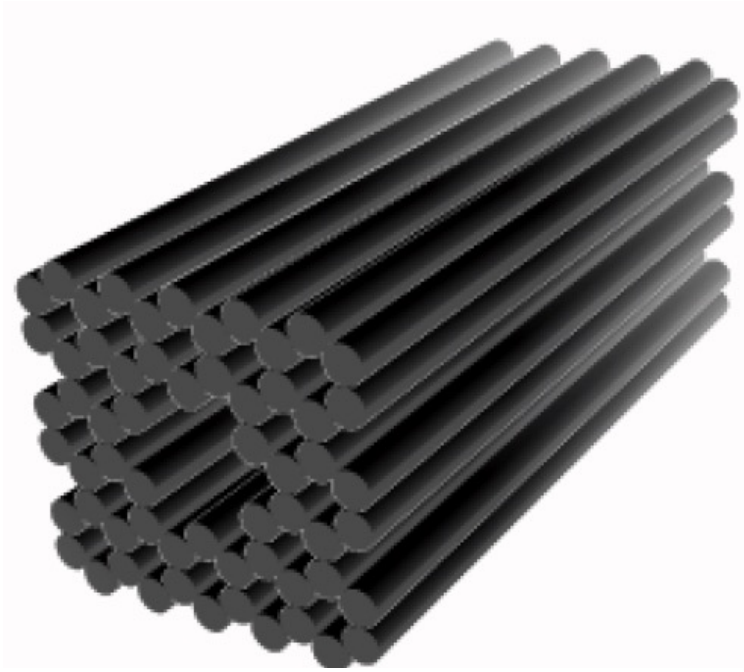

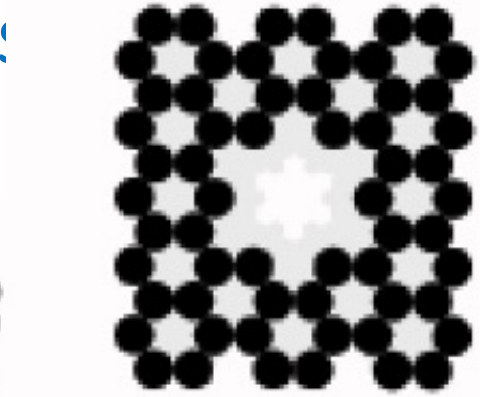

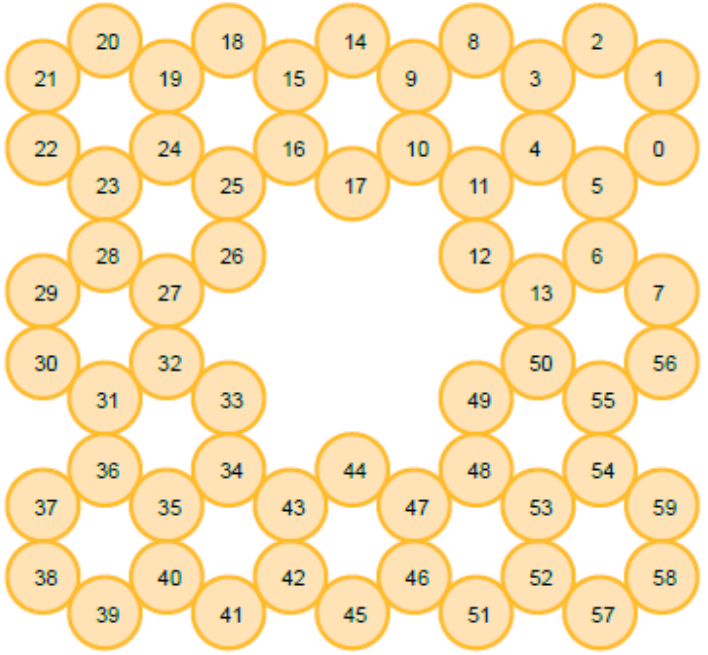

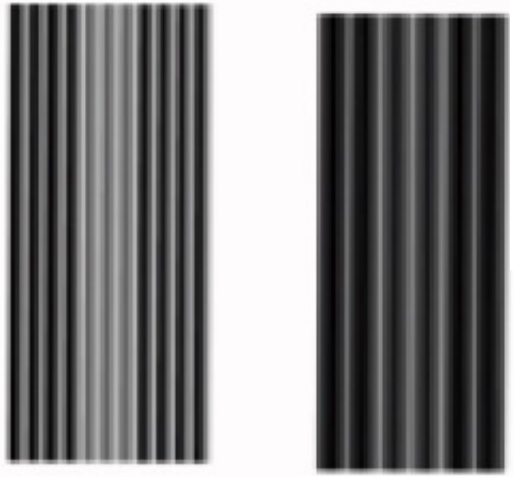

Douglas et al - Self-assembly of DNA into nanoscale three-dimensional shapes

Design Examples:
Slotted Cross

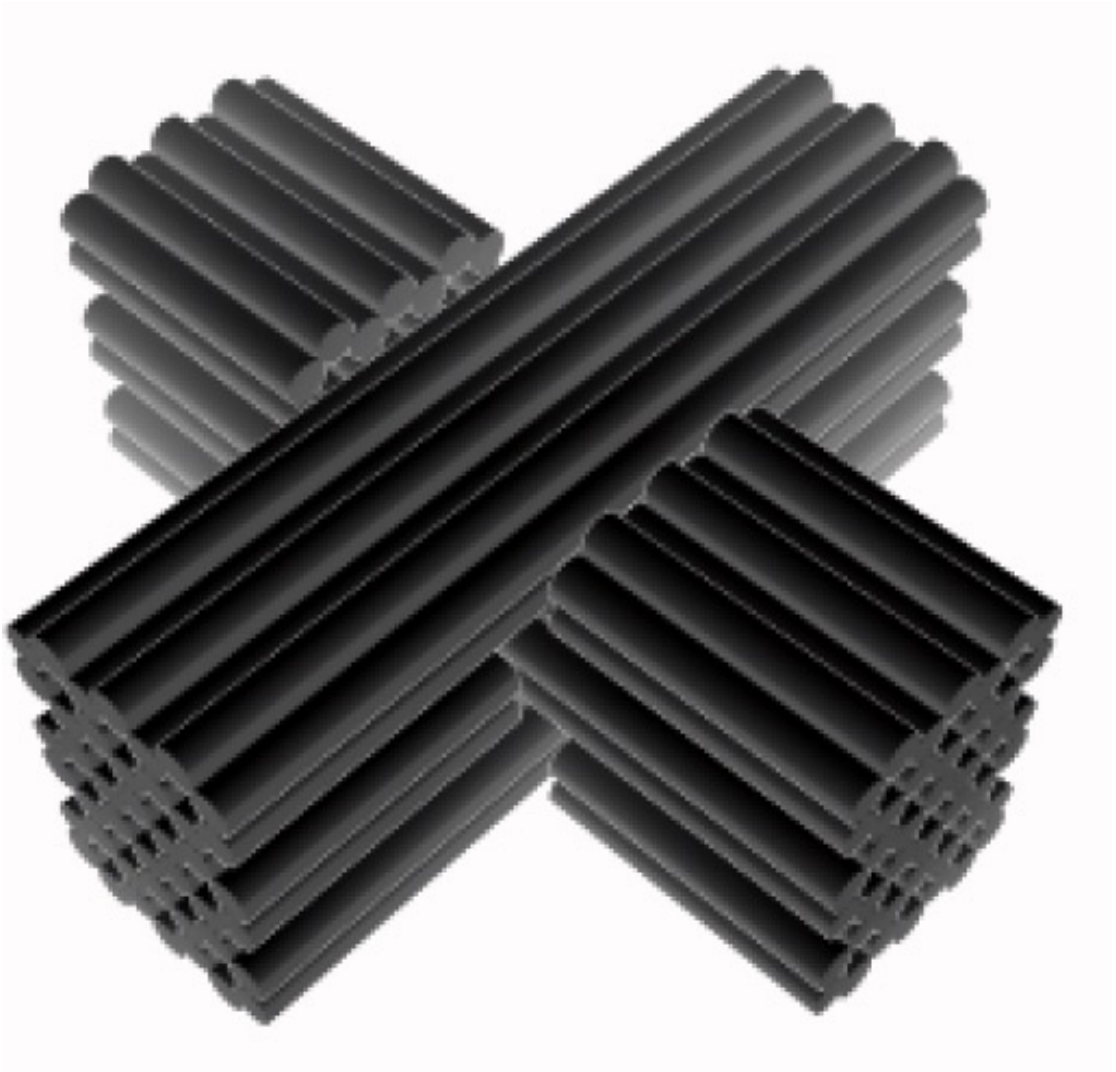

Douglas et al - Self-assembly of DNA into nanoscale three-dimensional shapes

Design Examples:

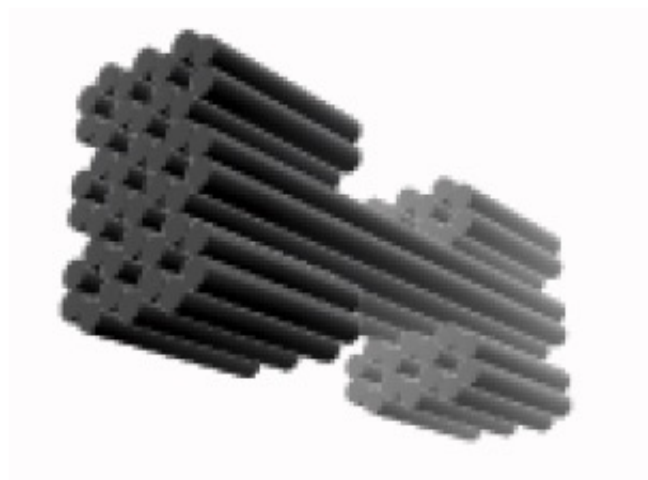

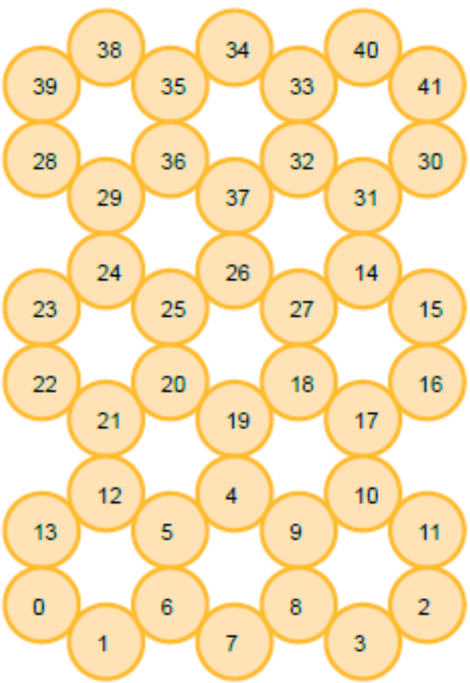

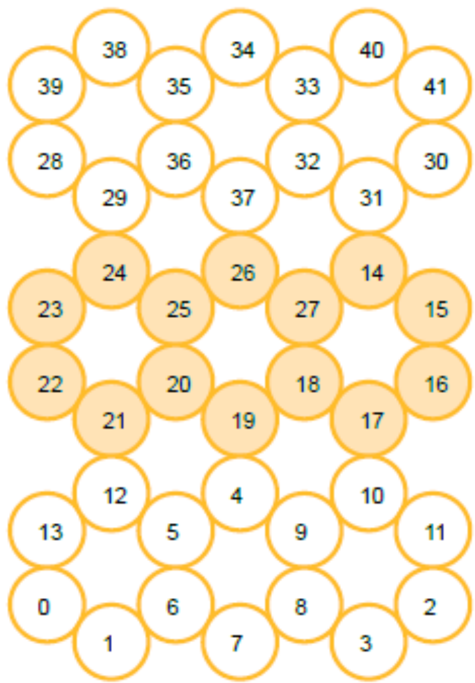

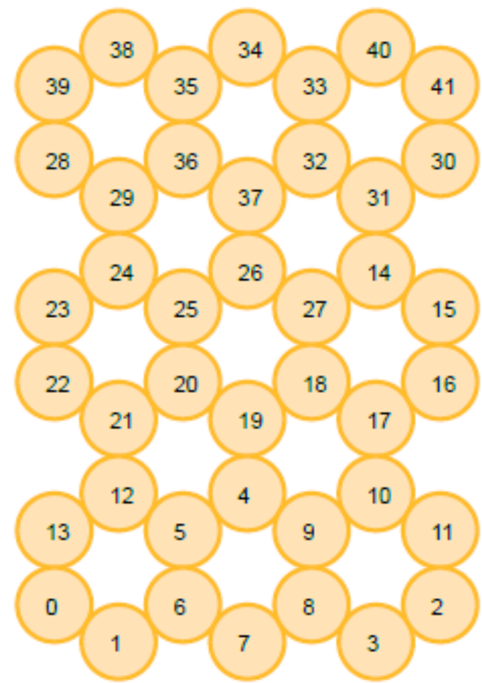

Douglas et al - Self-assembly of DNA into nanoscale three-dimensional shapes

Douglas et al - Self-assembly of DNA into nanoscale three-dimensional shapes

Design Examples:
Slotted Cross

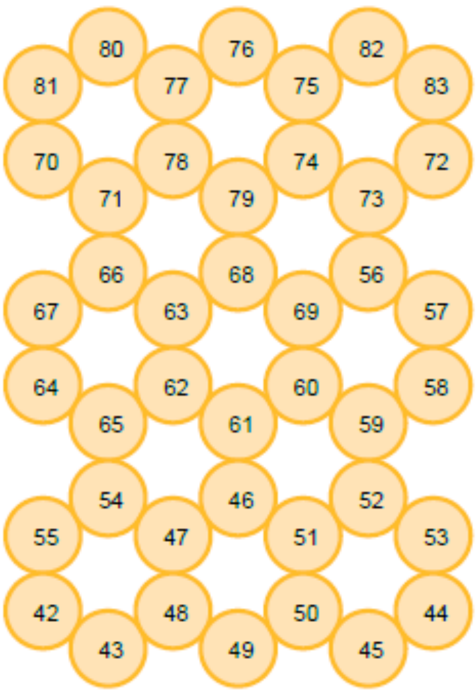

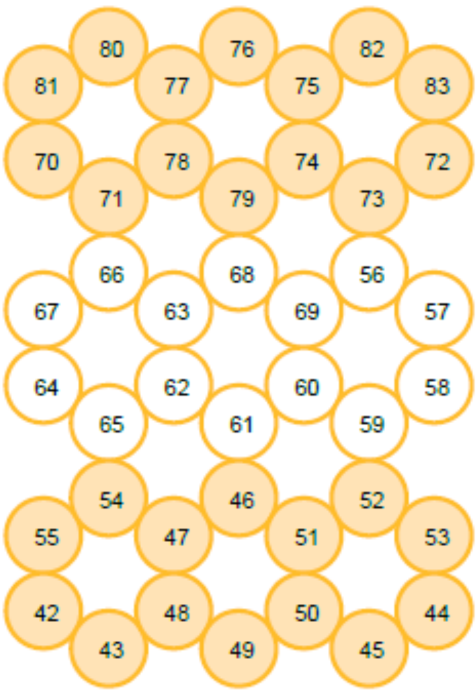

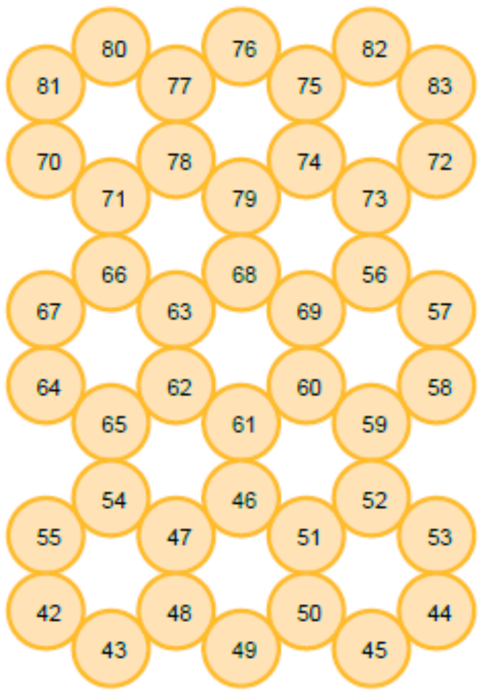

Douglas et al - Self-assembly of DNA into nanoscale three-dimensional shapes

Design Examples: Slotted Cross

Douglas et al - Self-assembly of DNA into nanoscale three-dimensional shapes

Alternative: Square Lattice:

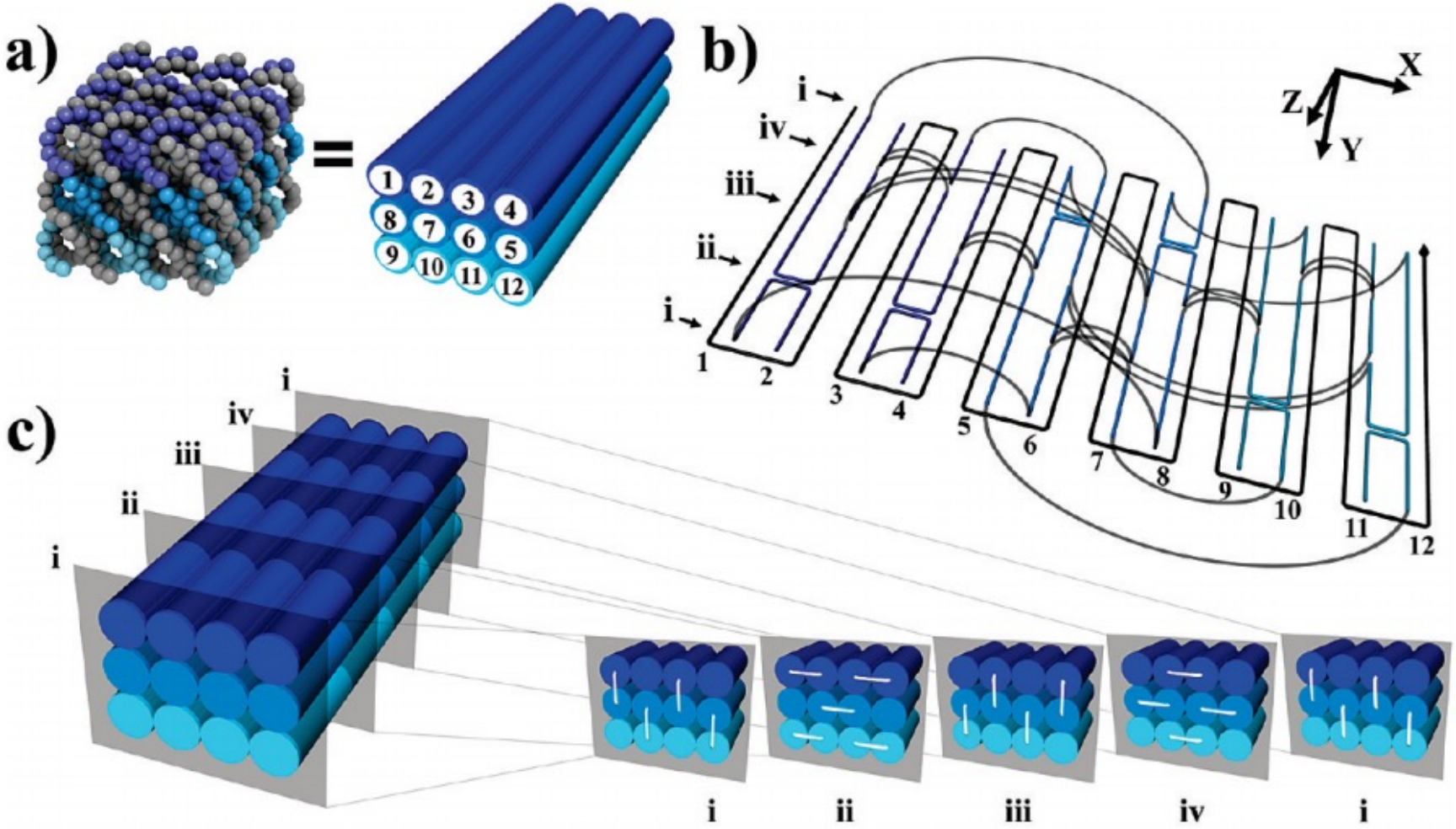

Ke, JACS 2009

Douglas et al - Self-assembly of DNA into nanoscale three-dimensional shapes

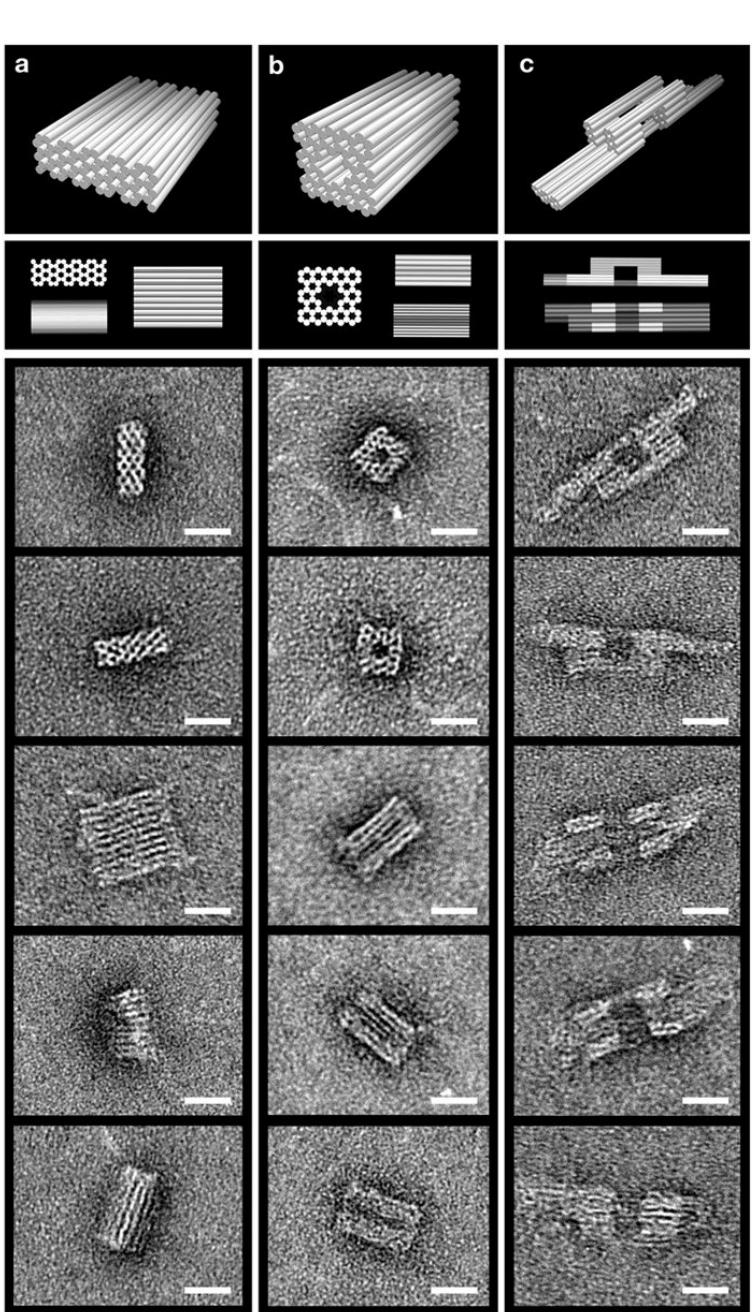

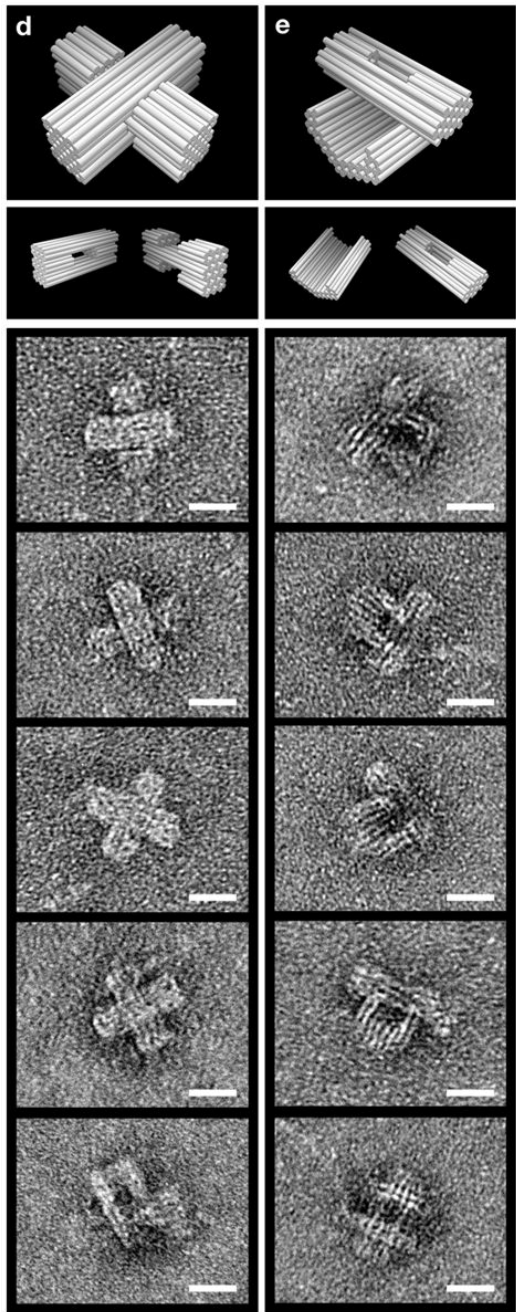

Figure 2 | Three-dimensional DNA origami shapes. The first and second rows show perspective and projection views of cylinder models, with each cylinder representing a DNA double helix. **a**, Monolith. **b**, Square nut. **c**, Railed bridge. **d**, Slotted cross. **e**, Stacked cross. Rows three to seven show transmission electron microscope (TEM) micrographs of typical particles. For imaging, samples were adsorbed (5 min) onto glow-discharged grids pre-treated with 0.5 M $MgCl_2$, stained with 2% uranyl formate, 25 mM NaOH (1 min), and visualized with an FEI Tecnai T12 BioTWIN at 120 kV.

Douglas et al - Self-assembly of DNA into nanoscale three-dimensional shapes

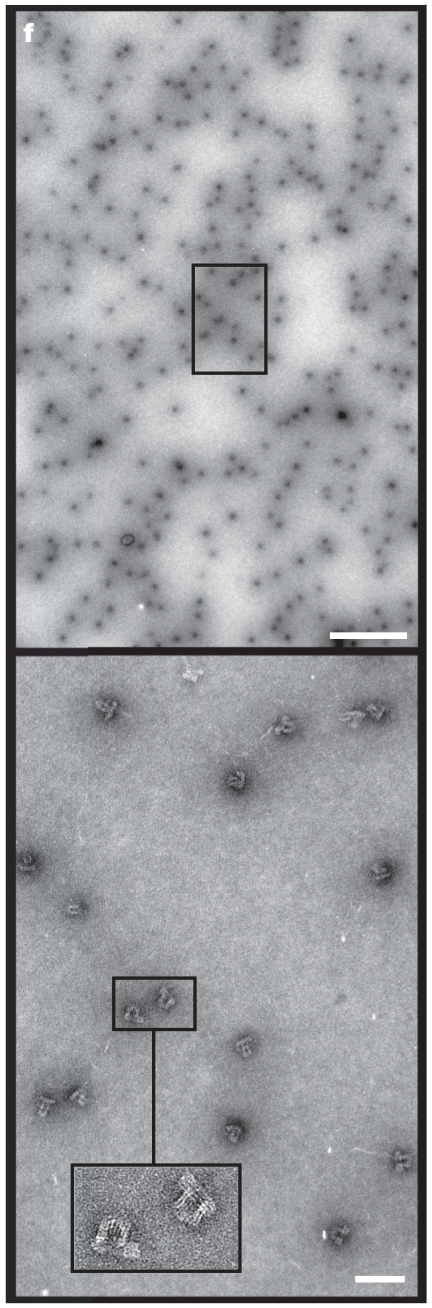

f, Top, field of homogeneous and monodisperse stacked-cross particles.

Bottom, expanded view of boxed area from above.

Douglas et al - Self-assembly of DNA into nanoscale three-dimensional shapes

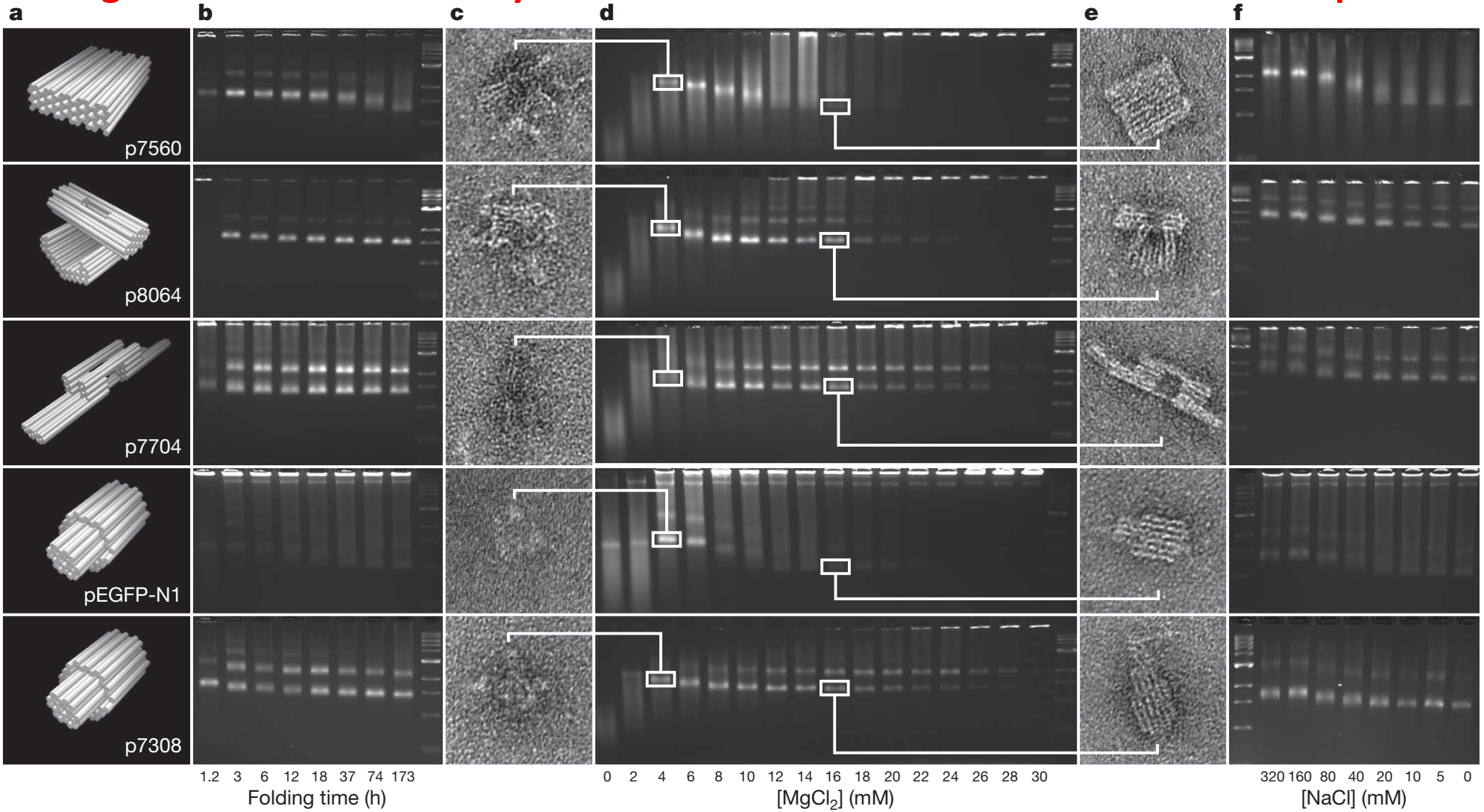

Gel and TEM analysis of folding conditions for three-dimensional DNA origami. **a**, Cylinder models of shapes: monolith, stacked cross, railed bridge, and two versions of genie bottle, with corresponding scaffold sequences. Labels indicate the source of scaffold used for folding the object (for example, p7560 is an M13-based vector of length 7,560 bases). **b**, Shapes were folded in 5 mM Tris + 1 mM EDTA (pH 7.9 at 20 °C) and 16 mM $MgCl_2$ and analysed by gel electrophoresis (2% agarose, 45 mM Tris borate + 1 mM EDTA (pH 8.3 at 20 °C), 11 mM $MgCl_2$) using different thermal-annealing ramps. For the 1.2 h ramp, the temperature was lowered from 95 °C to 20 °C at a rate of 1.6 min $°C^{-1}$. For the 3 h, 6 h, 12 h, 18 h, 37 h, 74 h and 173 h ramps, the temperature was lowered from 80 °C to 60 °C at 4 min $°C^{-1}$, and then from 60 °C to 24 °C at rates of 5, 10, 20, 30, 60, 120 or 280 min $°C^{-1}$, respectively). **c**–**e**, TEM and gel analysis of influence of $MgCl_2$ concentration on folding quality. **c**, The fastest-migrating bands in the 4 mM $MgCl_2$ lanes were purified and imaged, revealing gross folding defects. **d**, Shapes were folded with a 173 h ramp in 5 mM Tris + 1 mM EDTA (pH 7.9 at 20 °C) and $MgCl_2$ concentrations varying from 0 to 30 mM. **e**, As in **c**, leading bands were purified from the 16 mM $MgCl_2$ lanes and found to exhibit higher-quality folding when analysed by TEM. **f**, Excess NaCl inhibits proper folding. Shapes were folded with 173 h ramp in 5 mM Tris + 1 mM EDTA (pH 7.9 at 20 °C), 16 mM $MgCl_2$, and varying NaCl concentrations.

Douglas et al - Self-assembly of DNA into nanoscale three-dimensional shapes

2-Step Hierarchal Assembly of Larger 3D Structures:

(a) Assembly of Polymer-like Sequence of DNA Origami

(b-d) Assembly of Polyhedra from smaller parts

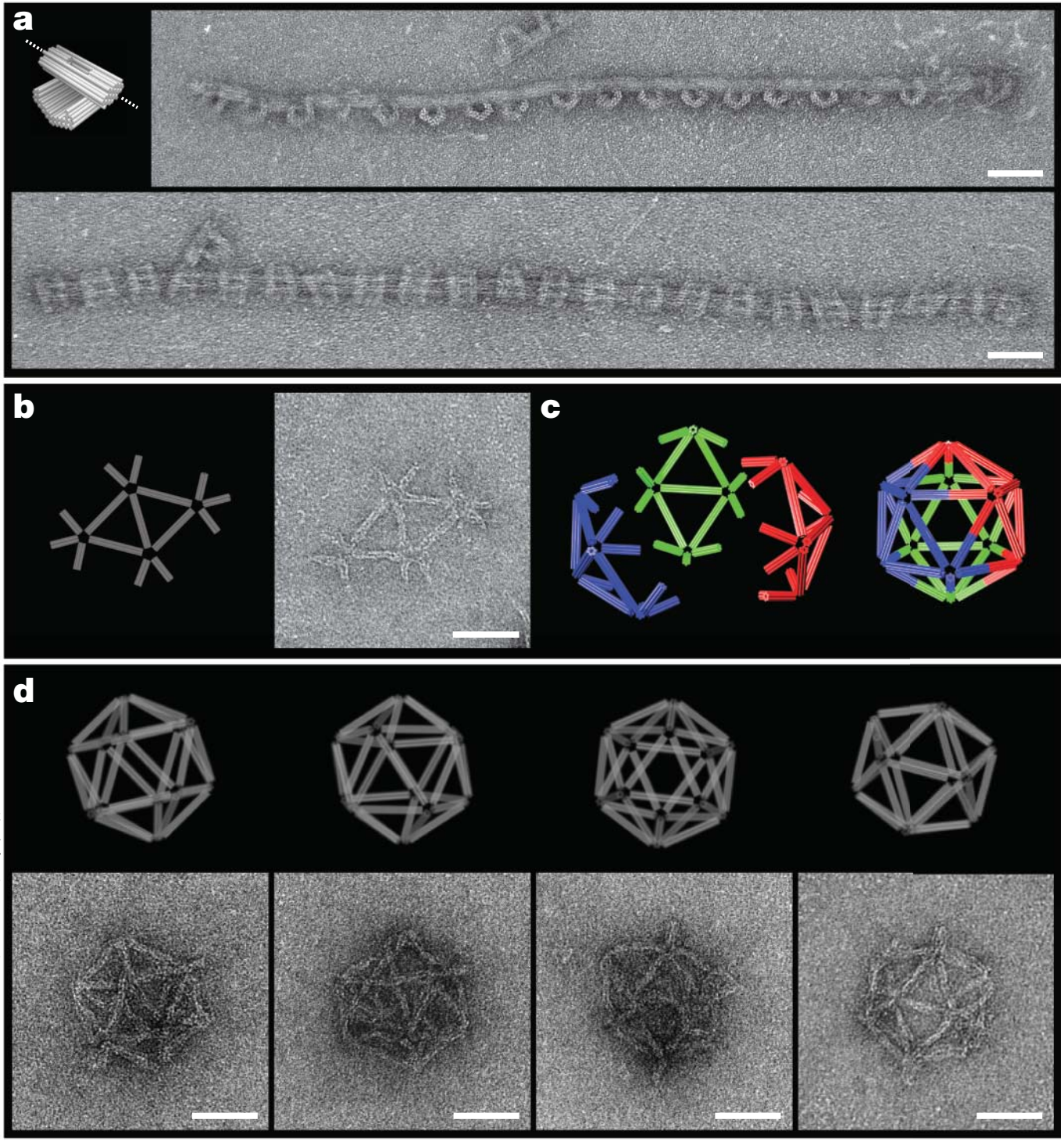

Two-step hierarchical assembly of larger three-dimensional structures and polymers. **a**, Left panel, Cylinder model of stacked-cross monomer (Fig. 2e), with dotted line indicating direction of assembly. Right panels, typical TEM micrographs showing stacked-cross polymers. Purified stacked-cross samples were mixed with a fivefold molar excess of connector staple strands in the presence of 5 mM Tris + 1 mM EDTA (pH 7.9 at 20 °C), 16 mM $MgCl_2$ at 30 °C for 24 h. Monomers were folded in separate chambers, purified, and mixed with connector staple strands designed to bridge separate monomers. **b**, Cylinder model (left) and transmission electron micrograph (right) of a double-triangle shape comprised of 20 six-helix bundle half-struts. **c**, Heterotrimerization of the icosahedra was done with a 1:1:1 mixture of the three unpurified monomers at 50 °C for 24 h. **d**, Orthographic projection models and TEM data of four icosahedron particles. Scale bars in **a**, **b** and **d**: 100 nm.

Douglas et al - Self-assembly of DNA into nanoscale three-dimensional shapes

Experimental Method

One-pot reaction

1. **Rapid heating → slow cooling**
2. **10 nM scaffold strands derived from M13 bacteriophage**
3. **50 nM of every oligonucleotide staple strand**
   (5x to 1x..why?) purified by reverse-phase cartridge
4. **Buffer, salts → 5 mM Tris + 1 mM EDTA (pH 7.9 at 20 uC), 16 mM MgCl2**
5. **Thermal-annealing ramp from 80 C to 60 C → 80 min then 60 C to 24 C → 173 h.**
6. **2% agarose gel containing 45 mM Tris borate + 11 mM EDTA (pH 8.3 at 20 C) , and 11 mM $MgCl_2$ at 70 V → Monomer bands were excised**
7. **Objects were electrophoresed**
   DNA was recovered by physical extraction from the excised band
   negative-staining by uranyl formate
8. **Objects were imaged using TEM**

Dietz et al - Folding DNA into Twisted and Curved Nanoscale Shapes

Dietz et al - Folding DNA into Twisted and Curved Nanoscale Shapes

- Goal: quantitatively control the degree of curvature
- A radius of curvature as tight as 6 nanometers was achieved.
- Bend angles ranged from 30° to 180°

→ Realized something close to the extreme bending of DNA found in the nucleosome

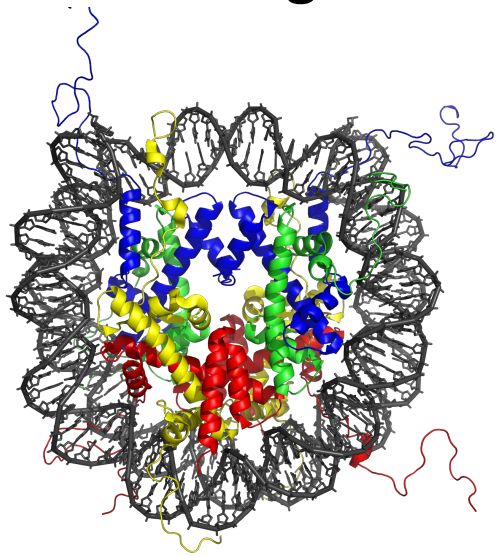

Source: Wikipedia.org/wiki/Nucleosome

Dietz et al - Folding DNA into Twisted and Curved Nanoscale Shapes

Twisting and Bending

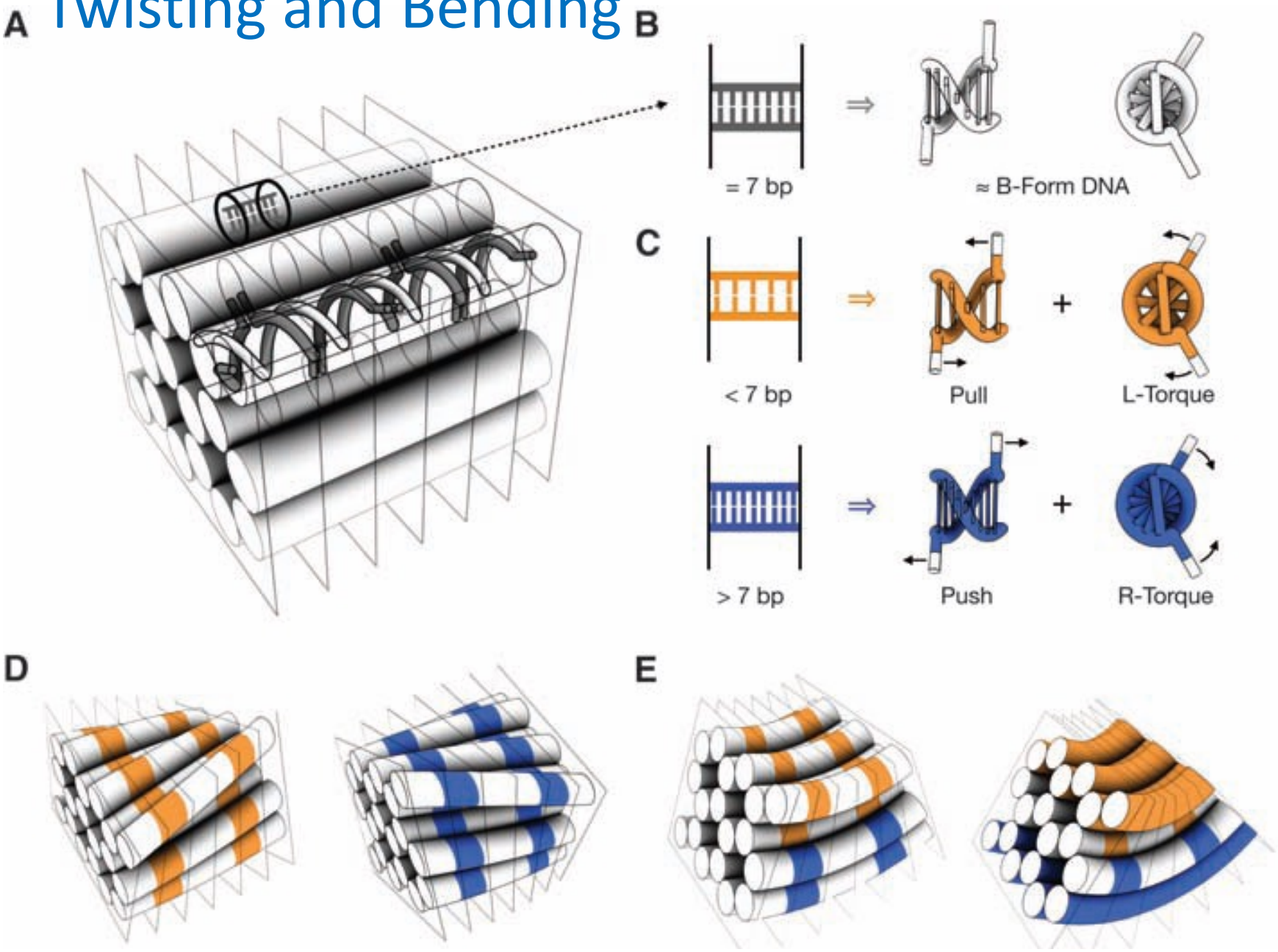

Dietz et al - Folding DNA into Twisted and Curved Nanoscale Shapes

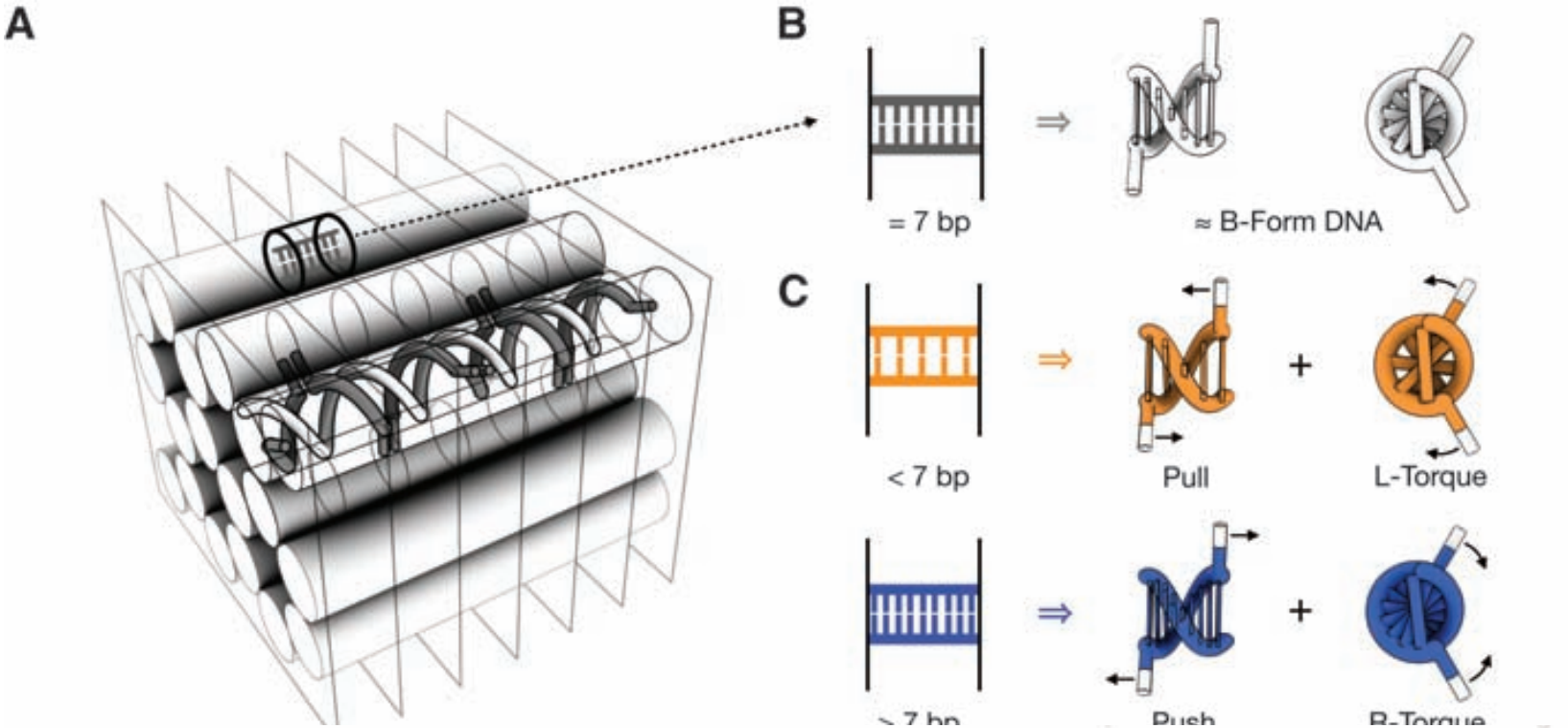

Design principles for controlling twist and curvature in DNA bundles. (**A**) Double helices are constrained to a honeycomb arrangement by staple-strand crossovers. Semi-transparent crossover planes mark the locations of strand crossovers between neighboring helices, which are spaced at 7-bp intervals along the helical axis. From left to right, each plane contains a class of crossovers rotated in-plane by 240° clockwise with respect to the preceding plane. The crossover planes divide the bundle conceptually into helix fragments that can be viewed as residing in array cells (one cell is highlighted). (**B**) Array cell with default content of 7 bp, which exerts no stress on its neighbors. (**C**) Above, array cell with content of 5 bp, which is under strain and therefore exerts a left-handed torque and a pull on its neighbors. Below, array cell with content of 9 bp, which is under strain and therefore exerts a right-handed torque and a push on its neighbors. Force vectors are shown on only two of the four strand ends of the array-cell fragment for clarity.

Dietz et al - Folding DNA into Twisted and Curved Nanoscale Shapes

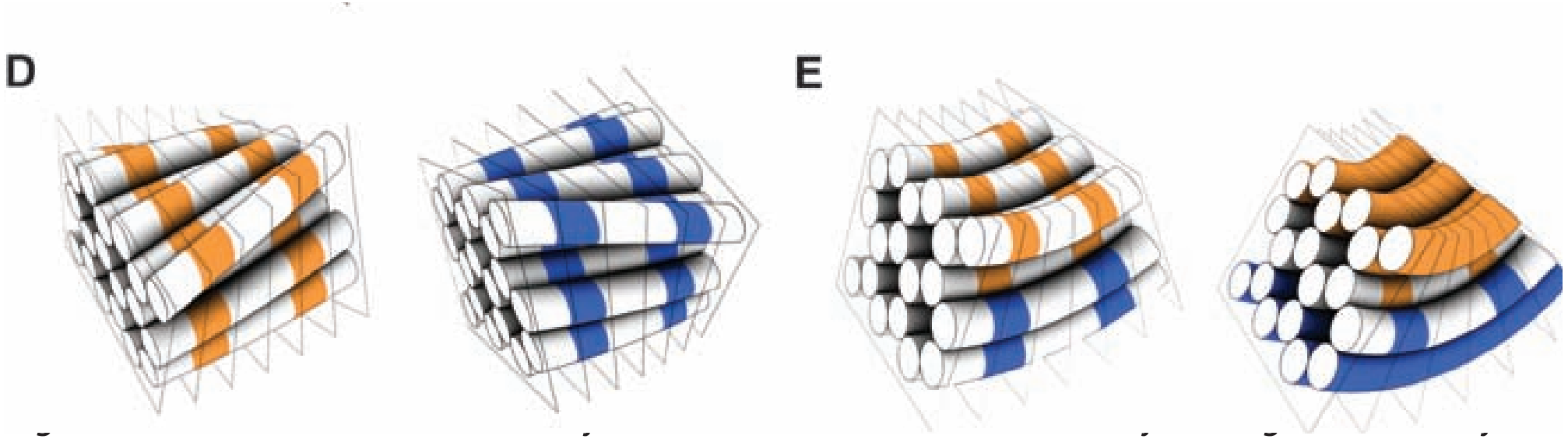

(**D**) (Left) Site-directed deletions installed in selected array cells indicated in orange result in global left-handed twisting with cancellation of compensatory global bend contributions; (right) site-directed insertions in selected array cells (shown in blue) result in global right-handed twisting. (**E**) Site-directed base-pair deletions (indicated in orange) and base-pair insertions (indicated in blue) can be combined to induce tunable global bending of the DNA bundle with cancellation of compensatory global twist contributions.

Dietz et al - Folding DNA into Twisted and Curved Nanoscale Shapes

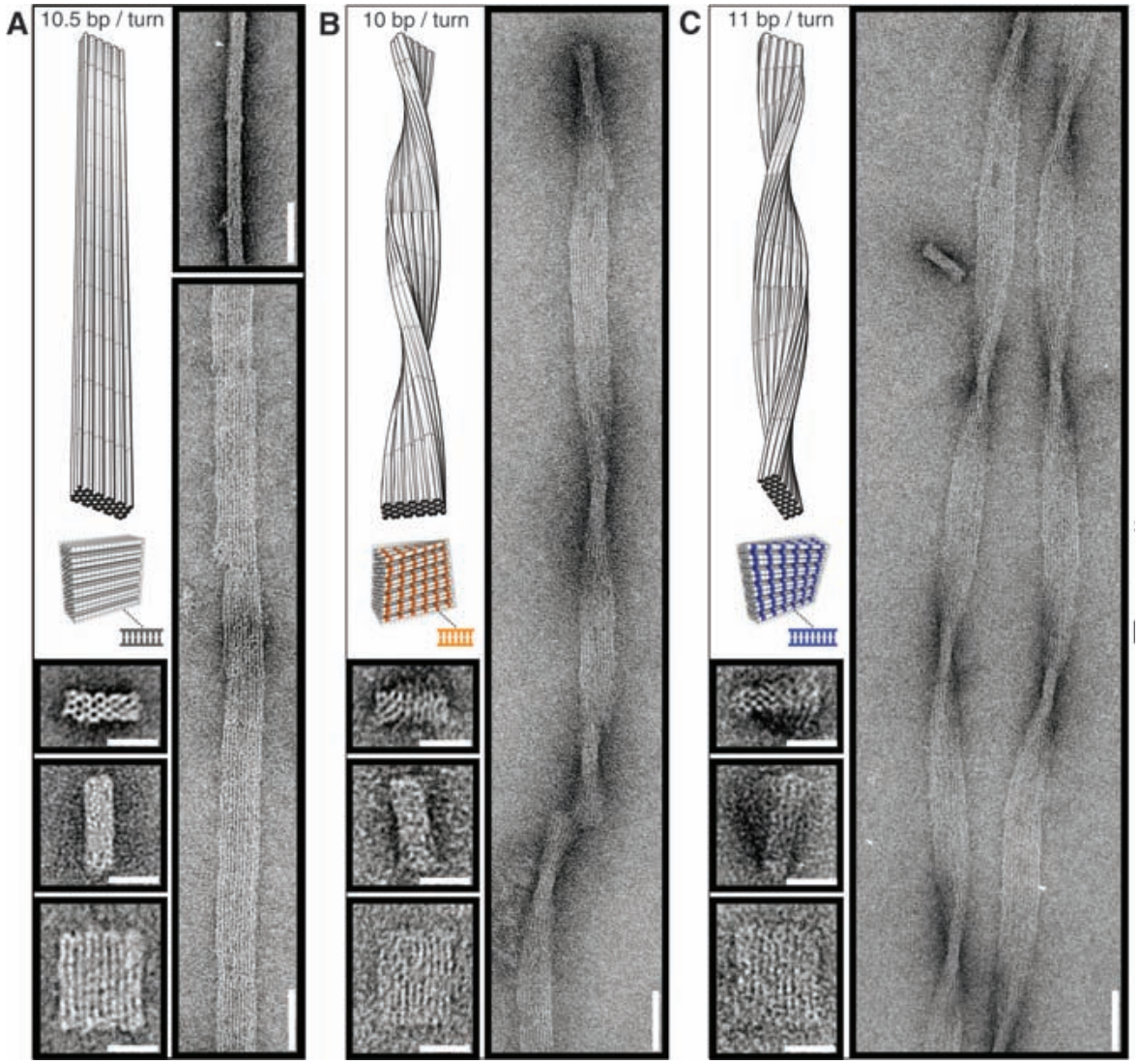

Deviations from 10.5 bp per turn twist density induce global twisting. (**A** to **C**) (Top left) Models of a 10-by-6–helix DNA bundle (red) with 10.5, 10, and 11 bp per turn average double-helical twist density, respectively, and models of ribbons when polymerized (silver). (Bottom left) Monomeric particles as observed by negative-stain TEM. Scale bars, 20 nm. (Right) Polymeric ribbons as observed by TEM. Scale bars, 50 nm. (**D**

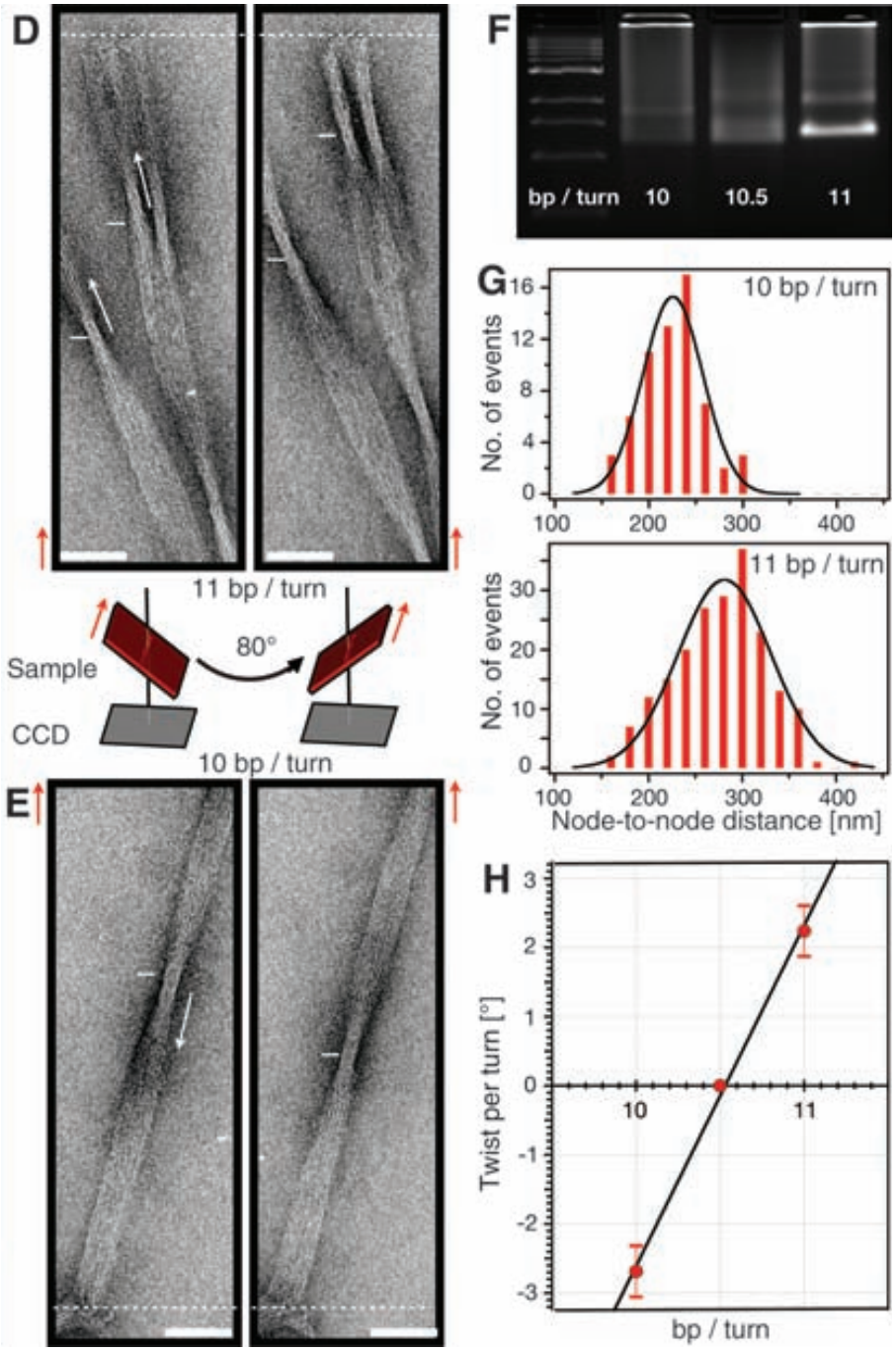

(**D** and **E**) Tilt-pair images of twisted ribbons polymerized from 11 bp per turn (D) and 10 bp per turn (E); 10-by-6–helix bundles, recorded at goniometer angles of 40° and –40°. Arrows indicate the observed upward (for 11 bp per turn) or downward (for 10 bp/turn) direction of movement of the twisted-ribbon nodes. The dashed line provides a reference point (ends of ribbons remain stationary on goniometer rotation). CCD, charge-coupled device. (**F**) Ethidium-bromide–stained 2% agarose gel, comparing migration of unpurified folded bundles. (**G**) Histograms of the observed node-to-node distance in twisted ribbons, as observed in negative-stain TEM micrographs. Left- and right-handed ribbons undergo half-turns every 235 ± 32 nm (n = 62 internode distances measured) and 286 ± 48 nm (n = 197), respectively (numbers after the ± sign indicate SD). (**H**) Plot of observed global compensatory twist per turn versus double-helical twist density initially imposed by design. A value of 0.335 nm per bp was used to calculate global twist per turn from values obtained in (G). Error bars indicate SD.

Dietz et al - **Folding DNA into Twisted and Curved Nanoscale Shapes**

Dietz et al - Folding DNA into Twisted and Curved Nanoscale Shapes

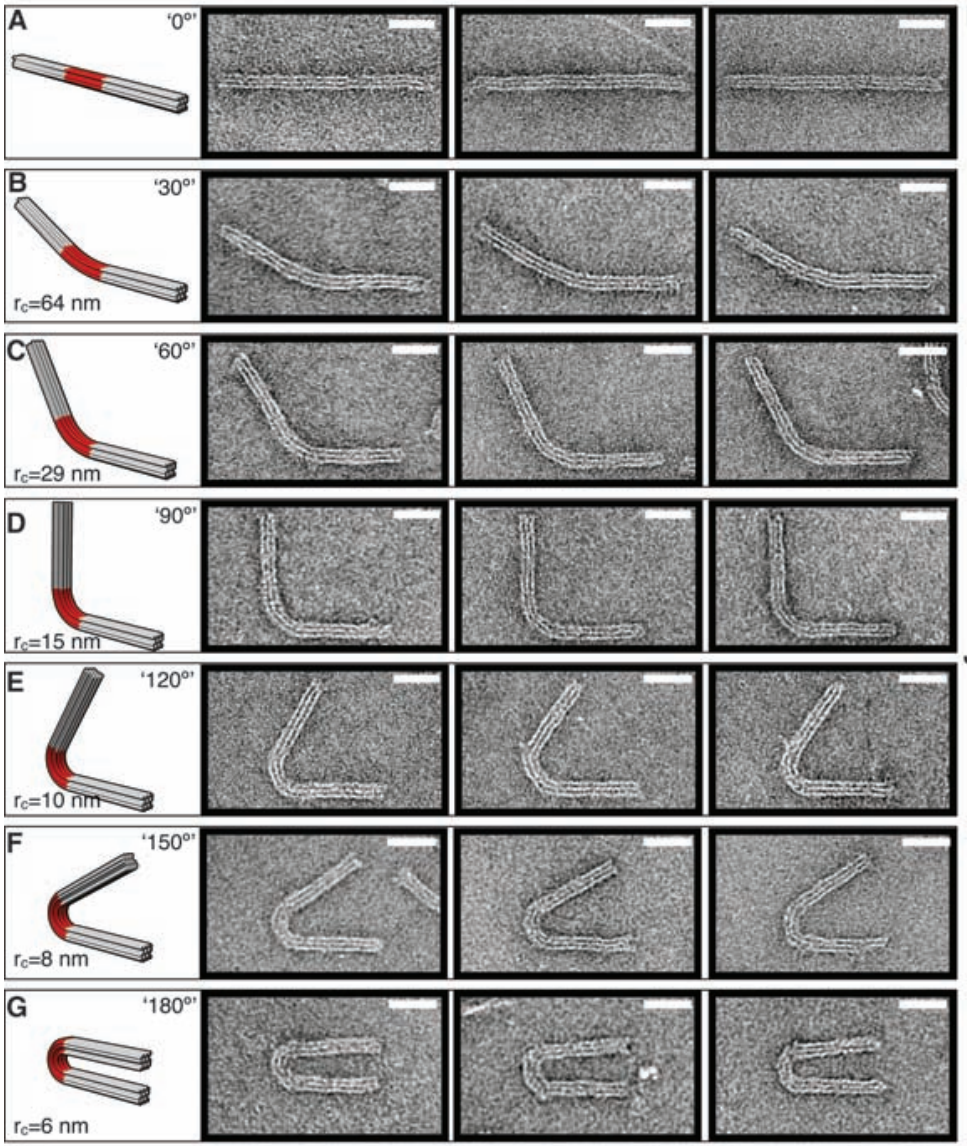

Combining site-directed insertions and deletions induces globally bent shapes. (**A** to **G**) Models of seven 3-by-6–helix-bundle versions programmed to different degrees of bending and typical particles, as observed by negative-stain TEM. r_c, radius of curvature. Scale bars, 20 nm.

Dietz et al - Folding DNA into Twisted and Curved Nanoscale Shapes

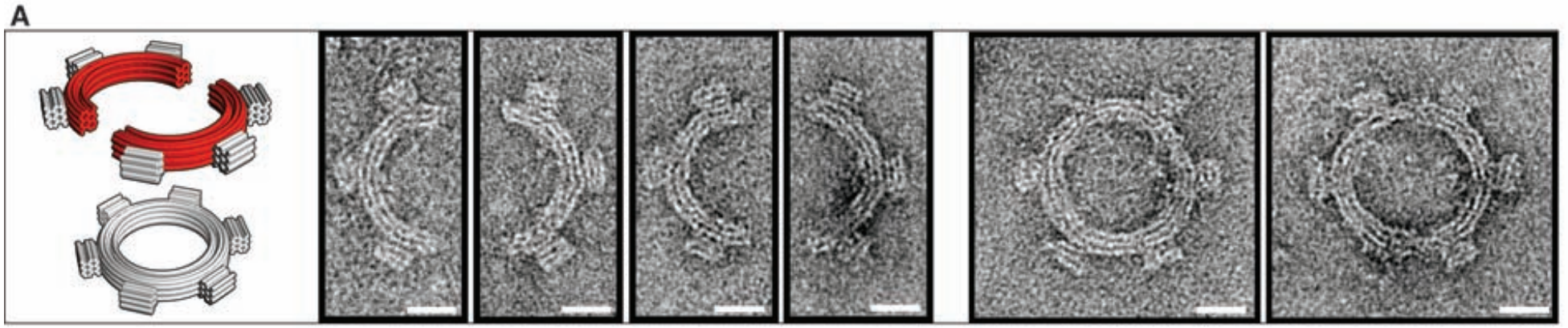

Bending enables the design of intricate nonlinear shapes. Red segments indicate regions in which deletions and insertions are installed. Scale bars, 20 nm. (**A**) Model of a 3-by-6–helix DNA-origami bundle designed to bend into a half-circle with a 25-nm radius that bears three non-bent teeth. Monomers were folded in separate chambers, purified, and mixed with connector staple strands to form six-tooth gears. Typical monomer and dimer particles visualized by negative-stain TEM.

Dietz et al - Folding DNA into Twisted and Curved Nanoscale Shapes

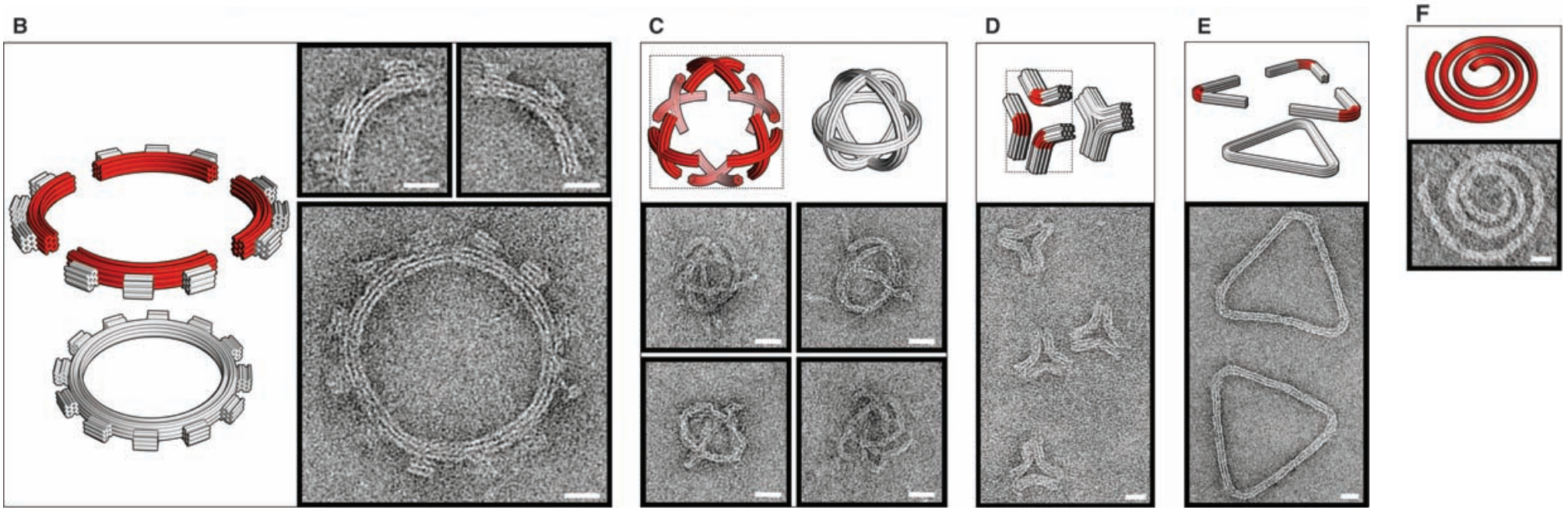

(**B**) 3-by- 6–helix bundle as in (A), modified to bend into a quarter circle with a 50-nm radius. Hierarchical assembly of monomers yields 12-tooth gears. (**C**) A single scaffold strand designed to fold into a 50-nm-wide spherical wireframe capsule resembling a beach ball and four typical particles representing different projections of the beach ball. The design folds as six bent crosses (inset) connected on a single scaffold. (**D**) A concave triangle that is folded from a single scaffold strand. The design can be conceptualized as three 3-by-6 bundles with internal segments designed to bend by 60°. (**E**) A convex triangle assembled hierarchically from three 3-by-6 bundles designed with a 120° bend (Fig. 3E). (**F**) A six-helix bundle programmed with varying degrees of bending folds into a spiral-like object.

Dietz et al - Folding DNA into Twisted and Curved Nanoscale Shapes

Origin of Stripes

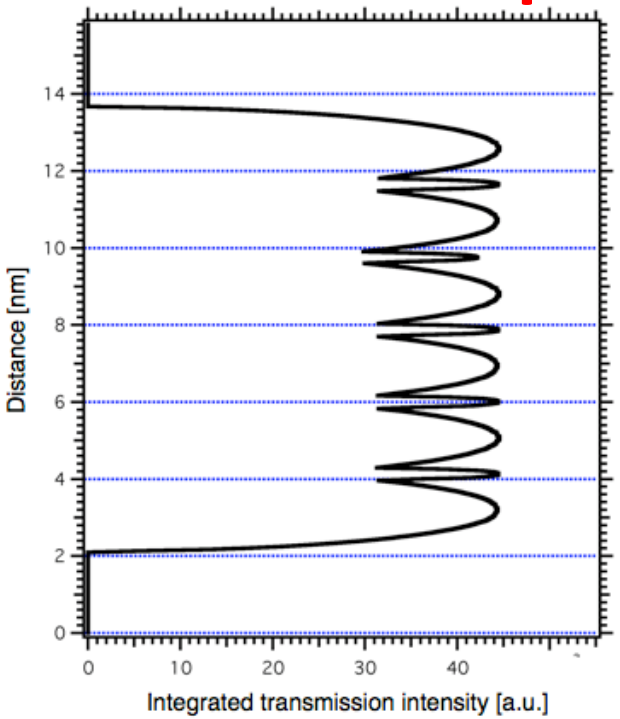

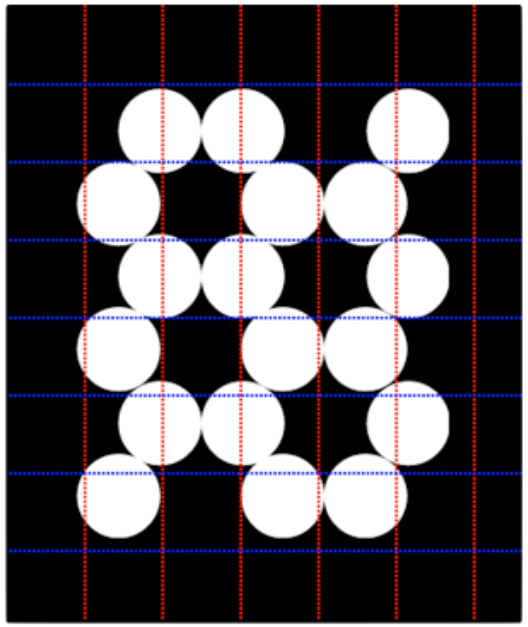

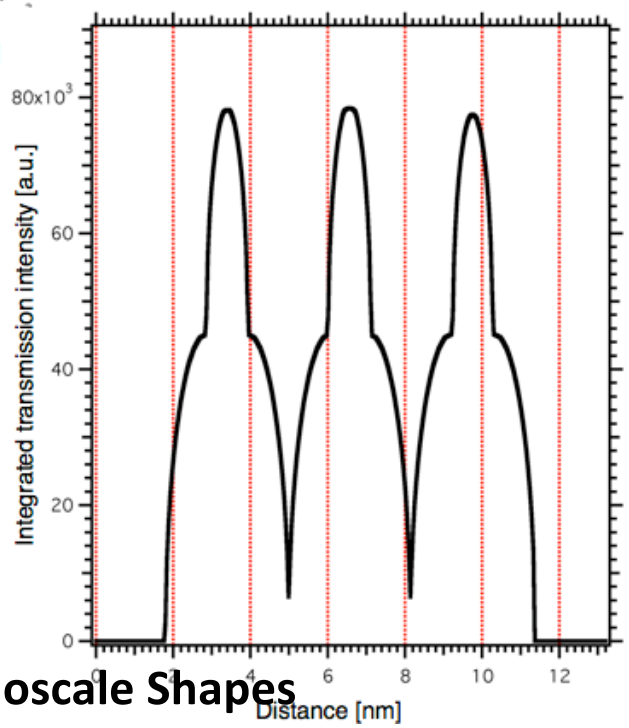

Claim: Clear stripes indicate well formed structures.

Dietz et al - **Folding DNA into Twisted and Curved Nanoscale Shapes**

Dietz et al - Folding DNA into Twisted and Curved Nanoscale Shapes

Yield Analysis

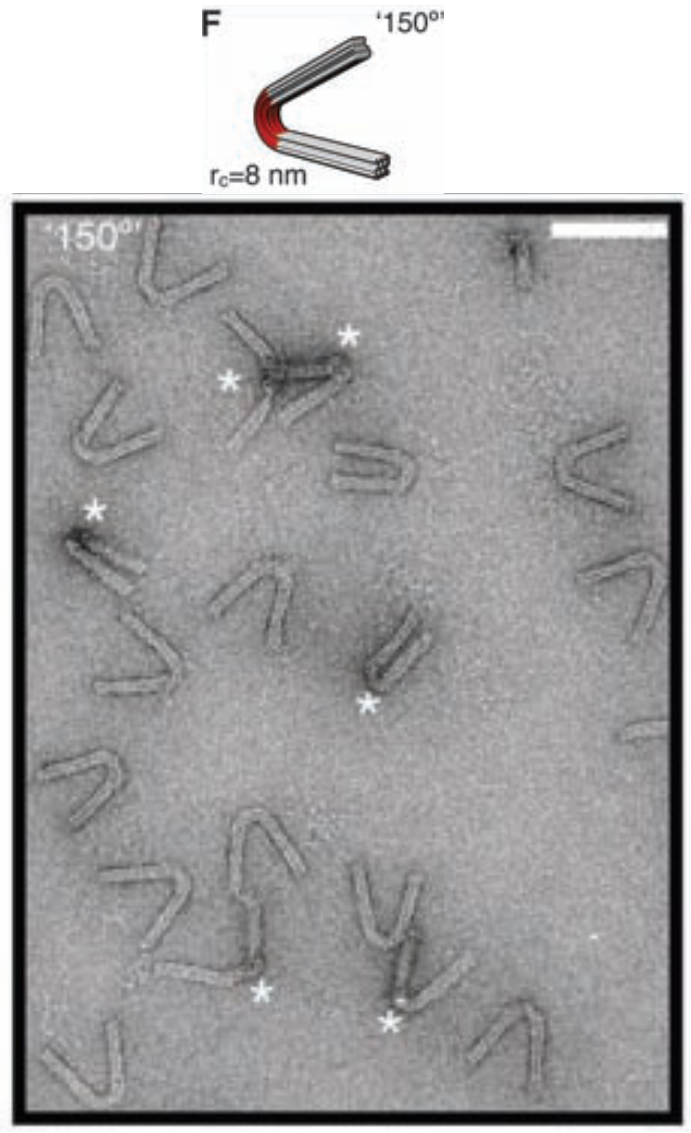

Dietz et al - Folding DNA into Twisted and Curved Nanoscale Shapes

Yield Analysis: 3D DNA Origami

- Yield ~ 50% at radius of curvature 10 nm
- Yield decreases as radius of curvature decreases
- Low yield for multimeric object such as gears, sometimes less than 10%

Dietz et al - Folding DNA into Twisted and Curved Nanoscale Shapes

Overview

- Gave a 3D extension of origami
- Implemented using the honeycomb lattice
- Sculpt away unnecessary parts of the lattice
- Change the number of bases per turn to twist or bend the honeycomb
- Long annealing schedule
- Carefully controlled cationic concentration
- Average to low yields

Han et al – DNA Origami with Complex Curvatures in Three-Dimensional Space

Han et al – DNA Origami with Complex Curvatures in Three-Dimensional Space

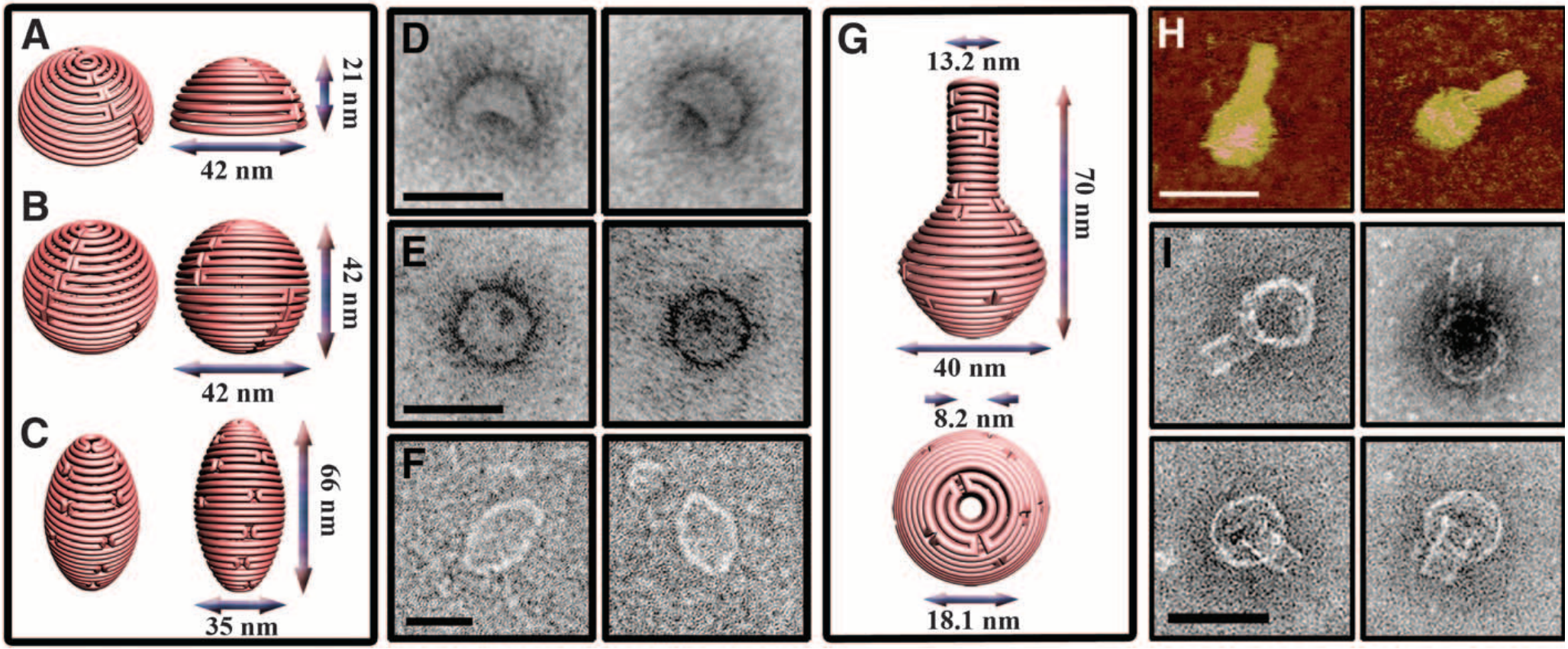

Han et al – DNA Origami with Complex Curvatures in Three-Dimensional Space

Design principles for DNA origami with complex curvatures in 3D space.

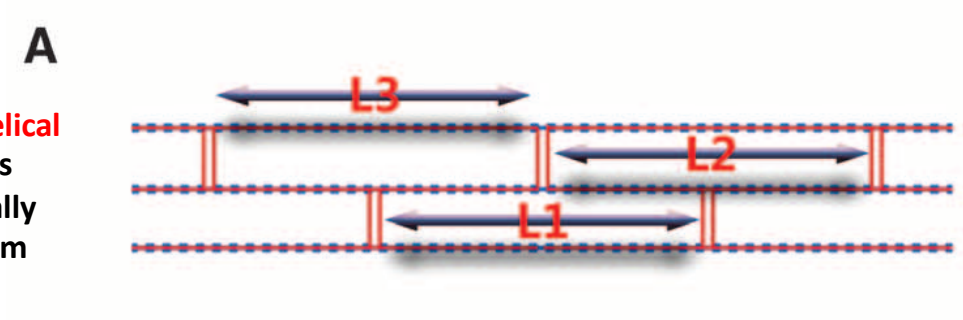

(A) A parallel arrangement of DNA double helices to make multihelical DNA nanostructures. **The distance between consecutive crossovers connecting adjacent helices (L1, L2, and L3) is constant and generally corresponds to 21 or 32 bps (about two or three full turns of B-form DNA).**

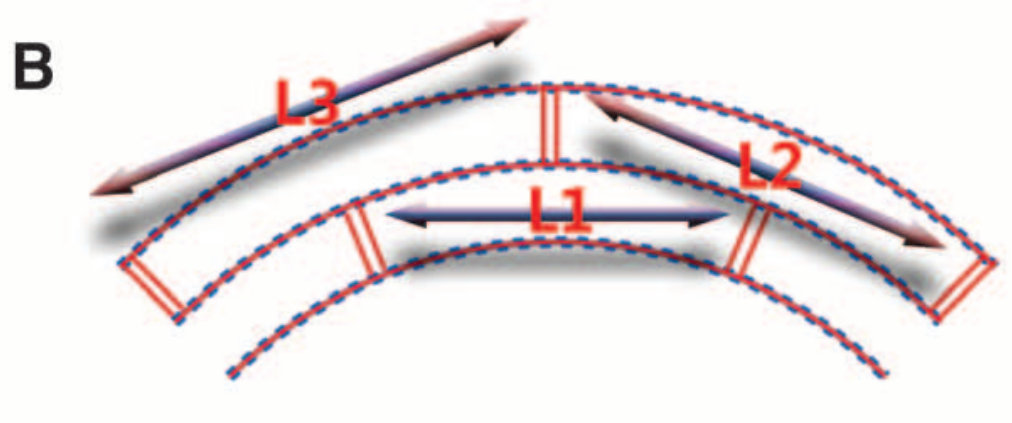

(B) Bending of DNA helices into concentric rings to generate in-plane curvature. **The distance between crossovers in the outer rings are greater than in the inner rings (L3 > L2 > L1). This distance is not required to be regular, or exactly equal to a whole number of full turns of B-form DNA for every helix.**

Han et al – DNA Origami with Complex Curvatures in Three-Dimensional Space

Design principles for DNA origami with complex curvatures in 3D space.

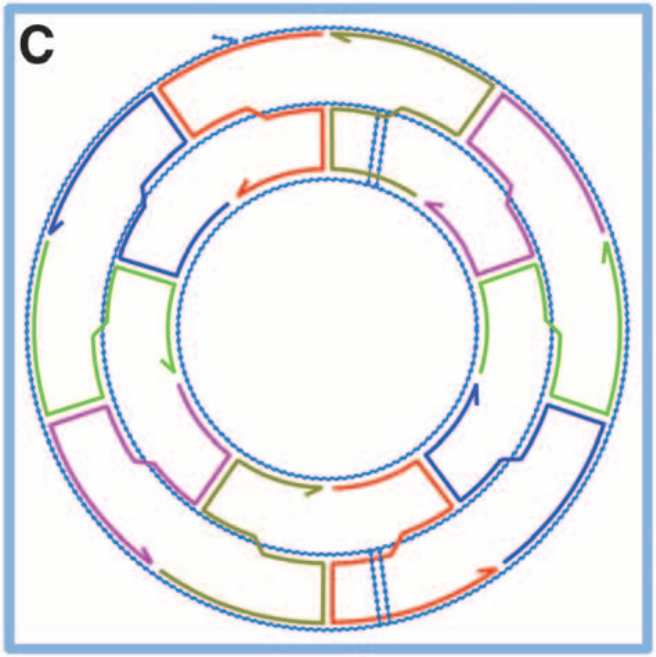

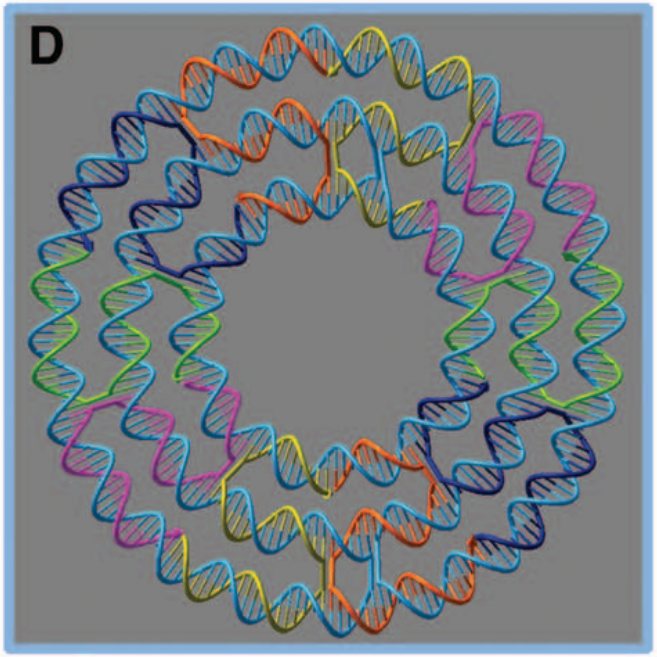

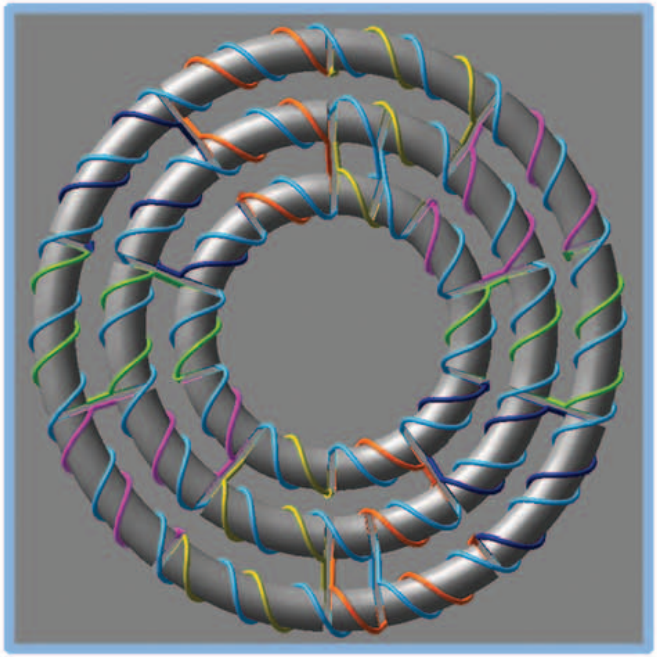

(C) Schematic diagram of a three-ring concentric structure. The long single-stranded DNA scaffold is shown in cyan, and short oligonucleotide staple strands are shown in various colors. Two scaffold crossovers are required between adjacent rings to achieve the three-ring arrangement. They are located far apart, on opposite sides of the rings. Five periodic, staple-strand crossovers connect the outer and middle rings and the middle and inner rings, respectively, constraining the three bent double-helical DNA rings to the same 2D plane.

(D) Helical and cylindrical view of the three-ring concentric structure.

Han et al – DNA Origami with Complex Curvatures in Three-Dimensional Space

Design principles for DNA origami with complex curvatures in 3D space.

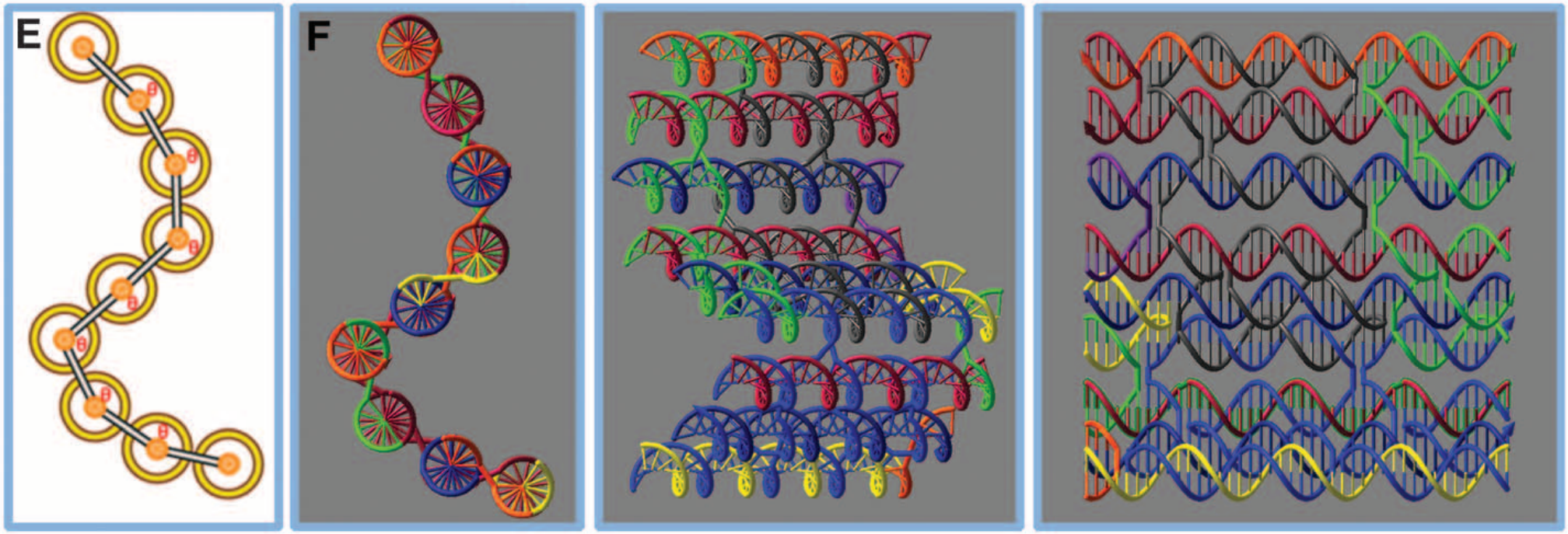

(E) A general method to introduce out-of-plane curvature in a multihelical DNA structure. All DNA helices exhibit a natural B-form conformation. There are 10 possible values of q ranging from ~34° to ~343°. Due to steric hindrance, not all values are allowed. Only a few of these values are demonstrated here.

(F) Various views of the structure shown in (E) viewed along the helical axes, tilted by 135°, and perpendicular to the helical axes.

Han et al – DNA Origami with Complex Curvatures in Three-Dimensional Space

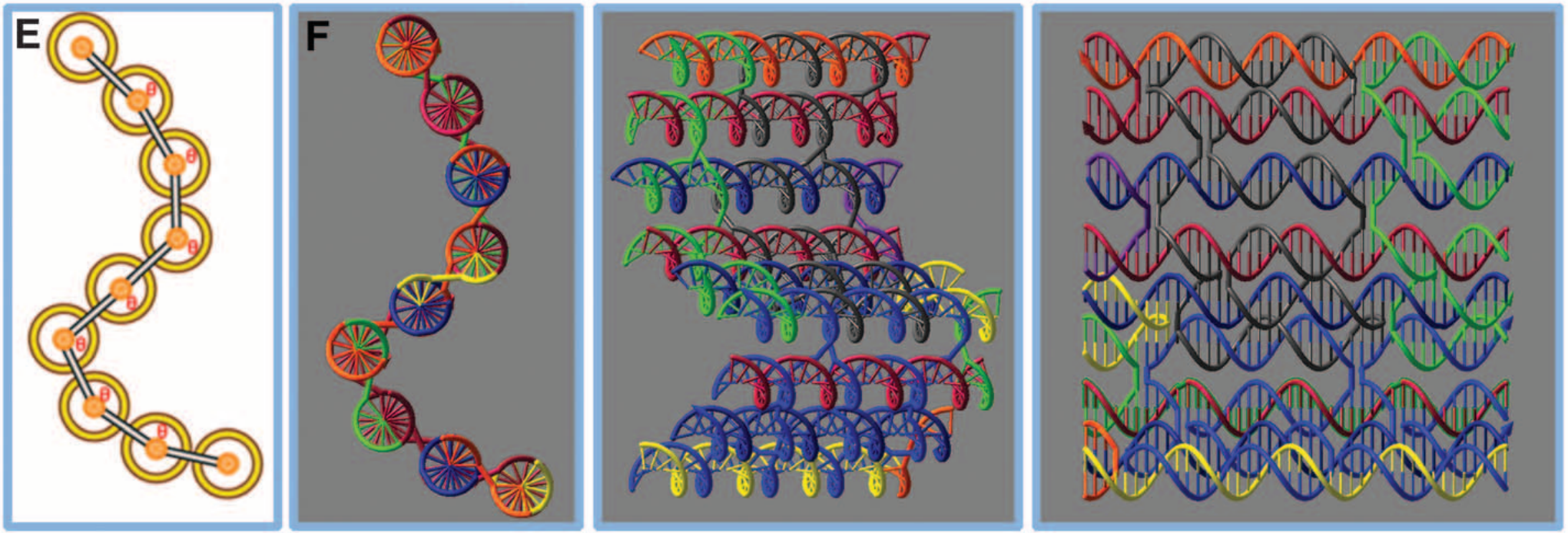

To produce a complex 3D object, it is necessary to create curvatures both in and out of the plane:

- **Out-of-plane curvature can be achieved by shifting the relative position of crossover points between DNA double helices (Fig. E and F).**
- **Typically, two adjacent B-form helices (n and n + 1) are linked by crossovers that are spaced 21 bps apart (exactly two full turns), with the two axes of the helices defining a plane.**
- **The crossover pattern of the two-helix bundle and those of a third helix can be offset by any discrete number of individual nucleotides (not equal to any whole number of half turns, which would result in all three helices lying in the same plane), and in this way, the third helix can deviate from the plane of the previous two.**
- **However, with B-form DNA, the dihedral angle (θ)—the angle between the planes defined by n and n + 1, and n + 1 and n + 2—can not be finely tuned, and ~34.3°/bp is the smallest increment of curvature that can be achieved.**

Han et al – DNA Origami with Complex Curvatures in Three-Dimensional Space

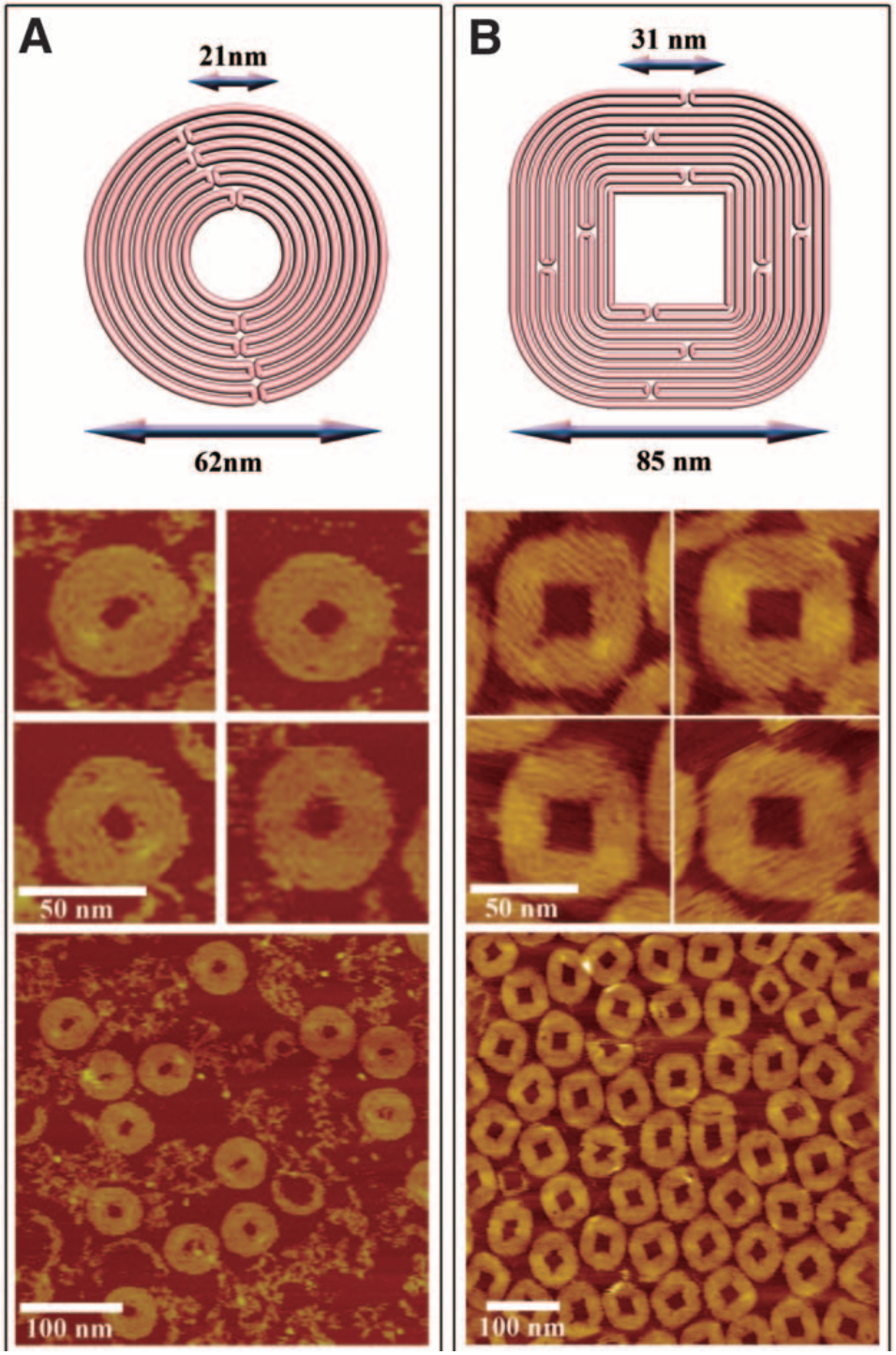

Curved 2D DNA nanostructures with various structural features. (**Upper panels**) Schematic designs. (**Middle panels**) Zoom-in AFM images with 50-nm scale bars. (**Lower panels**) Zoom-out AFM images with 100-nm scale bars. (**A**) Nine-layer concentric ring structure. Only 3600 of 7249 nucleotides of the scaffold strand are used in this structure, and the remaining single-stranded loop is left unpaired, attached to the outer ring (often visible due to formation of secondary structures). (**B**) Eleven-layer modified concentric square frame structure with rounded outer corners and sharp inner corners.

90% yield

Table 1. Design parameters for the nine-layer concentric-ring structure. The number of bps in each ring, number of crossovers between adjacent helices, conformation of the double helical DNA in bps/turn, and radius are listed, respectively.

Ring no.	bps	No. of crossovers	bps/turn	Radius (nm)
1	200	5	10	10.3
2	250	5	10	12.9
3	300	10	10	15.5
4	350	10	11.7	18
5	400	10	10	20.6
6	450	10	9	23.2
7	500	10	10	25.8
8	550	10	11	28.4
9	600	–	10	30.9

Han et al – DNA Origami with Complex Curvatures in Three-Dimensional Space

Hollow DNA nanostructures

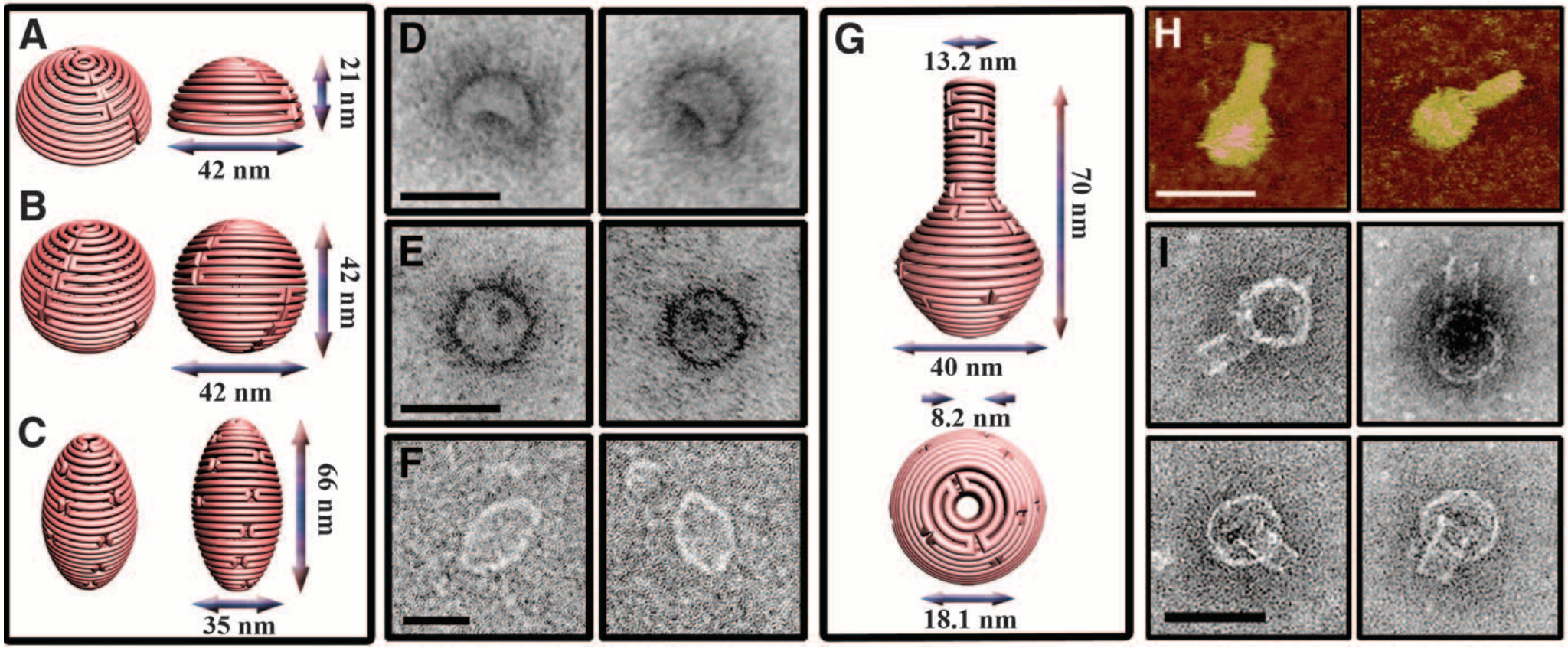

Schematic representations:
(A) The hemisphere.
(B) The sphere.
(C) The ellipsoid.

TEM images:
(D) TEM images of hemisphere.
(E) TEM images of the sphere
(F) TEM images of the ellipsoid

Scale bar for the TEM images in (D), (E) and (F) is 50 nm.

(G) Schematic representation of the nanoflask.

(H) AFM images of the nanoflask. Scale bar is 75 nm.

(I) TEM images of the nanoflask. The cylindrical neck and rounded bottom of the flask are clearly visible in the images. Scale on TEM grids. The cylindrical neck and rounded bottom of the flask are clearly visible in the images. Scale bar is 50 nm.

Automated design of 3D DNA origami with non-rasterized 2D curvature

Dan Fu, Hao Yan & John Reif, Science Advances, 2022

Overview of the DNAxiS design process:

(A) User input is a 3D model in STL file format generated in the user's graphics design software of choice.
(B) The vertices of the STL build a point cloud that is upsampled to avoid gaps when extracting the shape's outline
(C) A circle-based mesh is extracted from the point cloud.
(D) The structure can be made selectively multilayer by adding rings outward from the starting mesh.
(E) A helical twist is calculated from circumference and used to convert each circle of mesh into a DNA helix ring

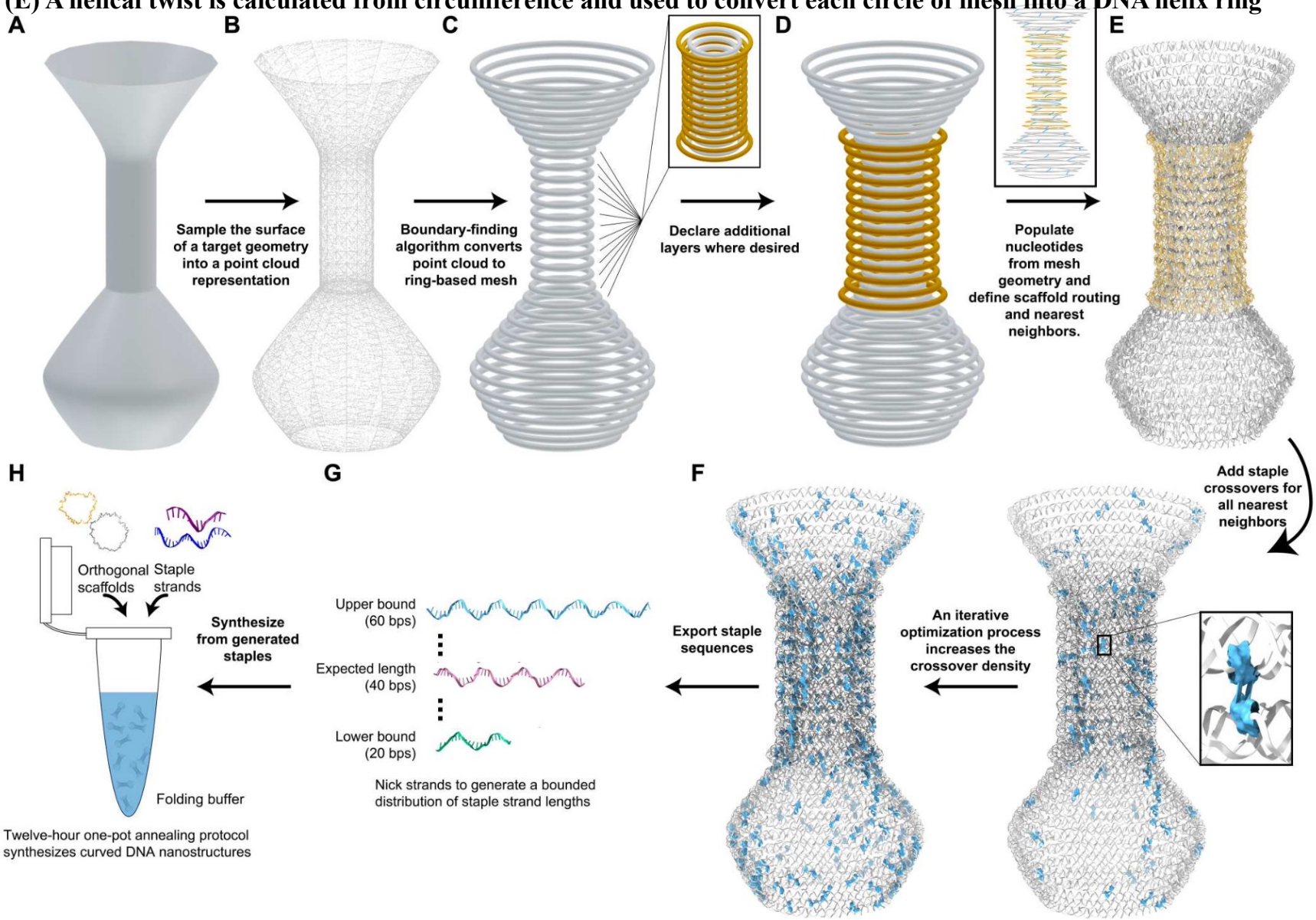

(F) Crossovers are densely applied upon the template using either a greedy algorithm or a simulated annealing algorithm.
(G) Conventional scaffold sequences are applied to generated corresponding staple sequences within specified length bounds.
(H) Staple sequences are annealed with the corresponding scaffolds, sometimes multiple orthogonal sequences as needed, in a one-pot reaction to produce DNA nanostructures of the designed shape.

Automated design of 3D DNA origami with non-rasterized 2D curvature

Dan Fu, Hao Yan & John Reif, Science Advances, 2022

Alignment principles for single/multilayer, curved, closed-shell DNA nanostructures:

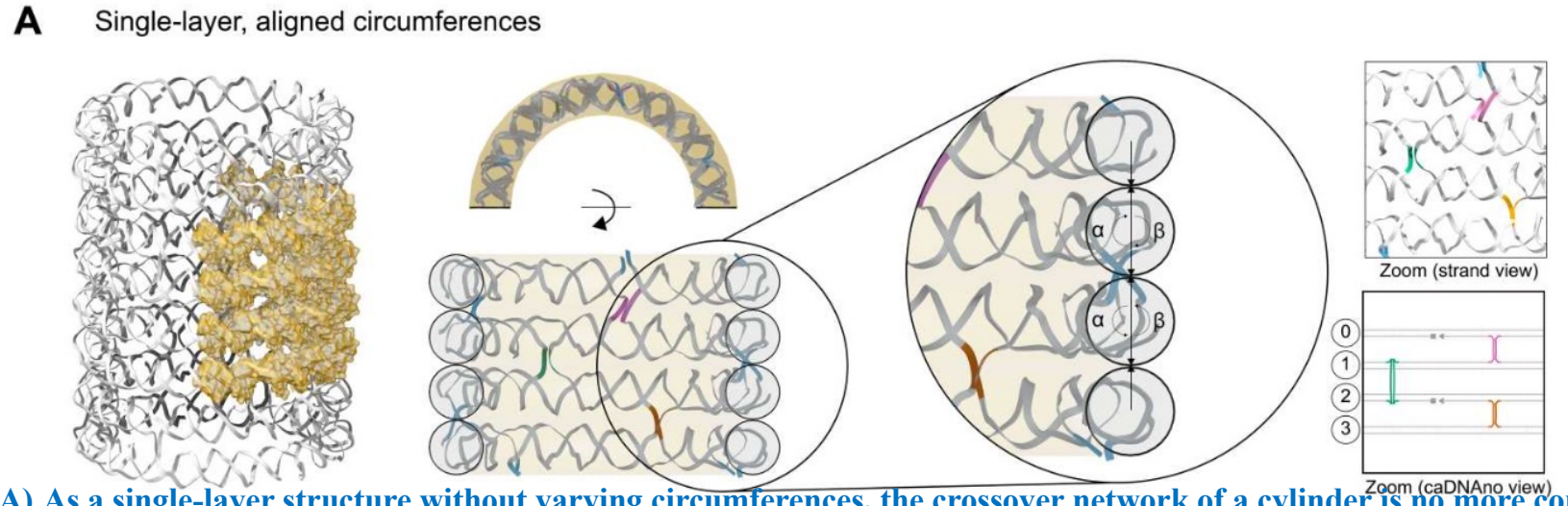

(A) As a single-layer structure without varying circumferences, the crossover network of a cylinder is no more complex than a flat DNA origami rectangle. Local patterns of a few crossovers can be repeated globally, as the dihedral angle and crossover periodicity are the same for all pairs of nearest neighbor helices.

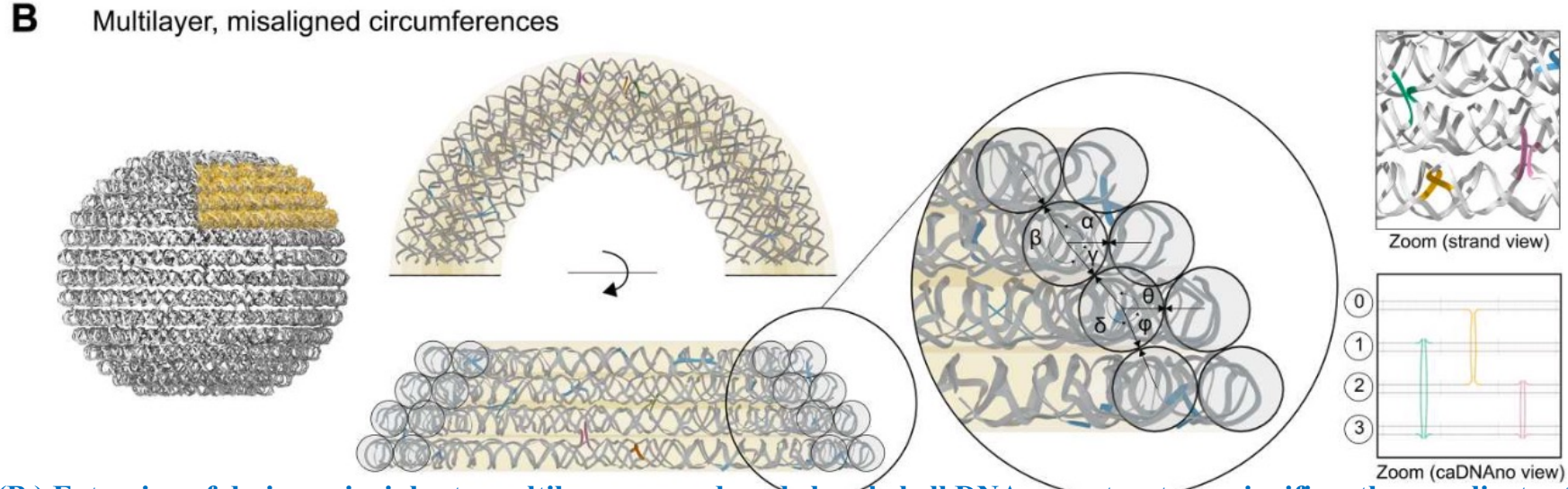

(B) Extension of design principles to multilayer, curved, and closed-shell DNA nanostructures significantly complicates the design space for determining valid crossovers. Each crossover pattern between pairs of nearest neighbor helices is unique because of a different dihedral angle and varying helical twists. Rather than repeating a simple local pattern, each crossover, typically up to 200 when fully using a single M13mp18 scaffold, must be carefully positioned. DNA origami nanostructures were designed using caDNAno software. DNA origami nanostructures were designed using caDNAno software.

Automated design of 3D DNA origami with non-rasterized 2D curvature

Dan Fu, Hao Yan & John Reif, Science Advances, 2022

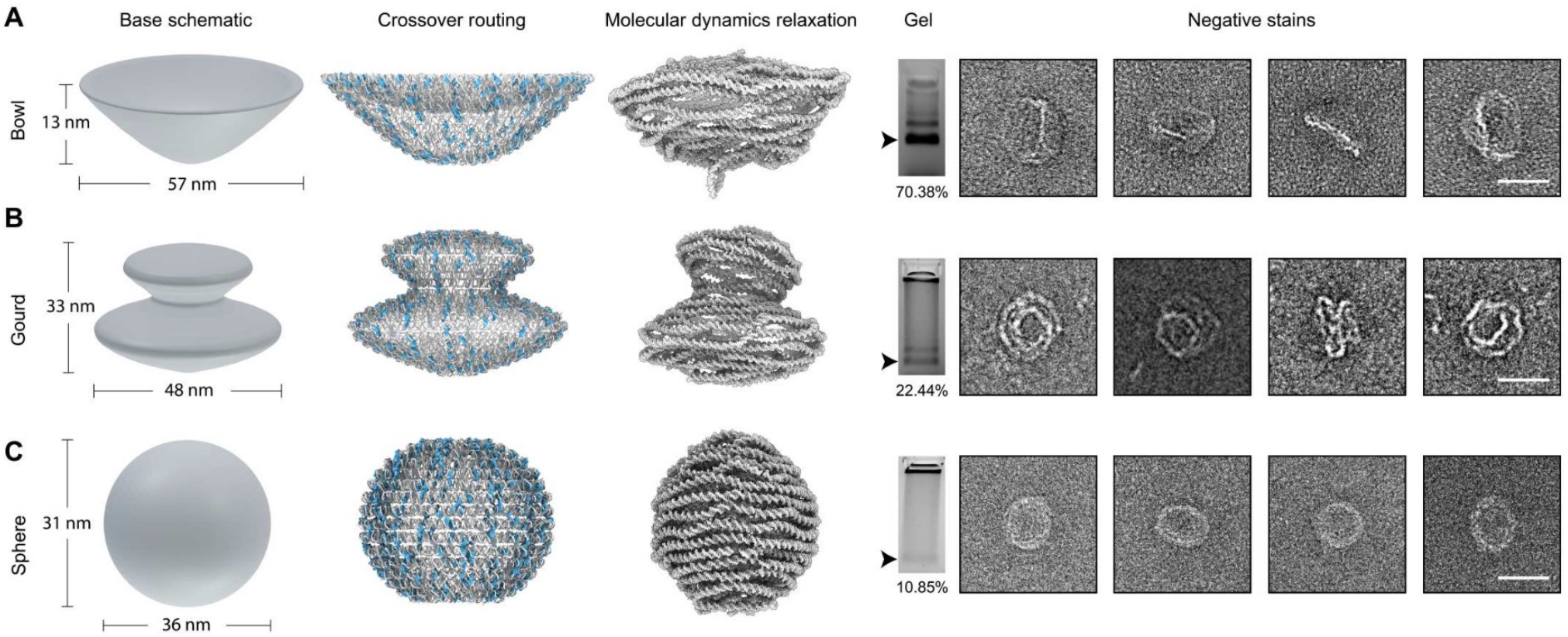

Experimental verification of automated design principles:

(A) Bowl design evaluates convex and concave inflection horizontally with respect to its axis of rotation. Scale bar, 40 nm.

(B) Gourd design evaluates convex and concave inflection vertically along its profile, perpendicular to the axis of rotation. Scale bar, 40 nm.

(C) Sphere is designed with two layers, one nested and one encapsulating, to evaluate the extension of design principles to multilayer structures. Scale bar, 40 nm.

Automated design of 3D DNA origami with non-rasterized 2D curvature

Dan Fu, Hao Yan & John Reif, Science Advances, 2022

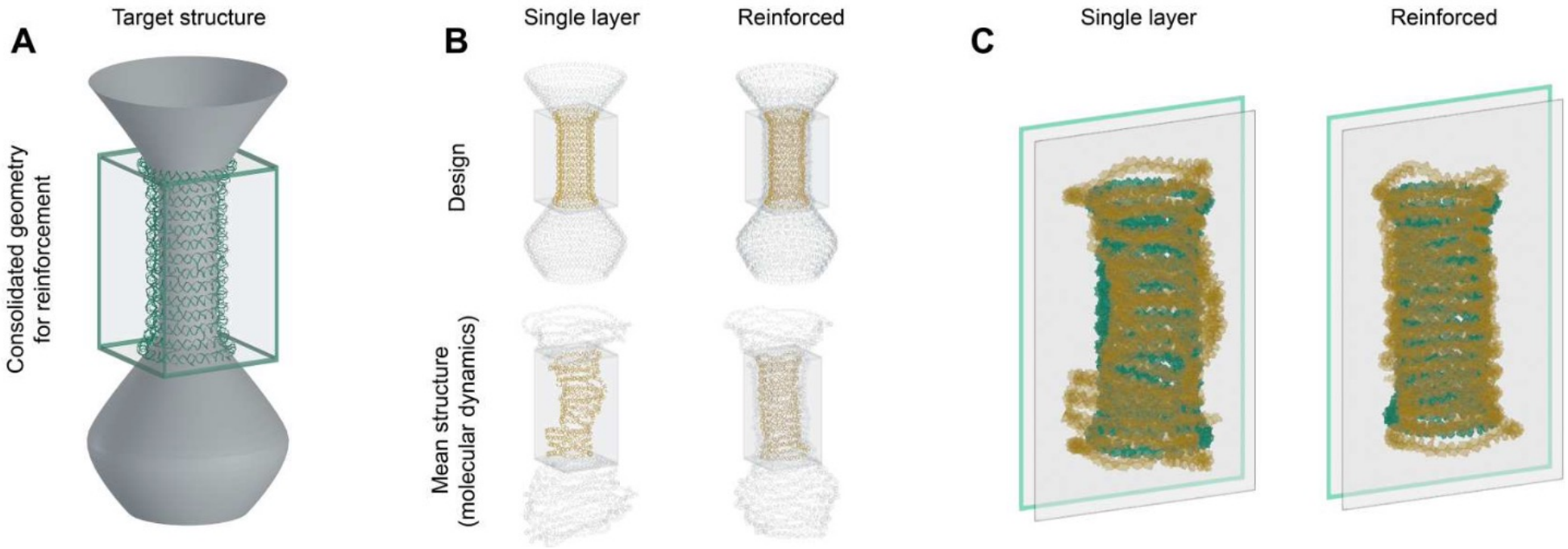

Characterization of reinforcement strategies:

(A) A portion of the vase is selected for targeted reinforcement via additional of coplanar helices.

(B) Designs generated from DNAxiS (top) are submitted into oxDNA (bottom), whereupon mean structures are calculated from 103 samples taken uniformly from 108 trajectory steps.

(C) The interior layer (yellow), which determines the shape of the cavity, for both the single layer and reinforced section is consolidated and compared to their intended shape (green). The overlay shows that the reinforced structure more closely conforms to the intended shape of the neck.

Automated design of 3D DNA origami with non-rasterized 2D curvature

Dan Fu, Hao Yan & John Reif, Science Advances, 2022

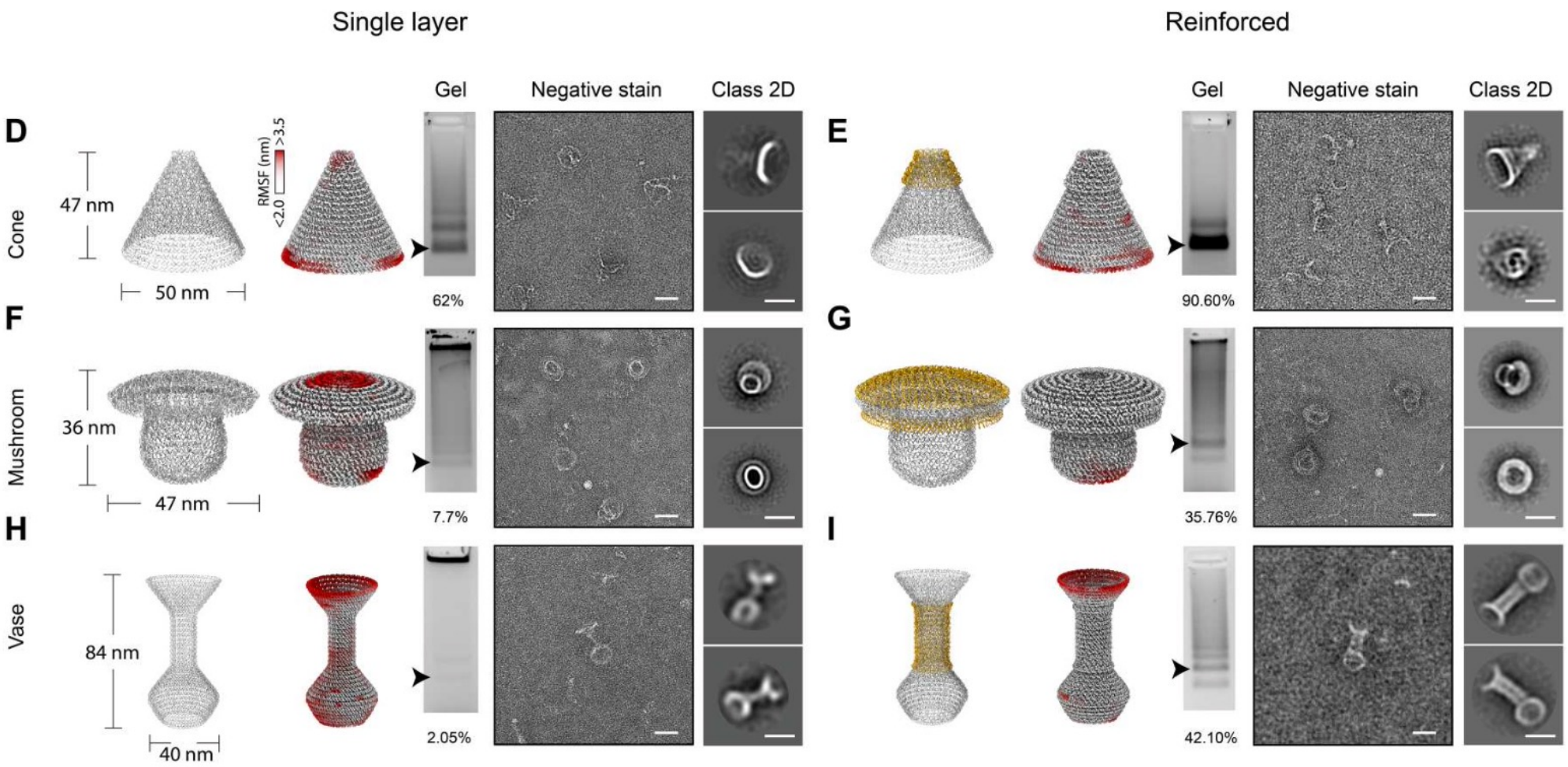

Characterization of reinforcement strategies, cont:

(D to I) Comparing additional geometries (gray) using RMSF calculations calculated from trajectory steps generated by oxDNA, yields and shown by AGE, TEM micrographs, and 2D class averages. Scale bars, 40 nm.

Automated design of 3D DNA origami with non-rasterized 2D curvature

Dan Fu, Hao Yan & John Reif, Science Advances, 2022

Exploration of axially asymmetric structures and generalized application of DNAxiS design principles:

(A and B) Modules defined as arcs can be linked together to create axially asymmetric shapes. Each module is a bent bundle of variable cross-sectional helices where design principles implemented in DNAxiS for multilayer structures can directly apply and were used to generate ellipse and clover shapes.

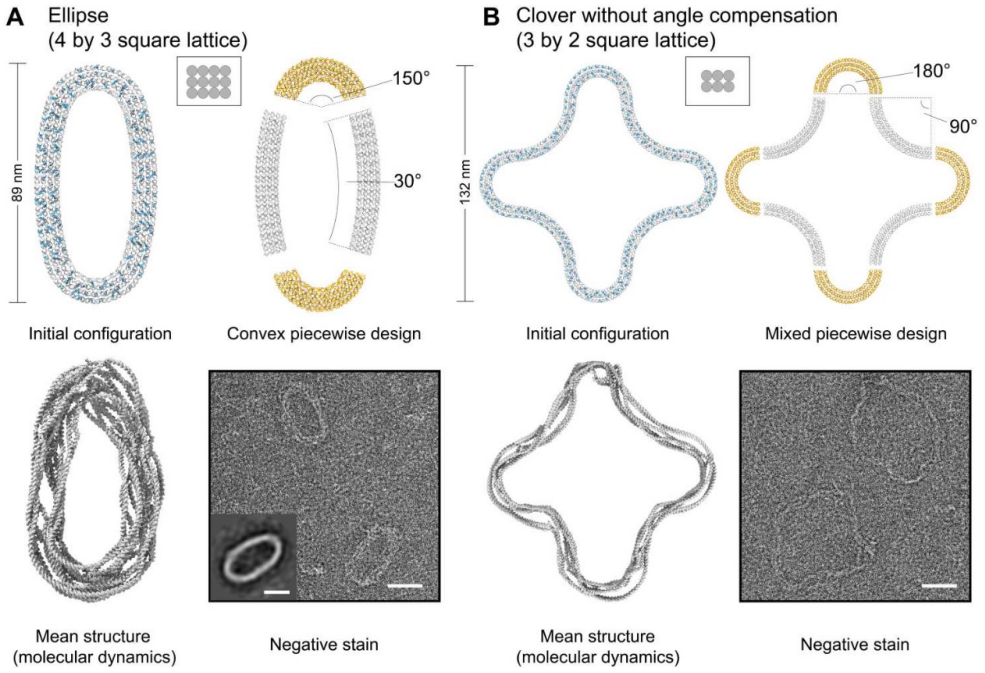

(C) The ellipse shape is repeated five times in a vertical extrusion and pitched by 20°. The cross-sectional area of each ellipse is reduced to fit the entire design within a limited length of scaffold sequence despite already using multiple scaffolds. Both parallel and antiparallel crossovers are created to increase the crossover count and yield of the design.

(D) The cross section of bundles is expanded to three by three to increase the upper-bounded stiffness of each module. This is necessary to achieve sufficient counteracting strain on inside corner modules to preserve the inflection between convex to concave segments of the structure without "rounding out" as it did in three-by-two clover. Scale bars (on TEM micrographs and 2D averages), 40 nm.

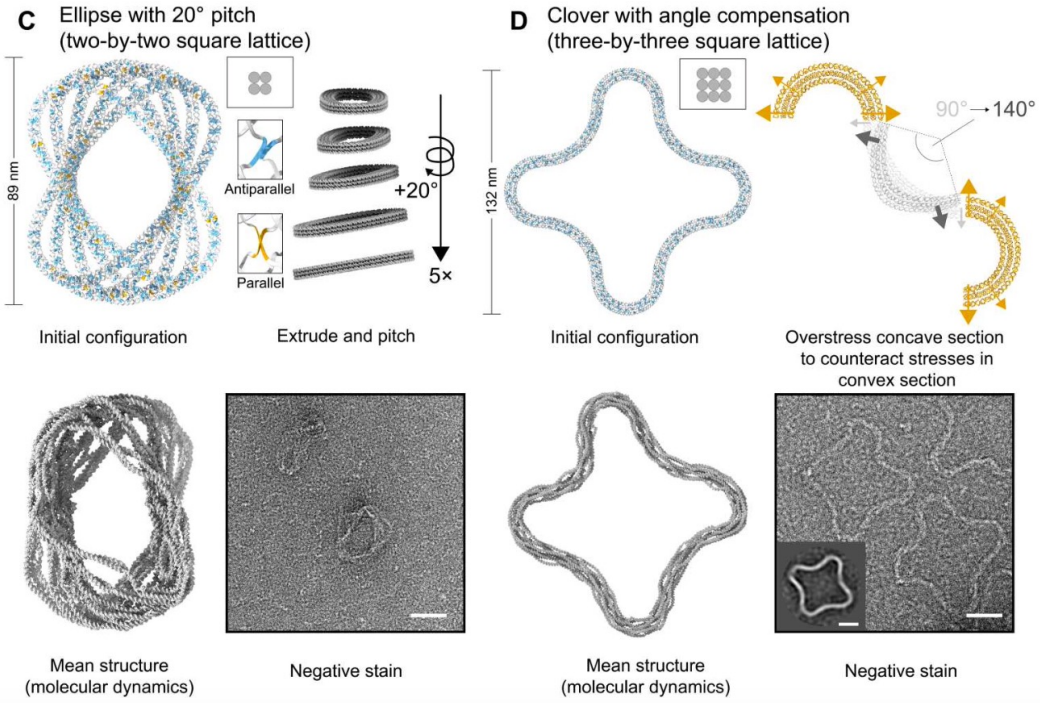

DNA origami capsids
Fu, Pradeep et al

DNA origami capsids
Fu, Pradeep et al

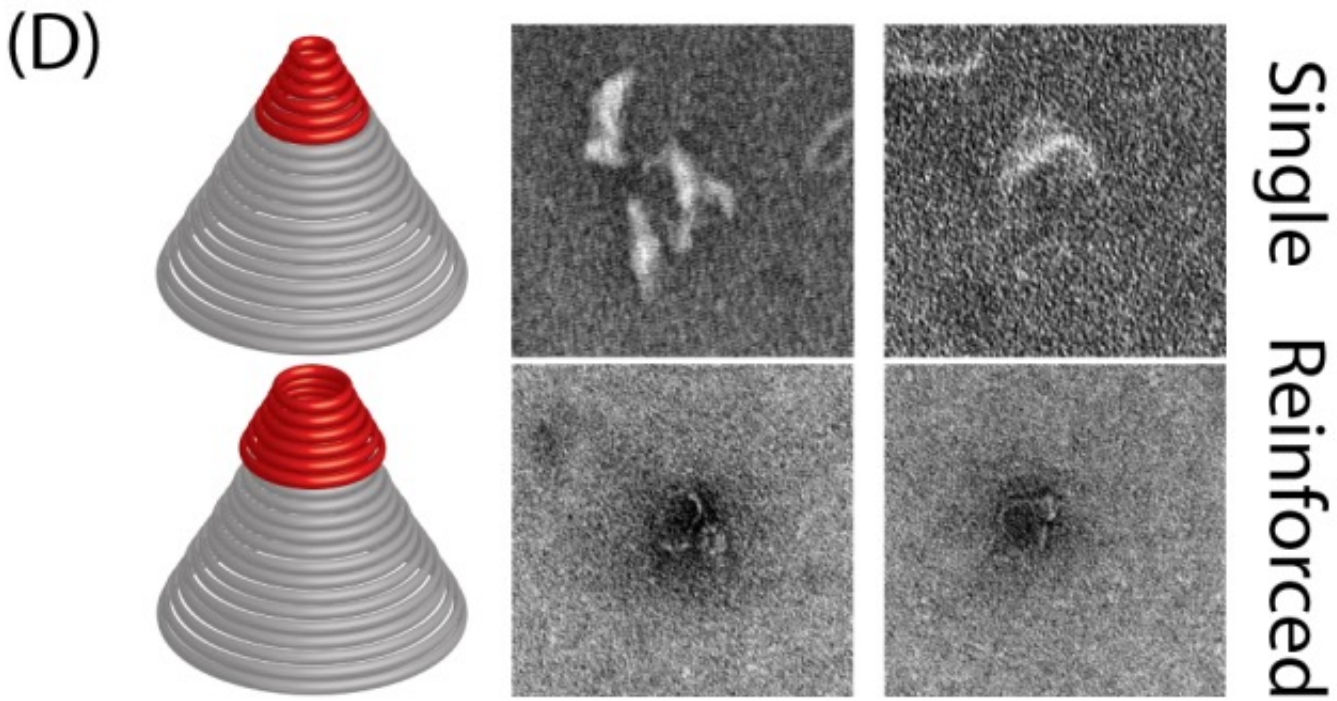

Rigidity increases with bundles, even if curved.

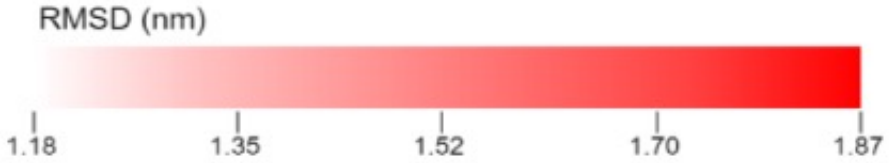

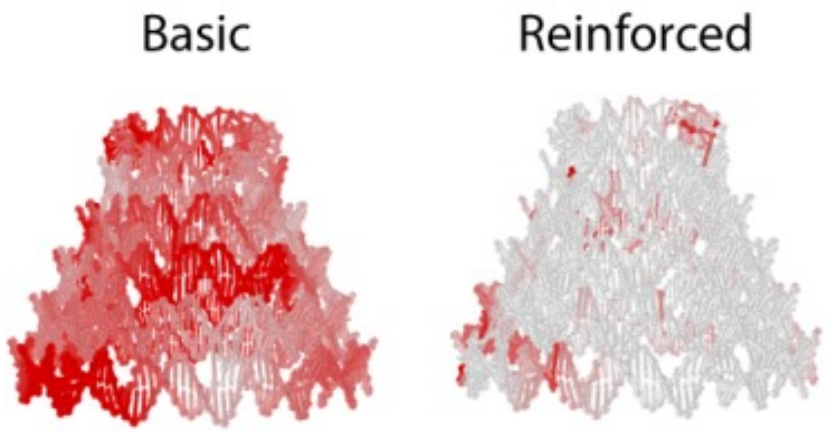

(Reinforced portion shown only)

Planar Polyhedral DNA Nanostructures

Benson et al, Nature 523(7561), 2015

Benson et al, Nature 523(7561), 2015
3D Polyhedral DNA Nanostructures

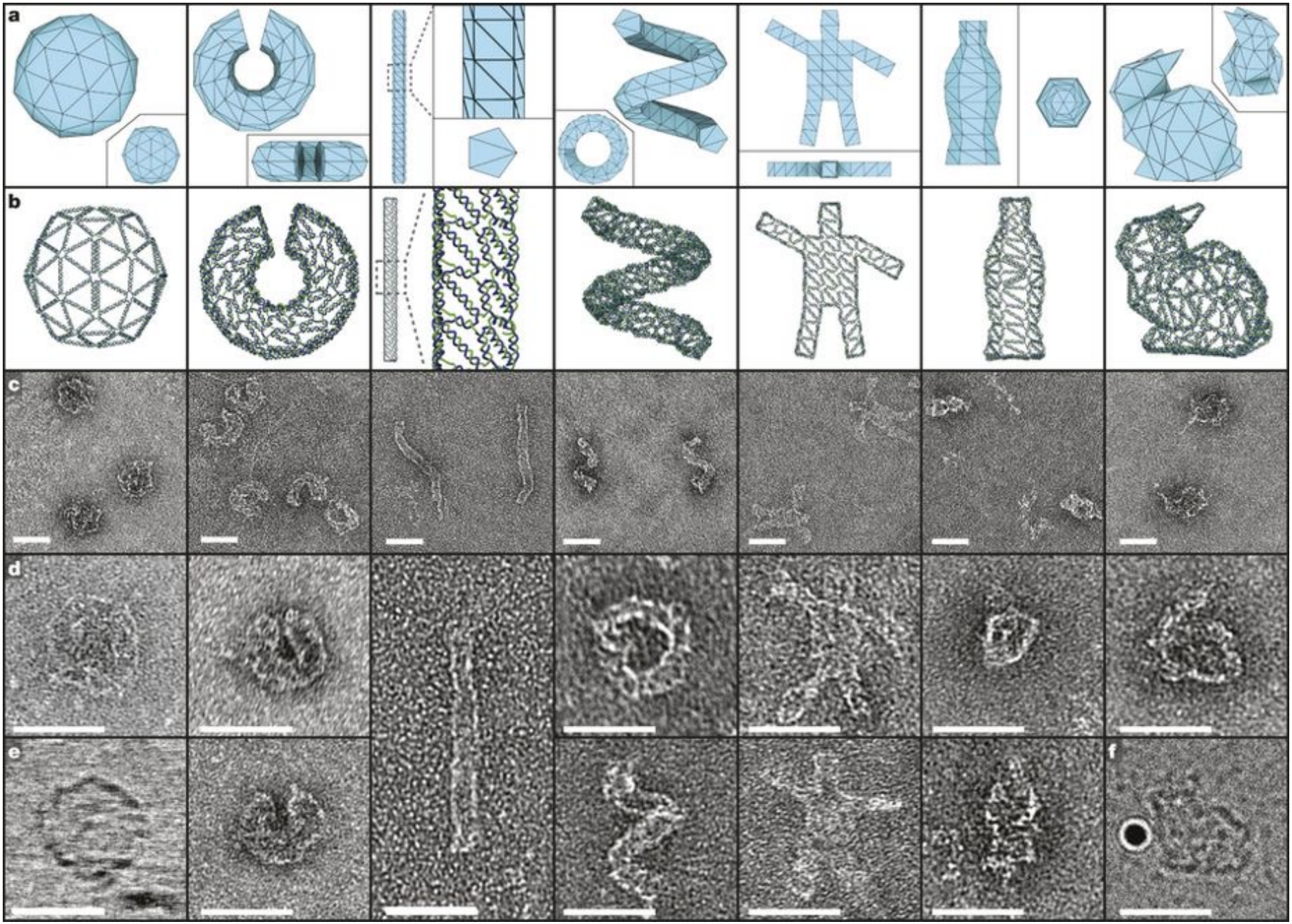

Benson et al, Nature 523(7561), 2015

Planar Polyhedral DNA Nanostructures

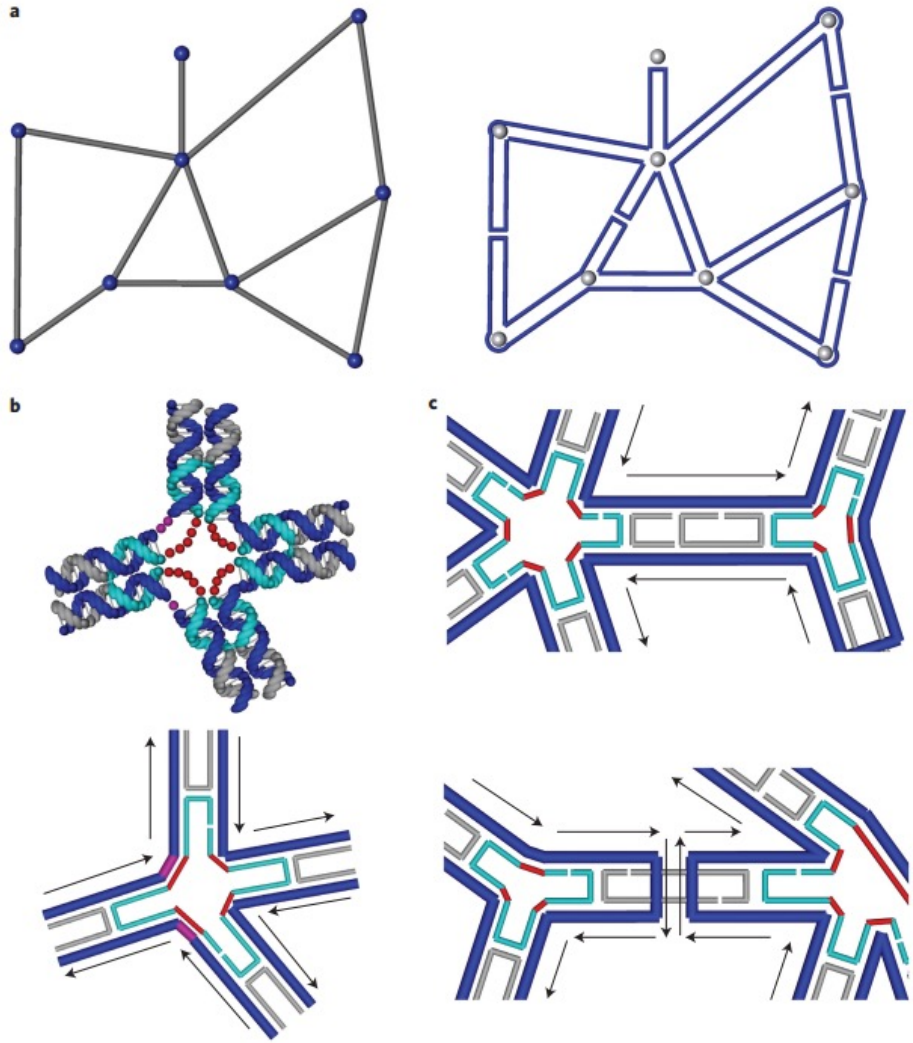

| Design principles. a, Left: an arbitrary wireframe pattern composed of line segments (grey) and vertices (blue). Right: steps to route a scaffold. First, double all the line segments from the original pattern. Second, connect the lines that meet at each vertex. Third, 'loop' and 'bridge' all the lines into one continuous scaffold. **b**, A DNA helical model of a 4 × 4 junction (top) and a line model of the 4 × 4 junction (bottom). Each vertex is designed as an $n \times 4$ junction. The angle of adjacent arms in one junction can be adjusted by inserting poly T loops (red dots) and leaving unpaired nucleotides in the scaffold strand opposite to the poly T loop (pink dots). **c**, Adding staple strands on two different types of edge (five-turn long edges are used here for illustration): the edge with two antiparallel scaffolds (top) and the edge with a scaffold bridge (Holliday junction) in the middle (bottom). Arrows indicate the direction from the 5′ end to the 3′ end of the DNA. In **b** and **c**, dark blue strands represent the scaffold strand and grey and cyan strands are the staple strands.

Benson et al, Nature 523(7561), 2015

Challenge of polyhedral DNA nanostructures:

Eulerian Path Problem:

Given a graph is it possible to construct a path that visits each edge exactly once?

Polynomial Time Solution: graph has Eulerian path iff each vertex has even number of edges

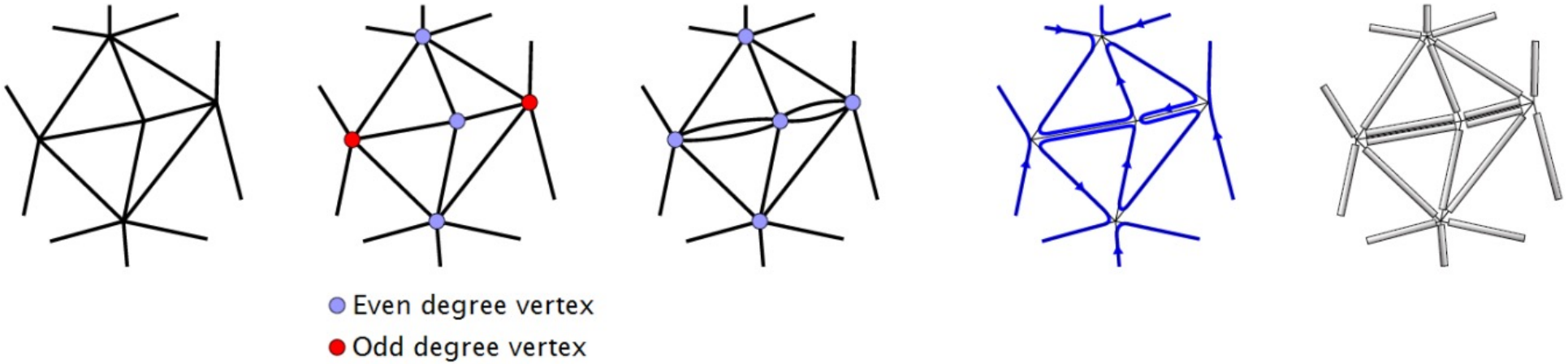

After identifying (and pairing) two odd degree nodes, we double the edges along a path connecting these nodes and implement the corresponding beams of the nanostructure by two DNA double helices.

Benson et al, Nature 523(7561), 2015

Benson et al, Nature 523(7561), 2015

Routing Scaffold Sequence using Singe or Doubled Eulerian Paths

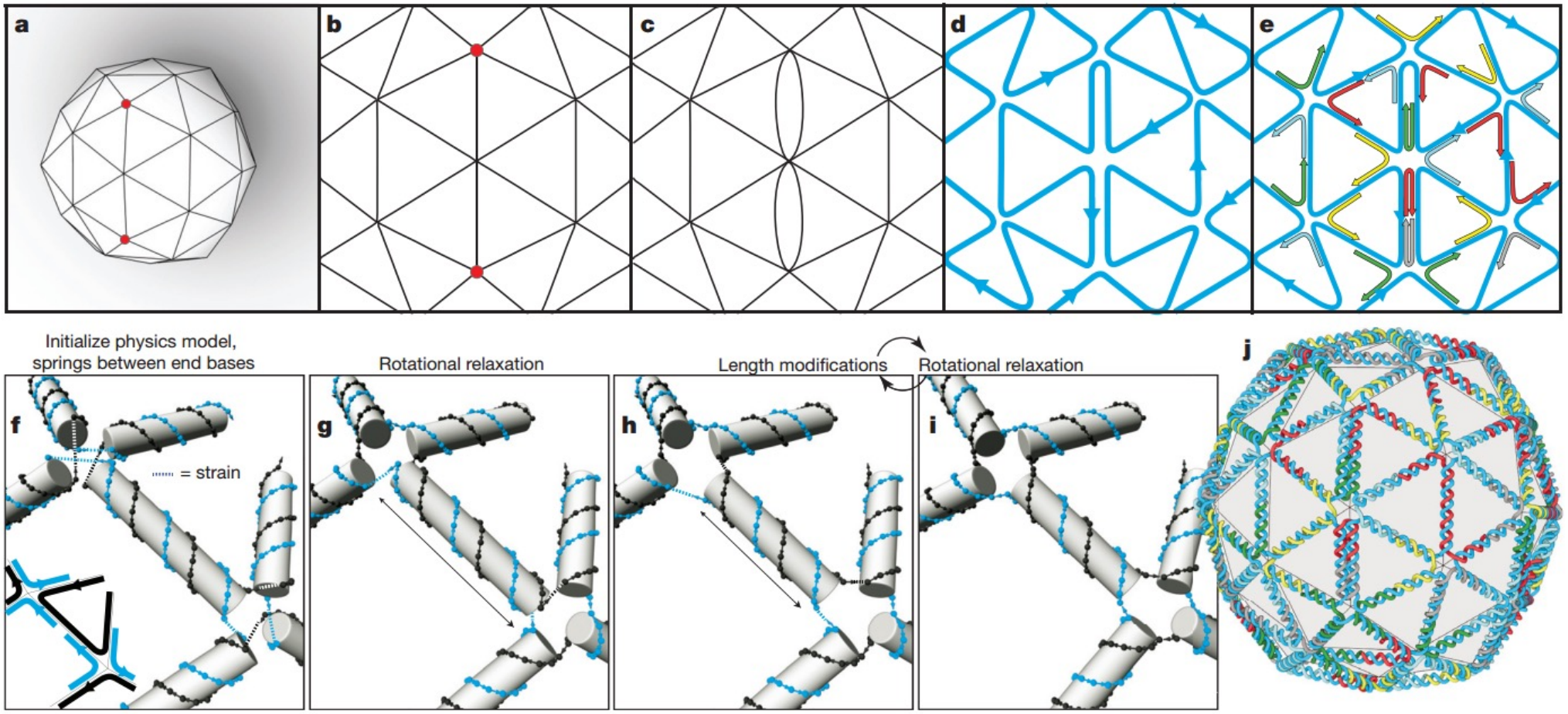

Design paradigm and automated workflow for scaffold-routeing sequence design of origami 3D meshes. **a**, A 3D mesh is drawn using 3D software. **b**, Using the minimum weight perfect matching algorithm, odd-degree vertices are paired. **c**, Double edges are introduced. **d**, The developed A-trails algorithm routes the scaffold according to the constraints. **e**, The staple-strand (multi-coloured) routeing follows implicitly from the scaffold (blue) routeing. **f–i**, Before computation of the sequences, a physics model is used to relax and evenly distribute strain in the design. Each double helix is treated as a stiff rod with springs connecting the bases at the ends of the scaffold strand and staple strand. Iterations of rotational relaxation (**g** and **i**) and length modification of helices (**h**) leads to the final design (**j**), where sequences are calculated after importing to vHelix.

Benson et al, Nature 523(7561), 2015

Benson et al, Nature 523(7561), 2015

Scaffold routing using Eulerian Paths

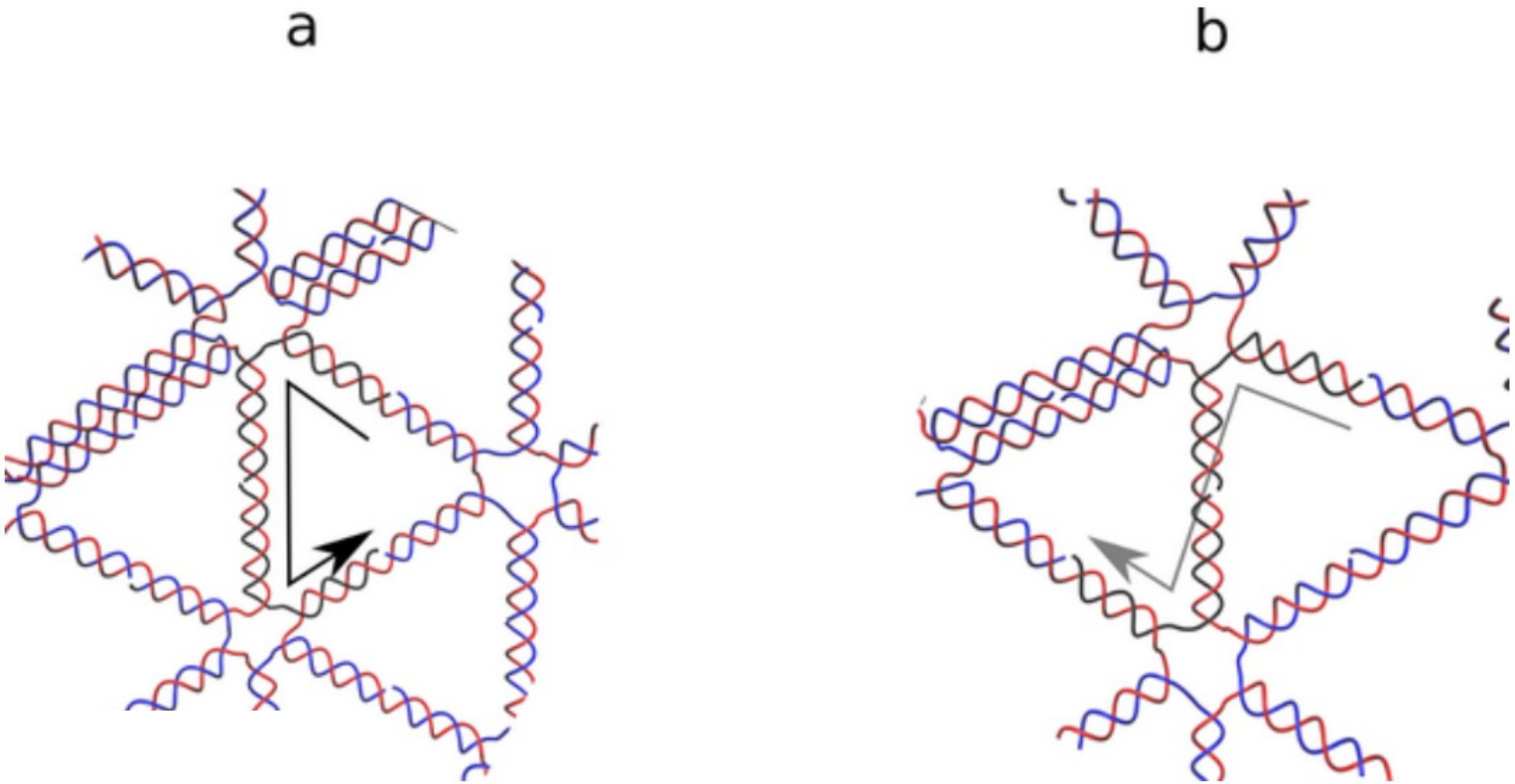

Figure S2.1: Non-crossing (a) and crossing (b) orientations of the scaffold and staples. As seen when considering the routing projected on the plane defined by the average of the normals of the two connected vertices. Depending on the two configurations, the allowed lengths are discretized into either in odd or even numbers of DNA half turn lengths.

Benson et al, Nature 523(7561), 2015

Gigadalton-scale shape-programmable DNA assemblies

Wagenbauer, Sigl, Dietz

DNA Origami Scaling Up Challenge:

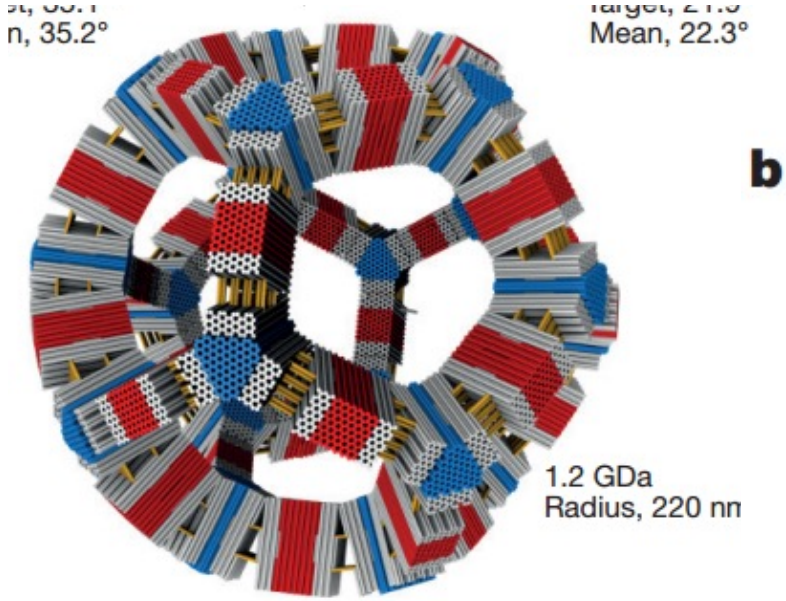

Gigadalton Polyhedra

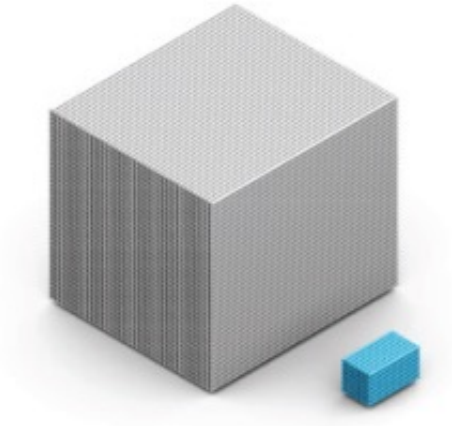

Gigadalton DNA bricks

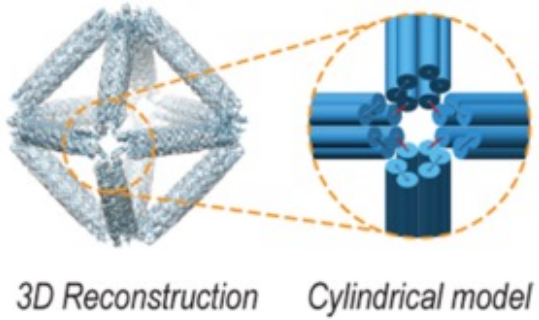

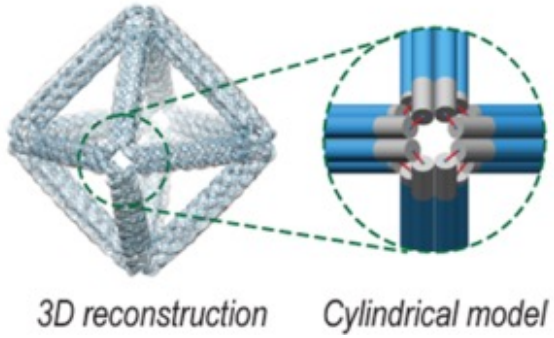

Helix bundle polyhedra

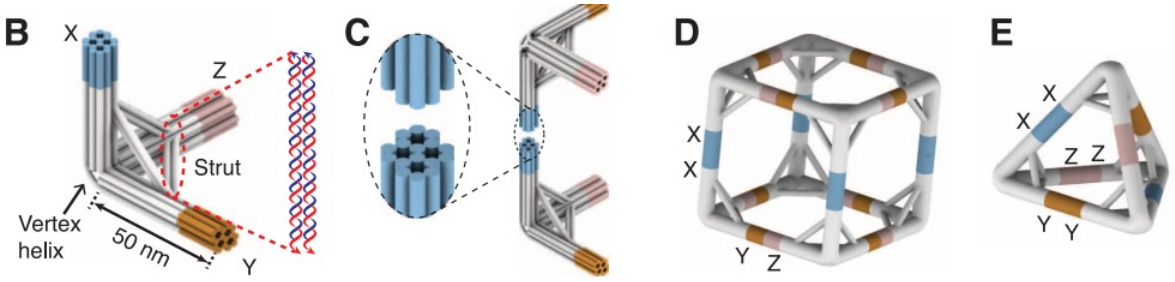

Strut Joint Polyhedra

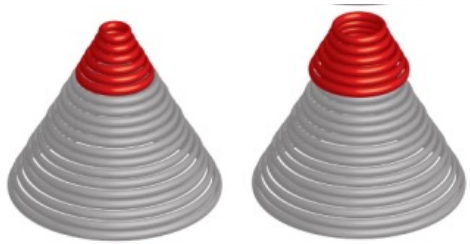

Reinforced curvature

Gigadalton-scale shape-programmable DNA assemblies
Wagenbauer, Sigl, Dietz

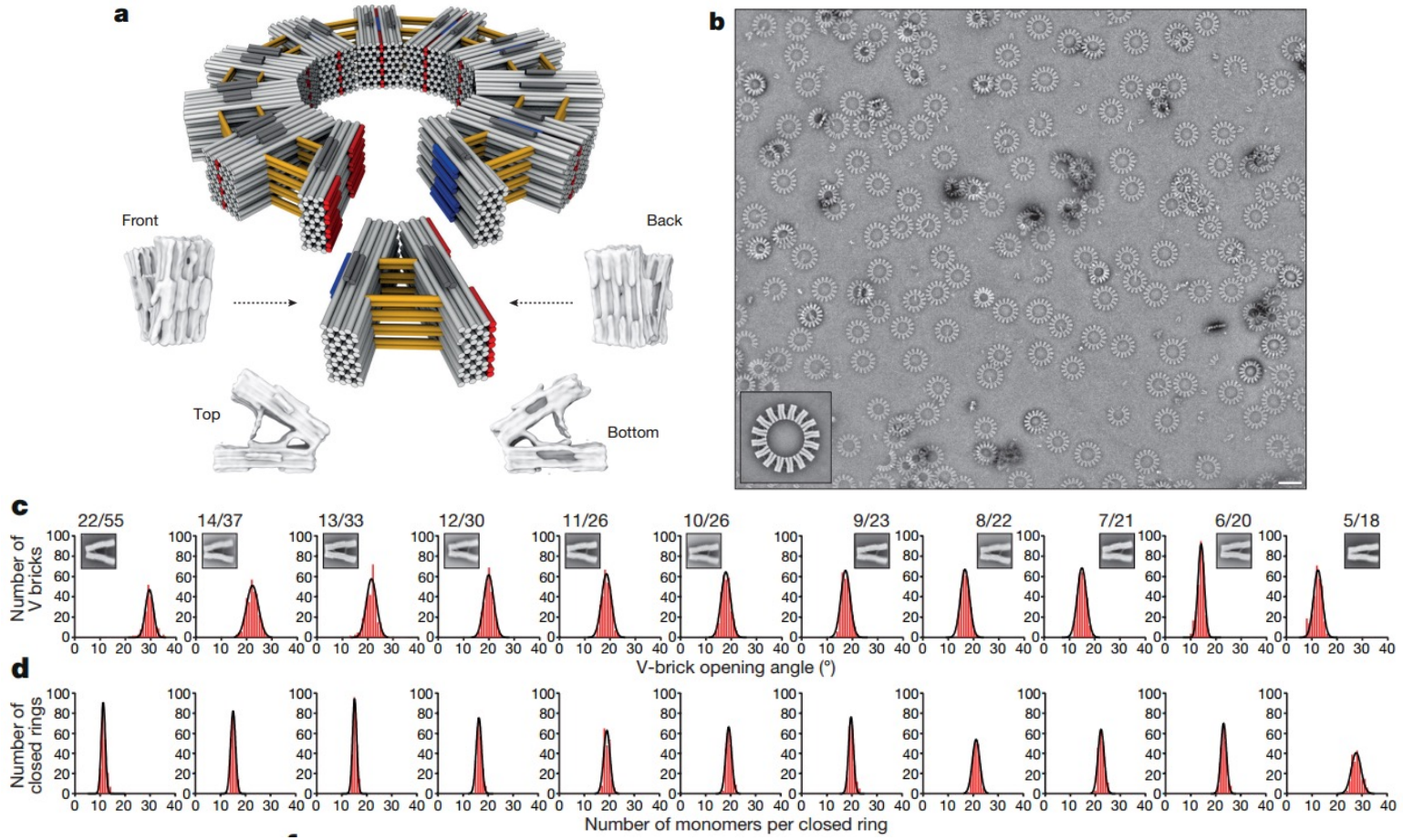

- **Repeatedly joining the same single geometric unit can self-assemble into large multiple unit structures.**
- **Controlling the angle affects the number of units necessary to fill 360°, thus controls size of formed structure.**

Gigadalton-scale shape-programmable DNA assemblies

Wagenbauer, Sigl, Dietz

Designing a 3-degree pivot:

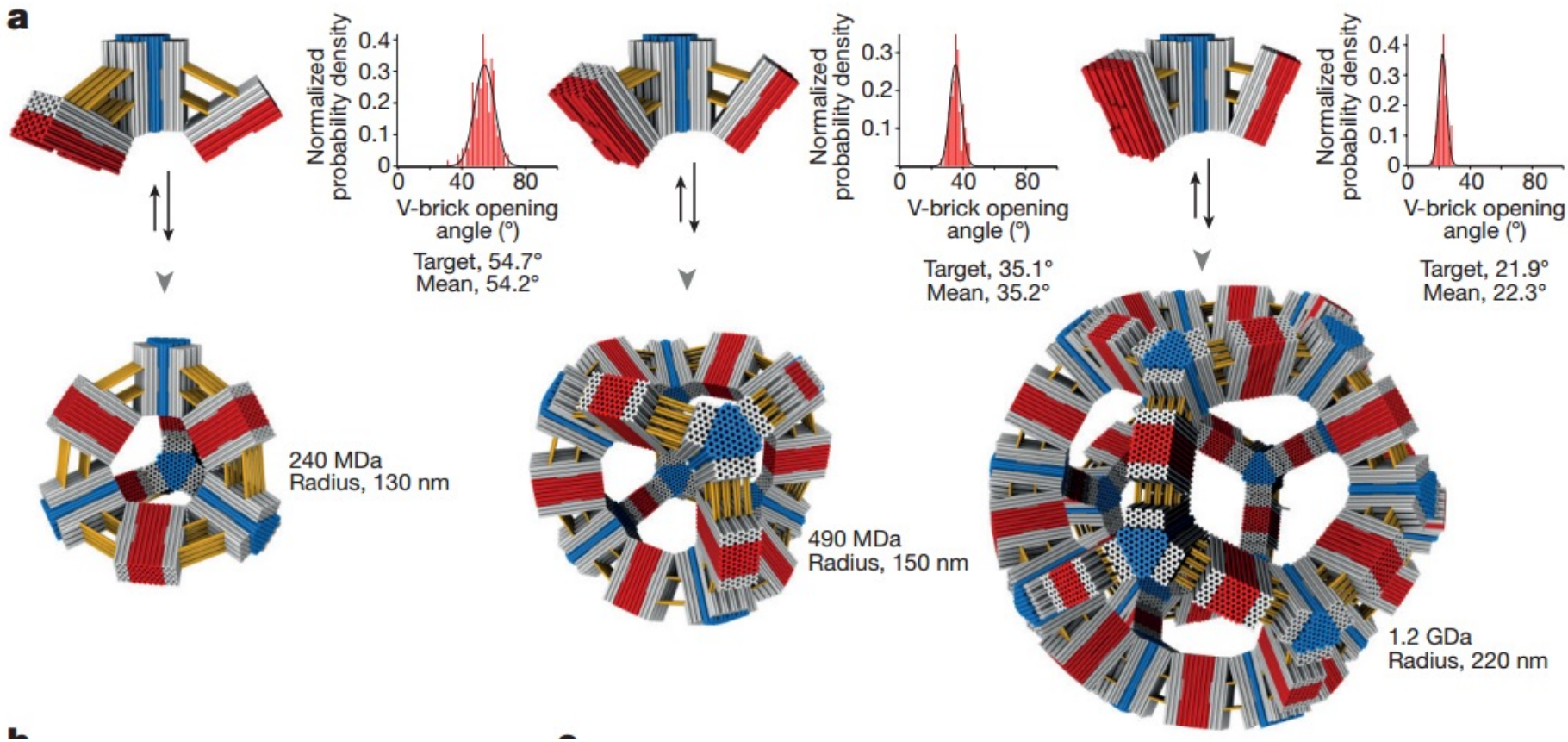

Gigadalton-scale shape-programmable DNA assemblies

Wagenbauer, Sigl, Dietz

Using a 3-degree pivot:

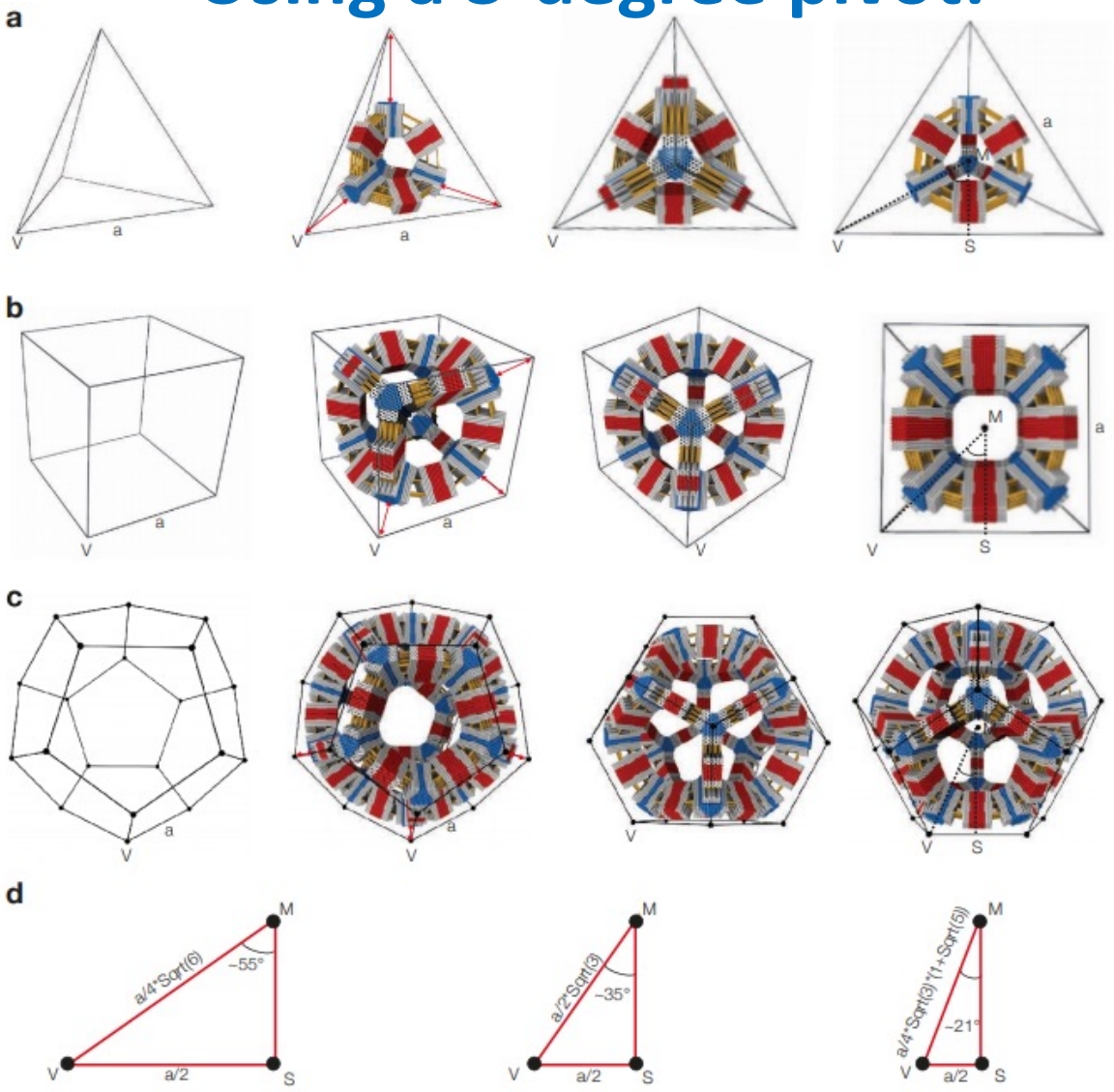

c Construction of closed higher-order polyhedron-like objects via self-limiting oligomerization of the reactive vertex objects. A tetrahedron, hexahedron, and a dodecahedron are shown as envelopes. **d** Sketch for calculating opening angles of the V-brick for each of the 3D finite-size assemblies. See V, M, S positions in a-c.

Helix Bundle Edges: Automated sequence design of 3D polyhedral wireframe DNA origami with honeycomb edges

Jun et al 2019 ACS Nano

Helix Bundle Edges:
Automated sequence design of 3D polyhedral wireframe DNA origami with honeycomb edges
Jun et al 2019 ACS Nano

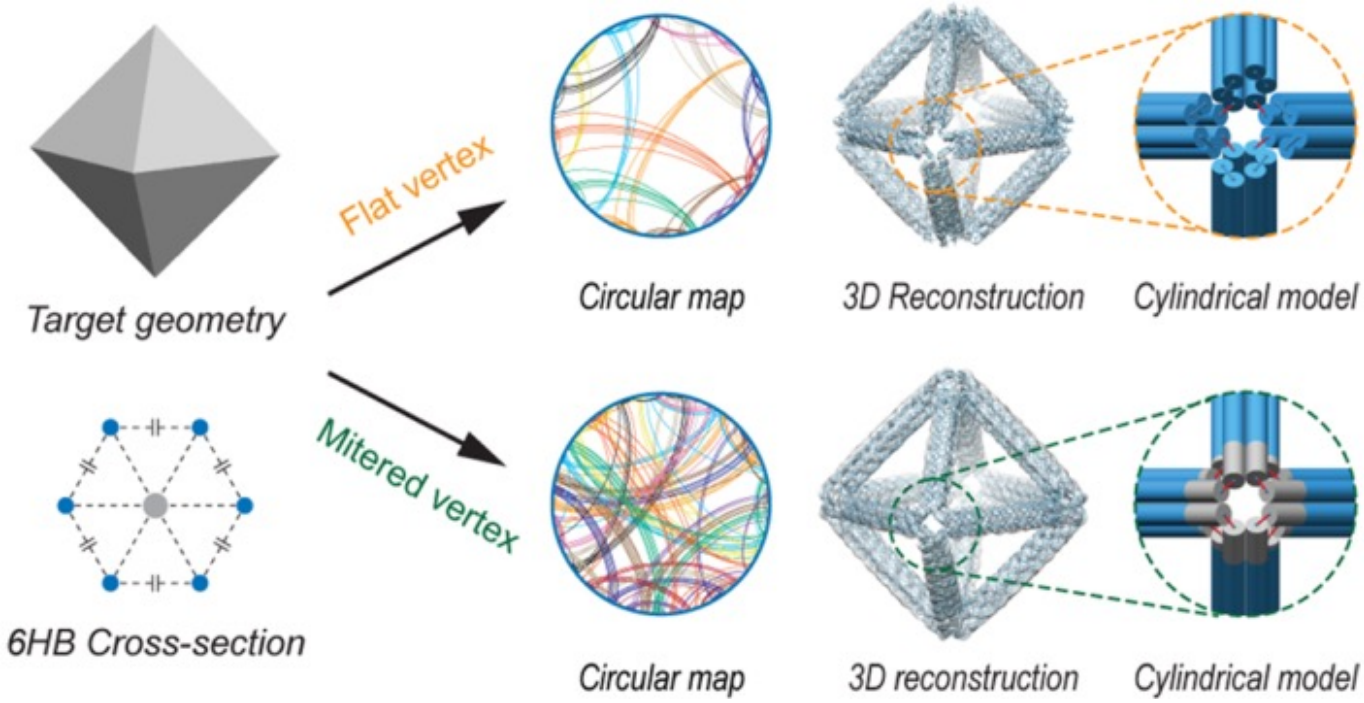

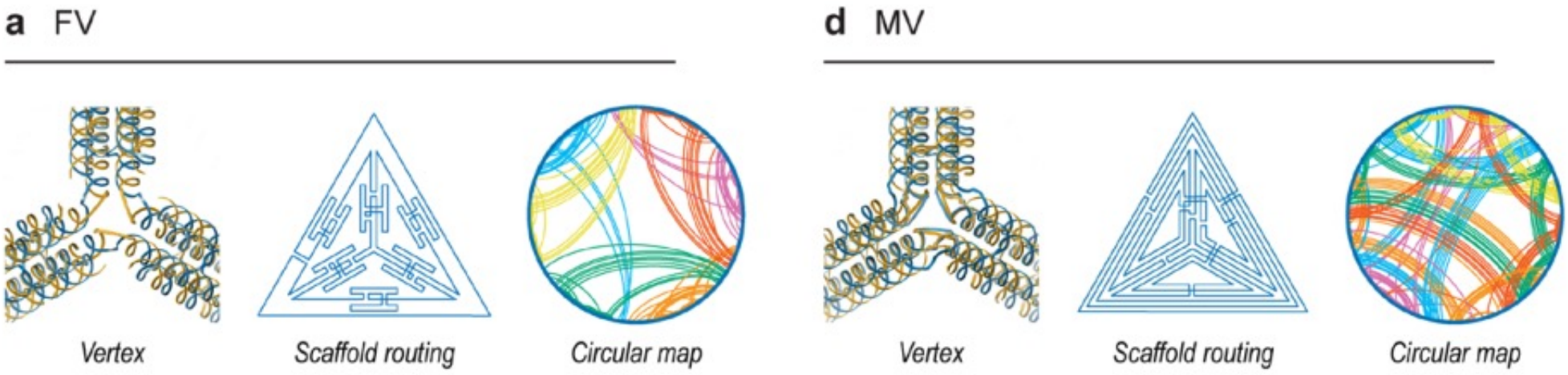

Helix Bundle Edges:
Automated sequence design of 3D polyhedral wireframe DNA origami with honeycomb edges
Jun et al 2019 ACS Nano

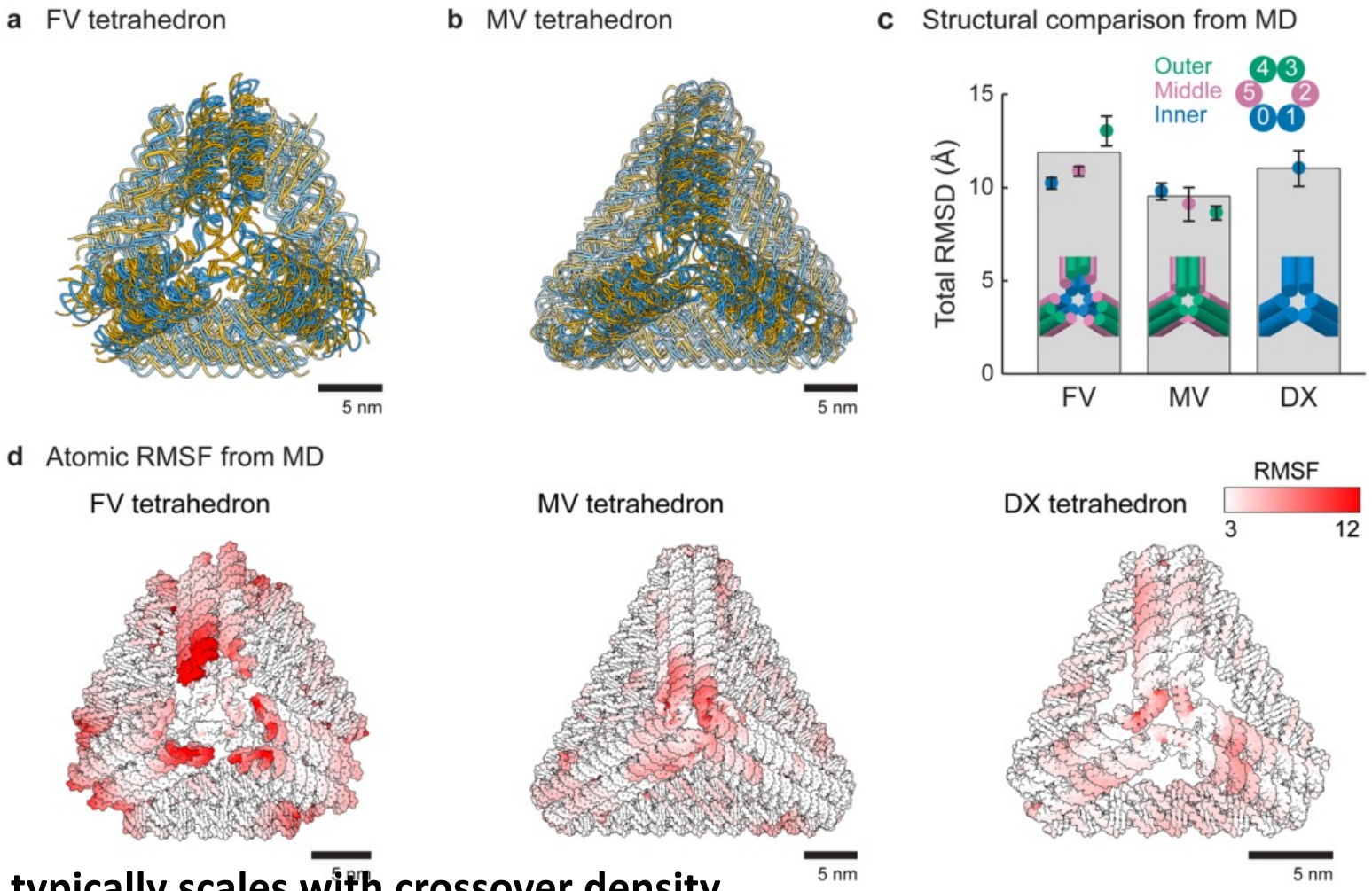

- **Rigidity typically scales with crossover density**
- **Crossover density – Number of crossovers per area typically increases with larger size bundles**

Strut-Supported Polyhedra
Iinuma et al Science 2014

Strut-Supported Polyhedra
Iinuma et al Science 2014

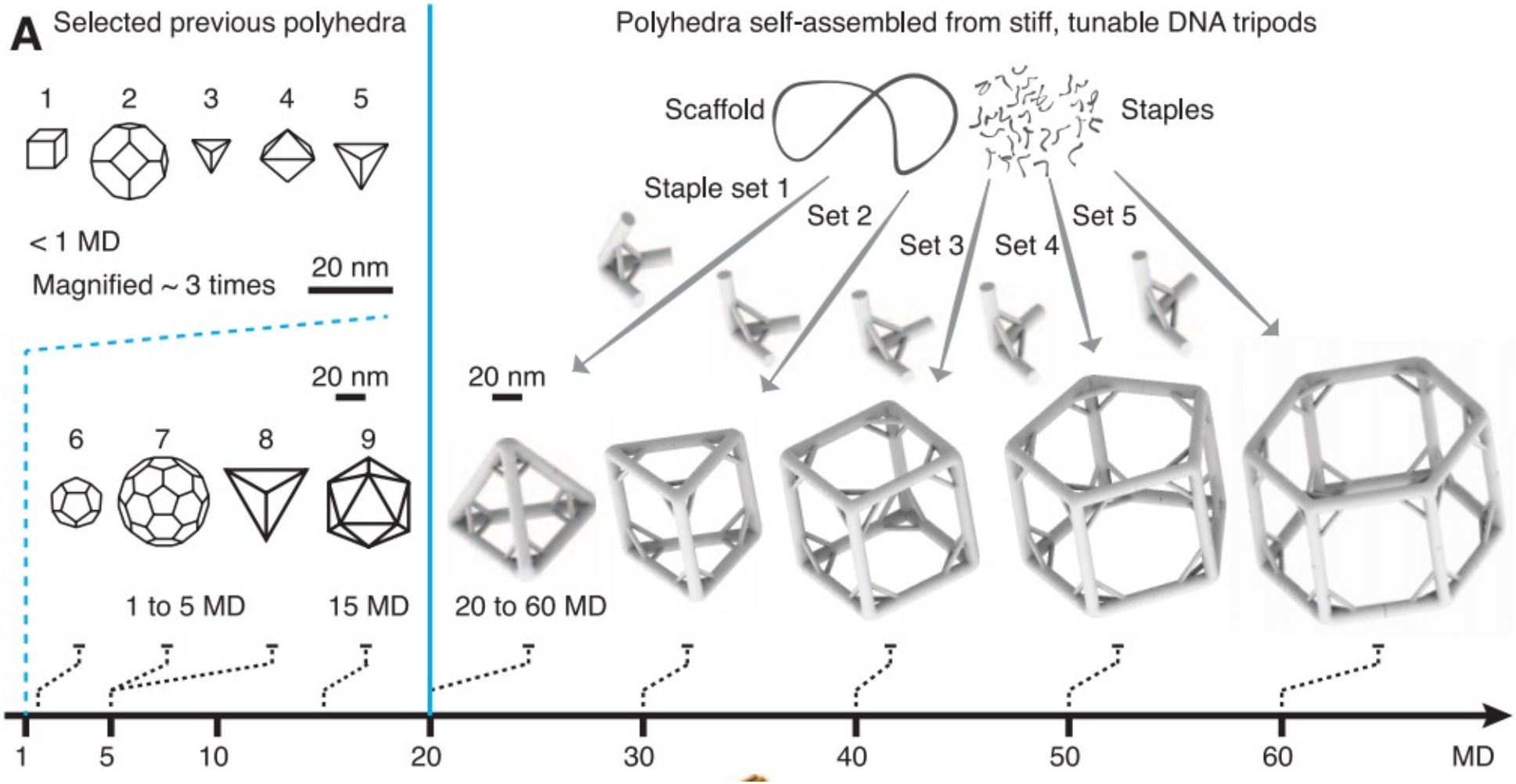

- **Weak vertices limited the variety of constructed polyhedral.**
- **Adding struts add rigidity and can explicitly set the angle.**

Strut-Supported Polyhedra
Iinuma et al Science 2014